DISTRIBUTION OF BETAINE/GABA TRANSPORTER BGT-1 IN EXCITOTOXIC BRAIN INJURY AND ITS ROLE IN OSMOREGULATON IN THE BRAIN

ZHU XIAOMING

(Bachelor of Medicine, Master of Science)

A THESIS SUBMITTED FOR THE DEGREE OF

DOCTOR OF PHILOSOPHY

DEPARTMENT OF ANATOMY

NATIONAL UNIVERSITY OF SINGAPORE

2005

ACKNOWLEDGEMENTS

First of all, I would like to express my deepest appreciation to my supervisor, **Associate Professor Ong Wei Yi**, Department of Anatomy, National University of Singapore, for his innovative ideas and invaluable guidance throughout this study. Not only does he train me in the field of neuroscience, but also set a role model as a hardworking and committed researcher.

I have to thank **Professor Ling Eng Ang**, Head of Anatomy Department, National University of Singapore, for his kind assistance in the matriculation and full support during my studies here.

I am very grateful to **Associate Professor Go Mei Lin**, Department of Pharmacy, National University of Singapore, for her generous financial support to execute some parts of this research. I am also greatly indebted to **Dr. Li Guodong**, National University Medical Institutes, National University of Singapore, for his kind assistance during my work in his laboratory.

I sincerely thank **Dr. Lim Sai Kiang**, Genome Institute of Singapore, for her technical guidance and kind support during that period of time when I indulged in the molecular work in her laboratory. Also thank **Miss Joan** and **Mr. Que Jianwen** in Dr. Lim's laboratory for their kind help.

I must acknowledge my gratitude to **Miss Chan Yee Gek** for her teaching in Electron Microscopy, **Mrs. Ng Geok Lan** and **Mrs. Yong Eng Siang** for their kind assistance, and **Mdm Ang Lye Gek Carolyne** and **Miss Teo Li Ching Violet** for their secretarial assistance. I would like to thank all other staff members and my

fellow postgraduate students at Department of Anatomy, National University of Singapore for their help and support.

A major credit also goes to my dearest parents, my dearest wife, **Xu Xinxia** and my dearest daughter, **Zhu Lingyi**, without their support this work would not have been completed.

Last, but not least, thanks to the National University of Singapore for supporting me with a Research Scholarship to bring this study to reality.

PUBLICATIONS

Various portions of the present thesis have been published, or have been submitted for publication.

International Refereed Journals:

Zhu XM, Ong WY (2004) A light and electron microscopic study of betaine/GABA transporter distribution in the monkey cerebral neocortex and hippocampus. J Neurocytol 33: 233-240.

Zhu XM, Ong WY (2004) Changes in GABA transporters in the rat hippocampus after kainate-induced neuronal injury: decrease in GAT-1 and GAT-3 but upregulation of betaine/GABA transporter BGT-1. J Neurosci Res 77: 402-409.

Zhu XM, Ong WY, Li G, Go ML (2005) Differential effects of betaine and sucrose on betaine / GABA transporter (BGT-1) expression and betaine transport in human U373 MG astrocytoma cells and rat hippocampal astrocytes. (In revision).

Conference papers:

Zhu XM, Ong WY (2004) Changes in GABA transporters in the rat hippocampus after kainate induced neuronal injury. **4th IBRO School, Hong Kong.**

Zhu XM, Ong WY, Li G, Go ML (2004) Differential effects of betaine and sucrose on betaine / GABA transporter (BGT-1) expression and betaine transport in human U373 MG astrocytoma cells and rat hippocampal astrocytes. **International Biomedical Science Conference, Kuming, Yunnan, China.**

TABLE OF CONTENTS

ABBREVIATIONS

BBB	blood - brain barrier
BGT-1	betaine/GABA transporter
BSA	bovine serum albumin
CA	cornu amonis
CA1	hippocampus CA1 area
CA3	hippocampus CA3 area
CAT	chloramphenicol acetyltransferase
CNS	central nervous system
CPM	count per minute
DAB	3, 3 - diaminobenzidine tetrahydrochloride
DNA	deoxyribonucleic acid
EDTA	ethylenediaminetetraacetic acid
ELISA	enzyme linked immunosorbent assay
EMSA	electrophoretic mobility shift assay
GABA	γ-aminobutyric acid
GABA - T	GABA transaminase
GAD	glutamic acid decarboxylase
GAT	GABA transport
GFAP	glial fibrillary acidic protein
GS	glutamine synthetase
[^{3}H]GABA	tritium labelled GABA

IC_{50}	concentration at 50% inhibition
KA	kainic acid
K_m	Michaelis constant
MDCK	Madin-Darby canine kidney
MW	molecular weight
NMR	nuclear magnetic resonance
OsO_4	osmium tetroxide
PB	phosphate buffer
PBS	phosphate-buffered saline
PCR	polymerase chain reaction
PKA	protein kinase A
PKC	protein kinase C
RNA	ribonucleic acid
RT - PCR	reverse transcription polymerase chain reaction
TauT	taurine transporter
TCA	tricarboxylic acid
TonE	tonicity-responsive enhancer
Tris	trihydroxymethylaminomethane

SUMMARY

Osmoregulation is critical for maintaining brain function. In response to hyperosmotic stress, brain cells, including neurons and glial cells can accumulate organic osmolyte: betaine, myo-inositol and taurine via the osmolyte transport. The betaine/GABA transporter BGT-1 has been extensively studied in MDCK cells, and it is responsible for the uptake of betaine into kidney cells when adapted to hyperosmotic environment. However, the localization and function of BGT-1 in the brain has been unclear. Although BGT-1 mRNA is widely expressed in the brain, previous studies on distribution of BGT-1 in the brain are only carried out at mRNA level using Northern blot and *in-situ* hybridization. The distribution and subcellular location of BGT-1 has to be addressed at protein level, in order to gain a thorough understanding of its function in the brain. BGT-1 is capable of transporting both betaine and GABA, as examined in *Xenopus oocytes* and various cell lines. But the physiological substrate of BGT-1 in the brain remains to be determined. Of particular interest is the elucidation of the role of BGT-1 in excitotoxic brain injury, since under such circumstances of neuronal injury, osmotic stress resulted to certain extent from the release of neuronal content, including the highly abundant betaine, as well as the altered levels of extracellular GABA, could be related to the function of BGT-1.

The present study first addressed the question of what is the normal distribution and subcellular location of BGT-1 in the brain. The use of a specific antibody to BGT-1 detected the presence of BGT-1 in the cell bodies and dendrites of pyramidal

neurons in the cerebral neocortex and CA fields of hippocampus. Electron microscopy reveals that BGT-1 is postsynaptically localized in asymmetric synapse. The distribution of BGT-1 on dendritic spines, rather than at GABAergic axon terminals, suggests that the transporter is unlikely to play a major role in terminating the action of GABA at a synapse. Instead, the osmolyte betaine is more likely to be the physiological substrate of BGT-1 in the brain, and the presence of BGT-1 in pyramidal neurons suggests that these neurons utilize betaine to maintain osmolarity.

Meanwhile, the present study explored the changes in the expression of GABA transporters in the rat hippocampus after kainate-induced neuronal injury, since changes in expression of GABA transporters/BGT-1 might result in alterations in levels of GABA/betaine in the extracellular space, with consequent effects on neuronal excitability or osmolarity. A decrease in GAT-1 and GAT-3 immunostaining, but no change in GAT-2 staining, was observed in the degenerating CA subfields. In contrast, increased BGT-1 immunoreactivity was observed in astrocytes after kainate injection. BGT-1 is a weak transporter of GABA as compared to other GABA transporters, and the increased expression of BGT-1 in astrocytes might be a protective mechanism against increased osmotic stress known to occur after excitotoxic injury. On the other hand, excessive or prolonged BGT-1 expression might be a factor contributing to astrocytic swelling after brain injury.

It is conceivable that BGT-1 could have been induced in astrocytes as a result of induction by betaine or hyperosmotic stress after excitotoxic injury. Finally, the present study investigated the possible changes in betaine transporter expression and its function in astrocytes, after treatment with high concentrations of betaine or

sucrose *in vitro*, as well as the effect of betaine on its transporter BGT-1 in reactive astrocytes *in vivo*. Treatment of human U373 MG astrocytoma cells for 12 hours with 1-100 mM of betaine, but not equivalent concentrations of sucrose, resulted in increased BGT-1 immunointensity by ELISA. The increased BGT-1 was present in the cytoplasm and cell membrane. Treatment of cells with 1-100 mM betaine also resulted in increased [^{14}C] betaine transport into the cells, consistent with increased BGT-1 transporter function. No increase in betaine uptake was observed when cells were treated with 1 and 10 mM sucrose, but a large increase was observed when cells were treated with 100 mM sucrose. In contrast to rats received intracerebroventricular injection with kainate plus saline, which showed loss of BGT-1 immunoreactivity in neurons and little induction of BGT-1 in astrocytes, a marked increase in BGT-1 immunoreactivity was observed in astrocytes in the degenerating CA fields and fimbria, in rats injected with kainate plus betaine. These astrocytes were found to have swollen mitochondria at electron microscopy. In view of the above findings, it is postulated that the release of betaine from dying neurons could be a factor contributing to increase BGT-1 expression in astrocytes. This might contribute to astrocytic swelling following head injury or stroke.

In summary, the present study has revealed the distribution of betaine/GABA transporter BGT-1 in normal brain and in excitotoxic brain injury, as well as the expression and functional changes of BGT-1 in astrocytes in response to hyperosmolarity *in vitro* and *in vivo*. Overall, the present study has dissected the role of BGT-1 in osmoregulation in the brain. Further studies are necessary to study the

mechanism by which betaine induces BGT-1 expression and the effects of BGT-1 inhibitors on astrocytic swelling.

CHAPTER 1

INTRODUCTION

1. Maintenance of osmolarity in living cells

Maintenance of osmotic balance is an important aspect of cellular homeostasis. When exposed to extracellular hyperosmolarity, cells initially lose water and shrink, thus concentrating intracellular inorganic ions. Accumulation of inorganic ions (e.g., sodium and potassium salts) and crowding of large intracellular molecules have been demonstrated to compromise the function of proteins, DNA and other cellular macromolecules (Yancey et al., 1982; Minton, 1983; Garner and Burg, 1994). Upon the prolonged hyperosmotic challenge, virtually all cells from bacterial to mammalian slowly accumulate certain small organic solutes, e.g., betaine, taurine and myo-inositol, to achieve osmotic balance. Compared to the high concentrations of intracellular inorganic ions, these small organic solutes generally do not perturb the function of macromolecules, so termed compatible (or non-purturbing) osmolytes (Yancey et al., 1982). Accumulation of specific osmolytes results from their intracellular synthesis or uptake from extracellular space via the corresponding osmolyte transporters (Burg, 1995). On the other hand, adaptation of cells to hypoosmotic condition requires the release of intracellular osmolytes (Kwon and Handler, 1995).

Since cell membrane is highly permeable to water, disturbance in osmoregulation would directly affect the cell volume, thus interfering with a multitude of cell functions (Lang et al., 1998).

1.1. Maintenance of osmolarity in the kidney

Maintenance of osmolarity is essential for the physiological functioning of kidney cells. The renal medulla is the site of final urine formation. The hyperosmolarity in renal medulla provides the driving force for extraction of water from the urine, thus concentrating urine. Osmolarity of the renal medulla can be easily raised to over 1000 mosM in humans and over 3000 mosM in rats (Garcia-Perez and Burg, 1991; Sone et al., 1995). To balance the high extracellular osmolarity, cells in the inner renal medulla accumulate large amounts of certain osmolytes, predominantly sorbitol, myo-inositol, betaine and taurine (Burg et al., 1997). These organic osmolytes help to protect the cells against hyperosmolarity. Therefore, physiological functioning of the kidney depends critically on the ability of the renal medullary cells to adapt to the hyperosmolarity.

1.2. Maintenance of osmolarity in the central nervous system

Osmoregulation plays a critical role in the brain, where changes in cell volume can not be tolerated due to the rigid, non-expandable skull and where alterations in ion composition would affect excitability (Strange, 1992; Gullans and Verbalis, 1993; Law, 1994a; Lang et al., 1998).

Hypernatremia and hyponatremia are very common clinical problems. Hyperosmolarity as a result of hypernatremic state leads to the cellular dehydration due to water movement from the intracellular space to the hyperosmotic extracellular space. In response to hyperosmolarity, brain cells subsequently accumulate osmolytes to restore to the normal volume level. Exposure of cultured

brain cells to hyperosmolarity shows a significant increase in the content of organic osmolyte (Strange et al., 1991; Beetsch and Olson, 1996). Studies of hypernatremic animals indicate that the organic osmolyte accumulation generally accounts for 30-50% of the total osmolyte accumulation (Chan and Fishman, 1979; Heilig et al., 1989; Lien et al., 1990). When hypernatremic state persists and exceeds the brain's ability to compensate for cellular dehydration, such neurological symptoms as irritability, stupor, hyperreflexia and coma would develop (Arieff, 1984; Gullans and Verbalis, 1993).

It is well documented that hyponatremia causes brain edema as a consequence of influx of water into brain. Due to increased intracranial pressure, brain edema leads to life-threatening cessation of the brain's blood supply and neuronal death (Kimelberg, 1995; Pasantes-Morales et al., 2002). To adapt to hypoosmolarity, brain cells exclude intracellular osmolytes, mainly the inorganic ions potassium (K^+) and chloride (Cl^-) and a number of organic osmolytes. Release of organic osmolytes has been shown to contribute significantly to the adaptive response to hyponatremia (Lien et al., 1991; Verbalis and Gullans, 1991; Sterns et al., 1993). *In vitro* studies in both neurons and astrocytes also demonstrate the persistent exclusion of organic osmolytes, e.g., taurine following hypoosmotic stimulus (Pasantes and Schousboe, 1988; Schousboe et al., 1991; Olson, 1999).

In addition, osmotic stress directly influences neuronal electrophysiological function. Alteration in ion concentrations in extracellular as well as intracellular spaces would affect membrane potential and the resulting neuronal excitability. Neuronal excitability increases significantly in hippocampal slices under

hypoosmotic conditions (Chebabo et al., 1995). The hypoosmotic-associated hyperexcitability has been shown in patients of hyponatremia with an increased susceptibility to seizures (Andrew, 1991). *In vitro* studies in brain slices reveal that osmolarity reduction enhances the synaptic transmission whilst raising osmolarity depresses synapses (Rosen and Andrew, 1990; Chebabo et al., 1995; Huang et al., 1997). When confronted with hyperosmolarity, neurons of primary culture show enhanced voltage-dependent Ca^{2+} currents and depressed K^{+} currents (Somjen, 1999).

2. Organic osmolytes

The different organic osmolytes that are accumulated by cells fall into three classes: methylamines, such as betaine and glycerophosphorylcholine; polyalcohols, such as myo-inositol and sorbitol; and amino acids or amino acid derivatives, such as glycine and taurine (Lang et al., 1998). The followings highlight some major osmolytes in the brain.

2.1. Betaine

Betaine (N, N, N-trimethylglycine) has been shown an osmoprotective role in many plant, animal and bacterial species (Yancey et al., 1982; Le Rudulier and Bouillard, 1983; Perroud and Le Rudulier, 1985; Bagnasco et al., 1986; Yancey and Burg, 1990). It is well documented that the kidney medulla becomes hyperosmotic when concentrating urea and large amounts of betaine is intracellularly accumulated (Bagnasco et al., 1986; Balaban and Burg, 1987; Garcia-Perez and Burg, 1991).

In addition to the uptake from the extracellular environment through transporter, betaine can be synthesized *in vivo* from its precursor, choline. Production of betaine by oxidation of choline has been reported in gut mucosa (Flower et al., 1972), liver (Glenn and Vanko, 1959; Wilken et al., 1970), and kidney (Haubrich et al., 1975). Fig 1 illustrates the metabolic pathway for betaine synthesis and degradation. Betaine is synthesized via two oxidative steps. Choline is oxidized by choline dehydrogenase (EC 1.1.99.1) to betaine aldehyde, which is further oxidized to betaine by betaine aldehyde dehydrogenase (EC 1.2.1.8) (Rothschild and Barron, 1954). Choline dehydrogenase itself may also be able to catalyze both steps (Tsuge et al., 1980).

Betaine degradation is catalyzed by betaine homocysteine methyltransferase (EC 2.1.1.5) (Skiba et al., 1987). In this reaction, a methyl group is transferred from betaine to homocysteine to form methionine. After donating its methyl group, betaine becomes dimethylglycine. It has been well-documented that in liver, betaine acts as a methyl donor in the detoxification of homocysteine (Gaitonde, 1970; Finkelstein et al., 1982). Clinically, betaine is used for treatment of homocystinuria, which caused by a genetic defect in cystathione β-synthase (an enzyme in the trans-sulfuration pathway of homocysteine metabolism) (Smolin et al., 1981; Wilcken and Wilcken, 1997; Walter et al., 1998).

Within the kidney, the production of betaine from choline occurs in proximal tubule (Wirthensohn and Guder, 1982; Miller et al., 1996) and renal medullary cells (Grossman and Hebert, 1989; Lohr and Acara, 1990), both of which contain choline dehydrogenase activity. It raises the possibility that alterations of betaine synthesis

in the renal medulla may contribute to its osmotic regulation. However, no evidence favors this. Hypernatremia, which results in major accumulation of betaine in renal medullas, does not show an increase in the activity of choline dehydrogenase (Grossman and Hebert, 1989). MDCK (Madin-Darby canine kidney) cells, which accumulate betaine when grown in hyperosmotic media, have little capacity to synthesize betaine and rely on uptake from the medium (Nakanishi et al., 1990). Thus, the role of betaine synthesis in osmoregulation is not well supported.

In contrast, betaine metabolism is poorly characterized in the central nervous system (CNS), although betaine has been detected in rat brain (Heilig et al., 1989; Lien et al., 1990; Lien, 1995; Koc et al., 2002). No information on betaine synthesis in CNS has been reported. The activity of betaine homocysteine methyltransferase, the enzyme responsible for betaine degradation, is absent in brain (McKeever et al., 1991). It is likely that betaine synthesized elsewhere, e.g. liver, kidney, is transported into the brain via blood-brain barrier (BBB), since betaine/GABA transporter BGT-1 is localized in BBB (Takanaga et al., 2001). High concentrations of betaine (100-300 mM) have been found in single neurons isolated from the abdominal ganglion from *Aplysia Californica* using nuclear magnetic resonance (NMR) spectroscopy. The levels of betaine in brain are increased following salt loading, suggesting a role of betaine in osmoregulation in the CNS (Lien et al., 1990). It is noteworthy that cerebral edema was clinically reported in patients treated with betaine (Yaghmai et al., 2002; Devlin et al., 2004).

2.2. Taurine

Taurine (2-aminoethanesulfonic acid) is widely distributed in the brain, and its intracellular concentration can reach tens of milliMolar (Palkovits et al., 1986; Huxtable, 1989). The highest levels of taurine are present in cerebral cortex, hippocampus, caudate-putamen, cerebellum and hypothalamic supraoptic nuclei, while lower levels are found in the brain stem (Palkovits et al., 1986). Taurine has been detected in neurons, e.g., cerebellar Purkinje neurons, neurons of cortex and hippocampus, as well as in glial cells (Hussy et al., 2000). The biosynthesis of taurine is primarily from cysteine derived in part from methionine via the cysteine sulfinate pathway, which includes oxidation of cysteine to cysteine sulfinate by cysteine dioxygenase and decarboxylation of cysteine sulfinate by cysteine sulfinate decarboxylase (Foos and Wu, 2002; Tappaz, 2004).

The role of taurine in osmoregulation in the brain has been well established. Efflux of taurine in response to osmotic reduction has been consistently shown in numerous preparations of *in vitro* studies, including neurons (Schousboe et al., 1991; Pasantes-Morales et al., 1994), astrocytes (Pasantes and Schousboe, 1988; Kimelberg et al., 1990; Vitarella et al., 1994), and brain slices (Oja and Saransaari, 1992; Law, 1994b). *In vivo* studies on hyponatremia confirm a decreased level of taurine in brain (Thurston et al., 1987; Verbalis and Gullans, 1991; Lien et al., 1991). On the other hand, intracellular accumulation of taurine as a result of hyperosmotic stimulus has been demonstrated in cultured astrocytes (Olson and Goldfinger, 1990; Sanchez-Olea et al., 1992), as well as *in vivo* studies (Thurston et al., 1980; Lien et

al., 1990). In addition, taurine-deficient astrocytes in culture show impaired volume regulation (Moran et al., 1994).

Besides biosynthesis, taurine transport significantly contributes to maintenance of high intracellular levels of taurine in the brain (Sanchez-Olea et al., 1992; Bitoun and Tappaz, 2000a; Bitoun and Tappaz, 2000b). In addition to osmoregulation, taurine has been assigned various roles in the brain, e.g., neuroprotection against neurotoxicity (Saransaari and Oja, 2000), and modulation of intracellular calcium homeostasis (Foos and Wu, 2002).

2.3. Myo-inositol

Myo-inositol is richly present in the brain with heterogenous distribution (2-15 mM) (Fisher et al., 2002). Myo-inositol serves as an osmolyte, such as by accumulation upon extracellular hyperosmolarity and exclusion in response to osmotic reduction, has been shown in numerous studies in the brain, both *in vitro* and *in vivo* preparations (Lien et al., 1990; Strange et al., 1991; Verbalis and Gullans, 1991; Paredes et al., 1992; Strange and Morrison, 1992; Strange et al., 1993; Isaacks et al., 1994). Uptake by myo-inositol transporter as well as de novo biosynthesis from D-glucose-6-phosphate plays an important role in maintaining myo-inositol intracellular concentration (Fisher et al., 2002).

3. Osmolyte transporters

3.1. Betaine/GABA transporter BGT-1

3.1.1. Cloning of BGT-1

Betaine, as a protective osmolyte has been shown in many plant, animal and bacterial species (Yancey et al., 1982; Le Rudulier and Bouillard, 1983; Perroud and Le Rudulier, 1985; Bagnasco et al., 1986; Yancey and Burg, 1990). *Escherichia coli* and *Salmonella typhimurium* utilize a high-affinity betaine transporter encoded by proU gene to accumulate betaine under hyperosmotic stress (Barron et al., 1987; Stirling et al., 1989). It has been recognized that large amounts of betaine is intracellularly accumulated in the kidney medulla (Bagnasco et al., 1986; Balaban and Burg, 1987; Garcia-Perez and Burg, 1991).

In studies on the accumulation of betaine and its transporter, Madin-Darby canine kidney (MDCK) cells have proved to be a valuable model system. A series of elegant experiments on MDCK cells have led to the cloning and characterization of the betaine/GABA transporter BGT-1 and subsequent elucidation of detailed mechanisms regarding the role of BGT-1 in osmoregulation in kidney cells. MDCK cells have shown to accumulate betaine when grown in hyperosmotic media (Nakanishi et al., 1988). Further studies revealed that the intracellular accumulation of betaine is due to increased Na^+-dependent uptake from the culture medium (Nakanishi et al., 1990). When MDCK cells were cultured at normal osmolarity in a defined betaine-free medium, no betaine was detected in the cells. After changing to a medium made hyperosmotic to 500 mosmol/kg H_2O by adding NaCl and containing 50 μM betaine, the level of intracellular betaine increased and lasted over

1 week. If the culture medium contained no betaine, the cells did not accumulate betaine even at the higher osmolarity. Additional kinetic analysis showed that under hyperosmotic media, the maximal velocity (Vmax) of Na^+-dependent betaine uptake increases with no apparent change in K_m, suggesting that extracellular hyperosmolarity induces an increase in the number of functional betaine transporter in the plasma membrane (Nakanishi et al., 1990). With the technological mature of heterologus expression in *Xenopus oocyte*, a variety of Na^+-dependent membrane transporters encoded by exogenous mRNA have been successfully expressed in *Xenopus oocyte* during the late 1980s (Hediger et al., 1987; Aoshima et al., 1988; Longoni et al., 1988; Sigel et al., 1988; Hagenbuch et al., 1990). Similarly, this technology was employed to express the mRNA from MDCK cells and assay the betaine uptake in *Xenopus oocyte* (Robey et al., 1991). The results are quite inspiring. Injection of mRNA from hyperosmotic MDCK cells into *Xenopus oocyte* induces significantly increased betaine uptake, compared to the mRNA from isosmotic MDCK cells. The greatest betaine uptake activity results from an mRNA fraction with a median size of approximately 2.8 kilobases. The above achievements pave the way for the successful cloning of the betaine/GABA transporter BGT-1 since neither the related sequence information nor the antibody to the transporter were available at that time.

Further efforts brought about the cloning of the betaine/GABA transporter cDNA from MDCK cells using the above mentioned heterologus expression in *Xenopus oocyte* to screen a cDNA library (Yamauchi et al., 1992). Interestingly, the cloned transporter is capable of utilizing both betaine and GABA, a principle

inhibitory neurotransmitter, as substrates; hence named BGT-1. It is worth to note that the first GABA transport GAT-1 has been previously cloned from rat brain (Guastella et al., 1990). The deduced amino acid sequence of BGT-1 exhibits highly significant sequence and topographic similarity to the rat brain GAT-1, suggesting that the kidney BGT-1 and brain GAT-1 are members of the same transporter gene family. Shortly after its identification in MDCK cells, BGT-1 was also cloned from the mouse brain (originally named mouse GAT-2) (Lopez-Corcuera et al., 1992), and subsequently from human kidney (Rasola et al., 1995), human brain (Borden et al., 1995b), rat liver (Burnham et al., 1996) and rabbit renal papilla cells (Ferraris et al., 1996).

3.1.2. Molecular structure of BGT-1

The entire BGT-1 gene from MDCK cells has been cloned and analyzed. It extends over 28 kilobases and consists of 18 exons. Three alternative first exons in the 5' end of the gene, together with alternative splicing, produces a complex mixture of mRNAs. Eight kinds of BGT-1 mRNA (classified into three types according to the 5' end sequence) have been identified. They diverge in their 5'-untranslated region and have the identical open reading frame. Each type of mRNA is expressed in a tissue - specific manner. Type A is found only in kidney medulla, while type B is present in brain, liver, kidney cortex and medulla, type C in brain, kidney cortex and medulla. Use of Northern blot analysis reveals that hyperosmolarity induces all three type mRNAs in MDCK cells. Primer extension and/or RNase protection assays as well as transfection assays into MDCK cells

demonstrate that the three alternative first exons each have an independent transcription initiation site controlled under an independent promoter (Takenaka et al., 1995).

The deduced amino acid sequence of canine BGT-1 reveals a single protein of 614 amino acids with 12 putative membrane-spanning domains. In addition, it contains several potential phosphorylation sites for protein kinase A and C, and two potential glycosylation sites, suggesting possible posttranslational regulation. Both N- and C-terminal domains containing potential phosphorylation sites are predicted to be located at the intracellular side of the transporter (Yamauchi et al., 1992).

The transporter BGT-1 cloned from human brain displays 91% amino acid identity with canine BGT-1 (Borden et al., 1995b), and the mouse brain BGT-1 (originally named mouse GAT-2) displays 88% amino acid identity with canine BGT-1 (Lopez-Corcuera et al., 1992). All of these share the similar hydropathy plot with a single protein of 614 amino acids. Despite their high overall amino acid identities, alignment of BGT-1 sequences from the human brain, mouse brain and MDCK cell reveals the differences in the number and location of potential phosphorylation sites (Borden et al., 1995b).

3.1.3. Distribution of BGT-1

The canine BGT-1 is present on the basolateral surface of MDCK cells (Yamauchi et al., 1991). Use of Northern Blot and *in situ* hybridization reveals a widespread distribution of BGT-1 mRNA that does not closely match the GABAergic pathways in the human and mouse brain, suggesting that BGT-1 might

not play a role in terminating the action of GABA at the synapse (Borden et al., 1995b).

Pietrini et al. utilized monolayer cultures of MDCK cells as a model system for the study of membrane protein sorting in neurons and found that BGT-1 was localized to the basolateral membrane, suggesting a dendritic localization in neurons (Pietrini et al., 1994).

3.1.4. Functional characterization of BGT-1

BGT-1 is capable of utilizing both GABA and betaine as substrates. Betaine and GABA transport are both Na^+- and Cl^--dependent. A coupling ratio of Na^+/Cl^- /organic substrate of 3:1:1 or 3:2:1 has been proposed (Matskevitch et al., 1999). Thus, BGT-1 can accumulate betaine inside the cell using the electrochemical gradient of sodium and chloride across the plasma membrane. Transport assay in oocytes expressing the canine BGT-1 reveals that the K_m for betaine is 398 μM and for GABA is 93 μM, suggesting that BGT-1 has a higher affinity for GABA than betaine. However, in view of the fact that the concentrations of betaine in plasma (~ 180 μM) far exceed those of GABA (< 1 μM), only betaine is accumulated to significant levels in the renal medulla (Yamauchi et al., 1992). It should be pointed out that BGT-1 is a weak transporter of GABA in comparison to other GABA transporters, given that the K_m of GAT-1 for GABA is 7 μM and K_m of GAT-3 for GABA is 0.8 μM (Guastella et al., 1990; Liu et al., 1993).

Pharmacological investigations indicate that nipecotic acid and β-alanine are weak inhibitors for both betaine and GABA uptake by BGT-1 (IC_{50} value ≥ 2 mM), as examined in the expressed oocytes (Yamauchi et al., 1992). NNC 05-2090 appears as a selective inhibitor of BGT-1 in inhibiting GABA uptake, showing at least 10 fold selectivity over GAT-1, GAT-2 and GAT-3 (Thomsen et al., 1997).

It is worth to note that Amino acid system transporter A might be able to transport betaine into cells when responding to hyperosmolarity (Petronini et al., 1994).

3.1.5. Transcriptional regulation of BGT-1 upon hyperosmolarity

Further investigations reveal that hyperosmolarity stimulates the transcription of BGT-1, leading to increased abundance of BGT-1 mRNA, increased transport activity of BGT-1 and subsequent accumulation of betaine in MDCK cells. When MDCK cells grown in isoosmotic medium are transferred to hyperosmotic culture medium, BGT-1 mRNA abundance has been shown to increase by both Northern Blot and ribonuclease protection assay (Yamauchi et al., 1992; Uchida et al., 1993). Transcription of the BGT-1 gene in response to hyperosmolarity, as examined by nuclear run-on assay, begins to rise within a few hours and reaches a peak at approximately 16 hours. The time course and magnitude of BGT-1 mRNA level closely follow those of BGT-1 transcription and precede the changes in BGT-1 transport activity by about 3-4 hours (Uchida et al., 1993). These results strongly indicate that the increase in transport activity of BGT-1 results from a

hyperosmolarity-induced increase in the transcription of BGT-1 gene and the resulting increase in BGT-1 synthesis.

3.1.5.1. Tonicity-responsive enhancer (TonE)

Following the cloning of the entire BGT-1 gene from MDCK cells, a regulatory sequence element termed tonicity-responsive enhancer (TonE) has been identified in the promoter region of the BGT-1 gene. Detailed studies confirm that TonE mediates the transcriptional stimulation in response to hyperosmolarity. This is accomplished by transfection of luciferase reporter gene constructs containing various DNA fragments of the 5'- flanking region of the BGT-1 into MDCK cells, followed by luciferase assay under isoosmotic or hyperosmotic environment. Further studies by electrophoretic mobility shift assay (EMSA) expressing mutants of TonE reveal that TonE contains a sequence of TGGAAAAGTCCAG and spans between 62 and 50 nucleotides upstream of the first exon of the BGT-1 gene. TonE acts in an orientation-independent manner and concatenation increases its function dramatically (Takenaka et al., 1994).

The function of TonE as an osmotic enhancer of transcription has also been demonstrated *in vivo*. Transgenic mice harboring 2.4 kb of the 5'-flanking region of the canine BGT-1 gene (including TonE) fused to the chloramphenicol acetyltransferase (CAT) reporter gene in their genome show increased expression of CAT in the renal medulla under systemic hyperosmotic conditions (Kaneko et al., 1997).

3.1.5.2. Transcription factor TonEBP

Using yeast one-hybrid screening and affinity chromatography purification, the transcription factor TonEBP (TonE binding protein) has been identified (Miyakawa et al., 1999; Ko et al., 2000). The DNA binding domain of TonEBP shares a 45% identity with those of the NFAT family of transcription factors; TonEBP is thus also known as NFAT5 (Lopez-Rodriguez et al., 1999). The TonEBP sequence that is C-terminal to the DNA binding domain contains many glutamine residues (18% of amino acids are glutamines). A truncated TonEBP without this glutamine-rich region acts as a dominant negative TonEBP, suggesting that this region mediates transcription activation (Miyakawa et al., 1999). TonBEP exists as a dimer, and dimerization is required for DNA binding and transcriptional activity (Lopez-Rodriguez et al., 2001). The resolved crystal structure of TonEBP-DNA complex reveals that TonEBP binds to TonE target through base-specific contacts as well as DNA encirclement (Stroud et al., 2002).

In response to increased osmolarity, TonEBP undergoes different levels of regulation. Within 30 minutes of exposure to hyperosmolarity, TonEBP becomes phosphorylated and translocates into the nucleus (Miyakawa et al., 1999; Ko et al., 2000; Dahl et al., 2001). Several hours later, the levels of TonEBP mRNA and protein as well as TonEBP activity, as measured by EMSA, increase significantly (Miyakawa et al., 1998; Miyakawa et al., 1999; Ko et al., 2000). In addition, it has been shown that hyperosmotic activation of TonEBP associates with phosphorylation of its transactivation domain (Ferraris et al., 2002b).

TonEBP is widely expressed in human tissues, the highest levels being in the renal medulla, brain and heart (Handler and Kwon, 2001). Under isoosmotic conditions, TonEBP is roughly equally distributed between cytoplasm and nucleus in MDCK cells (Woo et al., 2000a; Woo et al., 2000b; Dahl et al., 2001). In contrast, TonEBP is located primarily within the nuclei of neurons and glials in normal isoosmotic rat. Following acute systemic hyperosmotic induction, rapid and strong overexpression of TonEBP in neuronal nuclei and slight overexpression of TonEBP in glia nuclei are observed in the brain (Loyher et al., 2004).

3.1.5.3. Osmotic signaling pathway

The osmotic signaling pathway in yeast is well investigated. It includes both a two-component signal transducer and a Hog1 mitogen-activated protein kinase cascade. When yeast cells are exposed to hyperosmotic environment, the initial sensor Sln1p, a transmembrane protein containing cytoplasmic histidine kinase domain, initiates a multistep phosphorelay cascade that activates Hog1 kinase (Brewster et al., 1993; Han et al., 1994; Posas et al., 1996). Activated Hog1 directly participates in chromatin binding (Alepuz et al., 2001) and up-regulates the expression of a number of genes, including glycerol-3-phosphate dehydrogenase and glycerol-3-phosphatase isoform 2 (Posas et al., 2000; Rep et al., 2000). These two enzymes are required for the biosynthesis of glycerol, a dominant compatible osmolyte in yeast (Ohmiya et al., 1995; Pahlman et al., 2001).

In contrast, the osmotic signaling pathway in animal cells remains to be elucidated, although some kinase pathways are involved in TonEBP activation. To

date, the osmotic sensors have not been identified in mammalian cells. Studies have revealed that protein kinase A (PKA) activity is necessary for TonEBP-mediated osmotic response (Ferraris et al., 2002a). In addition to PKA, two other kinases, p38 and Fyn, both contribute to activation of TonEBP (Ko et al., 2002).

3.2. Taurine transporter (TauT)

Taurine transporter (TauT) cDNA has been cloned from numerous resources in mammalian species, e.g., MDCK cells (Uchida et al., 1992), mouse brain (Liu et al., 1992a), rat brain (Smith et al., 1992), human thyroid (Jhiang et al., 1993), human placenta (Ramamoorthy et al., 1994) and bovine endothelial cells (Qian et al., 2000). TauT consists of 590-655 amino acids, and has molecular weight of 65-74 KDa. Mammalian TauTs share more than 90% amino acid sequence identity; belong to the Na^+- and Cl^--dependent family. Hydropathy plots reveal that TauT has 12 transmembrane domains with the N-terminal and C-terminal both facing to the cytosolic side (Tappaz, 2004; Lambert, 2004).

Kinetic analysis suggests that TauT requires two Na^+ ions and one Cl^- ion to transport one taurine molecule across the plasma membrane. K_m of TauT for taurine is in the low μM range and uptake of taurine is inhibited by β-alanine and hypotaurine (Foos and Wu, 2002; Chen et al., 2004).

Exposure of cells to a hyperosmotic medium results in increased Vmax of TauT and/or increased abundance of TauT mRNA (Tappaz, 2004). This has been consistently shown in a wide variety of cells, including liver endothelial cells (Weik et al., 1998), intestinal Caco-2 cells (Satsu et al., 1999), MDCK cells (Uchida et al.,

1991; Uchida et al., 1992; Jones et al., 1995), astrocytes in primary cultures (Beetsch and Olson, 1996; Bitoun and Tappaz, 2000b) and brain capillary endothelial cells (Kang et al., 2002). Following acute salt-loading, a significant increase in the level of TauT mRNA has been detected in rat brain (Bitoun and Tappaz, 2000a).

Although the promoter region in TauT gene has been cloned and characterized (Han et al., 2000), no tonicity-responsive element has yet been identified for TauT. It has been shown that both PKA and PKC pathways are involved in the regulation of TauT activity (Tappaz, 2004).

3.3. Myo-inositol transporter

As BGT-1, myo-inositol transporter cDNA was originally cloned from MDCK cell. A single protein of 718 amino acids with 12 transmembrane domains is deduced from its cDNA. Myo-inositol transporter belongs to the Na^+-dependent transporter family, and is termed SMIT (sodium myo-inositol transporter) (Kwon et al., 1992). Transport of myo-inositol by SMIT is pH-dependent and requires two Na^+ ions for one myo-inositol molecule; phlorizin is a potent competitive inhibitor (Hager et al., 1995). Subsequently, human SMIT gene was cloned (Berry et al., 1995), and is a complex multiexon transcriptional unit subject to alternate splicing (Porcellati et al., 1998).

SMIT is widely distributed in the brain and present in both neural and non-neural cells (Inoue et al., 1996). Upregulation of SMIT in response to hyperosmolarity has been shown in numerous studies, including *in vitro* cell culture (Paredes et al., 1992; Yamauchi et al., 1993; Strange et al., 1994; Wiese et al., 1996;

Isaacks et al., 1997), and *in vivo* preparations (Ibsen and Strange, 1996; Bitoun and Tappaz, 2000a).

It has been shown that transcription of SMIT gene can be regulated by multiple tonicity-responsive enhancers scattered throughout the 5'-flanking region of the gene (Rim et al., 1998). Activation of PKC could lead to an inhibition of SMIT activity in human astrocytoma cells (Batty et al., 1993).

4. The GABAergic system in the central nervous system

4.1. Metabolism of GABA

GABA (γ-aminobutyric acid) was discovered in mammalian brain in 1950 by Awapara et al. (Awapara et al., 1950) and by Roberts and Frankel (Roberts and Frankel, 1950). In 1970's, GABA was identified as an inhibitory neurotransmitter in the adult mammalian brain (Roberts, 1976). GABA is widely distributed as GABAergic neuron and released at nearly 40% of brain synapses (Fonnum F, 1987; Sivilotti and Nistri, 1991). Lately, diverse functional role of GABA has been revealed. It acts as a neurotrophic factor (Barbin et al., 1993; Lauder et al., 1998), induces neural migration (Behar et al., 1994; Behar et al., 1996), and facilitates neurite extension (Behar et al., 1994; Owens and Kriegstein, 2002).

The metabolism of GABA in the brain is tightly linked to tricarboxylic acid (TCA) cycle in the mitochondria (Tillakaratne et al., 1995). Three enzymes, namely, glutamic acid decarboxylase (GAD, E.C. 4.1.1.15), GABA transaminase (GABA-T, E.C. 2.6.1.19) and succinic semialdehyde dehydrogenase (SSADH, E.C. 1.2.1.24) are responsible for GABA metabolism. Among them, GAD is a specific marker of GABAergic neurons. Two isoforms of GAD encoded by two distinct genes, GAD_{65} and GAD_{67}, are identified in GABAergic neurons. GAD_{65} is preferentially present near neuronal synaptic vesicles, where GAD_{67} is a soluble cytoplasmic protein (Soghomonian and Martin, 1998). GAD_{67} is responsible for the synthesis of >90% of GABA in the brain (Watanabe et al., 2002).

In mature brain, GABA is primarily produced through the decarboxylation of glutamic acid catalyzed by GAD. GAD is the rate-limiting enzyme for GABA

synthesis and requires pyridoxal phosphate as a cofactor. This reaction from glutamic acid to GABA is essentially irreversible (Roberts and Kuriyama, 1968). Precursor glutamic acid is derived from α-ketoglutarate generated by the TCA cycle and from glutamine catalyzed by phosphate-activated glutaminase (PAG). GABA may also be synthesized by other alternative routes, involving deamination and decarboxylation reactions from putrescine, spermine, spermidine and ornithine, but these routes do not contribute significantly to the synthesis of GABA in the brain (Martin, 1993).

GABA catabolism is catalyzed by the mitochondrial enzyme GABA-T, which transfers the amino group from GABA to α-ketoglutarate, producing glutamate and succinic semialdehyde. The resulting succinic semialdehyde is rapidly converted by the mitochondria enzyme SSADH into succinate, which enters the TCA cycle. During this procedure, GABA-T serves as both a synthetic (production of glutamate) and degradative (degradation of GABA) enzyme. This particular dual role allows the conservation of the transmitter pool of GABA. The metabolism of GABA is often called the “GABA shunt”, because it bypasses the TCA cycle (Tillakaratne et al., 1995).

GABA is synthesized exclusively by GABAergic neurons in the brain. In contrast, GABA-T and SSADH, the two enzymes required for GABA catabolism, are also present in non-GABAergic neurons, e.g., astrocytes. Glial cells are responsible for the degradation of GABA that is not recaptured by the GABAergic terminal (Martin, 1993). In glial cells, the glutamate formed from the GABA degradation is converted into glutamine, which is catalyzed by the cytosolic enzyme

glutamine synthetase (GS). The resulting glutamine is exported to neurons and converted to glutamate by the mitochondrial enzyme PAG. Therefore, glial glutamine is an important precursor for both neuronal glutamate and GABA (Farrant, 2002). For a summary of GABA metabolism in the context of a GABAergic synapse, refer to Figure 2.

4.2. Function of released GABA

Once released from GABAergic axon terminal, GABA molecules act on GABA receptors. To date, three types of GABA receptors have been identified: $GABA_A$, $GABA_B$ and $GABA_C$. The $GABA_A$ and $GABA_C$ receptors belong to the ligand-gated Cl^- channel superfamily and mediate the fast inhibitory action of GABA. $GABA_A$ receptor is widely distributed in the brain and located at postsynaptic membrane. In contrast, $GABA_C$ receptor is expressed predominantly in the retina. Structurally, $GABA_A$ and $GABA_C$ receptors are both pentameric heterooligomer. Drugs such as benzodiazepines and barbiturates enhance $GABA_A$ receptor-mediated inhibition, and they are clinically important anticonvulsant (Chebib and Johnston, 2000; Watanabe et al., 2002; Farrant, 2002).

$GABA_B$ receptor is a GTP-binding protein-coupled receptor, and thus differs from the $GABA_A$ and $GABA_C$ receptor pharmacologically as well as electrophysiologically. Two main $GABA_B$ receptor subunits encoded by distinct genes have been identified, named $GABA_BR1$ and $GABA_BR2$ (Isomoto et al., 1998; Kaupmann et al., 1998). The native structure of $GABA_B$ receptor may be a heterodimer of $GABA_BR1$ and $GABA_BR2$ through an interaction between the coiled

regions of their intracellular C-termini (Kuner et al., 1999; Marshall et al., 1999). $GABA_B$ receptor is present at postsynaptic membrane of inhibitory synapse, as well as both excitatory and inhibitory axon terminals. Activation of postsynaptic $GABA_B$ receptors results in the activation of K^+ channels and subsequent hyperpolarization of the postsynaptic membrane. On the other hand, activation of presynaptic $GABA_B$ receptors leads to the inhibition of neurotransmitter release from presynaptic terminals. This inhibition attributes to the blocking of presynaptic voltage-gated Ca^{2+} channels (Bowery and Enna, 2000; Watanabe et al., 2002).

$GABA_B$ receptor plays an important role in modulation of neurotransmitter release. Baclofen, a selective agonist of $GABA_B$ receptor, decreases neurotransmitter release in the brain (Bowery et al., 1980). Baclofen has been shown to suppress epileptiform electrical activity in the hippocampus (Swartzwelder et al., 1986). Presynaptically, $GABA_B$ autoreceptor controls the release of GABA, while $GABA_B$ heteroreceptor regulates the release of glutamate, dopamine, noradrenalin, 5-hydroxytryptamine and somatostain (Watanabe et al., 2002).

In addition to acting on GABA receptors, GABA released from the presynaptic axon terminals, is largely removed by uptake into both glial cells and GABAergic neurons through high-affinity GABA transporters. Once recovered into glial cells or GABAergic neurons, GABA undergoes catabolism as described above. Vigabatrin, an irreversible inhibitor of GABA-T, can increase the levels of brain GABA and has been used clinically as an anticonvulsant (Farrant, 2002).

4.3. Plasma membrane GABA transporters

In the 1960s, studies have revealed the existence of specific plasma membrane transport proteins for GABA in the mammalian brain (Varon et al., 1964; Iversen and Neal, 1968; Iversen and Neal, 1969). In the year 1990, cloning and expression of the first GABA transporter (GAT-1) from rat brain is the starting point for the characterization of related plasma membrane GABA transporters (Guastella et al., 1990). To date, four plasma membrane GABA transporters, termed GAT-1, GAT-2, GAT-3, and BGT-1 have been cloned and identified according to their differential amino acid sequences and pharmacological properties. They show approximately 50% amino acid sequence similarity, and belong to the family of Na^+- and Cl^--dependent neurotransmitter transporters with 12 putative transmembrane spanning domains. Both fairly large N- and C-terminal domains containing potential phosphorylation sites are situated at the cytoplasmic side (Masson et al., 1999; Soudijn and Van Wijngaarden, 2000).

The plasma membrane GABA transporters mediate high-affinity GABA uptake into presynaptic axon terminals and glial processes, thereby regulating the magnitude and duration of GABA synaptic action (Isaacson et al., 1993; Mager et al., 1993). Additional function of GABA transporters is that by removing GABA, they allow it to be reused, either directly or indirectly (Borden, 1996). The plasma membrane GABA transporters may also release GABA into the extracellular space in a Ca^{2+}-independent, non-vesicular manner (Pin and Bockaert, 1989; Attwell et al., 1993). This can occur in ischemia or seizures, due to the changes in the transmembrane sodium or voltage gradient. The reversal functioning of GABA

transporters could exert a protective effect during seizures, by reducing electrical excitability (Phillis et al., 1994; Borden, 1996).

It is worth to note that there exist specific vesicular membrane GABA transports, which carry GABA molecules into synaptic vesicles. Two vesicular membrane GABA transporters have been identified in the brain, named VGAT and VIAAT (McIntire et al., 1997; Sagne et al., 1997).

The followings give a detailed characterization of plasma membrane GABA transporters, GAT-1, GAT-2 and GAT-3. For BGT-1, refer to the above descriptions.

4.3.1. GAT-1

The pioneering work of cloning and identification of the first neurotransmitter transporter, GAT-1, was accomplished by Kanner and colleagues through an international collaboration. A GABA transporter from rat brain was first purified to homogeneity and microsequenced. Oligonucleotide probes designed according to the corresponding amino acid sequence were then used for screening a rat brain cDNA library. The isolated rat GAT-1 cDNA was subsequently expressed in *Xenopus oocytes* to examine its functional properties. The rat GAT-1 cDNA predicts a protein of 599 amino acids with a molecular weight of 67 kDa. Hydropathy analysis reveals that GAT-1 is a single protein of 12 transmembrane domains, with three potential glycosylation sites on the putative extracellular loop between transmembrane domain 3 and 4. Pharmacological studies indicate that uptake of GABA by GAT-1 is more sensitive to ACHC and L-DABA than to β-alanine, a feature traditionally known as the neuronal GABA transporter (Radian et al., 1986; Guastella et al.,

1990). GAT-1 has also been cloned from human (Nelson et al., 1990) and mouse brains (Liu et al., 1992b), exhibiting 97% and 99% sequence identity with rat GAT-1 respectively. Electrophysiological studies on GAT-1 in diverse expression systems, including synaptosomes, *Xenopus oocytes* and mammalian cells, show the cotransport of one GABA molecule with two Na^+ and one Cl^- (Keynan et al., 1992; Mager et al., 1993; Mager et al., 1996; Risso et al., 1996).

In contrast to BGT-1, GAT-1 is expressed exclusively in the central nervous system (Gadea and Lopez-Colome, 2001). Use of radiolabelled oligonucleotide probes and in situ hybridization histochemistry reveals that GAT-1 mRNA is widely spread in the brain, including retina, olfactory bulb, neocortex, ventral pallidum, hippocampus and cerebellum. Overall, the distribution of GAT-1 mRNA in the brain matches closely with that of GABAergic neurons, as examined by the localization of GABA or GAD. However, in cerebellum, GABAergic Purkinje cells do not express GAT-1 mRNA, whilst Bergmann glia cells express high levels of GAT-1 mRNA (Rattray and Priestley, 1993; Durkin et al., 1995; Borden, 1996). Immunohistochemical studies using antibodies to GAT-1 have consistently shown that GAT-1 is present in axon terminals of GABAergic neurons and also in astrocytic processes in rat brain (Radian et al., 1990; Minelli et al., 1995; Johnson et al., 1996; Ribak et al., 1996a; Ribak et al., 1996b). GAT-1 has been localized to non-pyramidal neurons in human and monkey cerebral cortex (Conti et al., 1998; Ong et al., 1998), but is also found in astrocytic processes in human and monkey cerebral cortex (Conti et al., 1998).

Various studies have demonstrated the alterations of GAT-1 expression in epilepsy. An increase in GAT-1 mRNA was detected bilaterally in the rat hippocampal CA subfields and dentate gyrus at 4 hour earlier after amygdala-kindled seizures (Hirao et al., 1998). The expression of GAT-1 protein increases bilaterally in the rat hippocampus at 5 to 15 days, and returns to normal levels by 30 days in focal epilepsy induced by amygdaloid ferric iron injection (Ueda and Willmore, 2000). In contrast, reductions in GAT-1 mRNA in various brain regions have been shown in genetically epileptic-prone rats following audiogenic stimulus (Akbar et al., 1998). A decreased GAT-1 expression is also found in the CA3 region of epilepsy patients with mesial temporal sclerosis (Mathern et al., 1999). During et al. have demonstrated the impaired function of GABA transporters in the human epileptic hippocampus (During et al., 1995).

GABA analogues, e.g., nipecotic acid and guvacine, have been studied as inhibitors for GAT-1. However, due to their poor penetration through the BBB, these inhibitors are of experimental interest only. Recently, a variety of potent and selective inhibitors of GAT-1 have been synthesized, with nipecotic acid or guvacine coupled to a lipophilic moiety, e.g., NNC-711, Tiagabine, SK&F 89976-A and Cl-966. These lipophilic inhibitors display anticonvulsant activity *in vivo*, probably due to the prolonged action of synaptically released GABA. Of these, Tiagabine has proved clinically useful in the treatment of epilepsy (Borden, 1996; Soudijn and van, I, 2000).

4.3.2. GAT-2

GAT-2 cDNA has been first isolated from a rat brain cDNA library by homologous screening. It has a predicted open reading frame of 1806 nucleotides encoding a protein of 602 amino acids. GAT-2 is also present in liver and kidney as examined by Northern blot and RT-PCR (Borden et al., 1992). Mouse GAT-2 (originally termed mouse GAT-3) has also been cloned, and it shares a 51% amino acid identity with mouse GAT-1. Mouse GAT-2 has a much lower affinity for GABA than mouse GAT-1 (Liu et al., 1993).

GAT-2 is present primarily in the leptomeninges, choroid plexus and ependyma of the rat brain (Ikegaki et al., 1994; Durkin et al., 1995; Conti et al., 1999). Within the rat retina, GAT-2 is localized to the retinal pigment epithelium layer, nerve fiber layer and ciliary body epithelium (Honda et al., 1995; Johnson et al., 1996).

A role for GAT-2 in regulating GABA levels in the cerebrospinal fluid has been proposed (Conti et al., 1999). Since mRNA levels of GAT-2 are more abundant in neonatal than in adult mouse brain, GAT-2 might play a role in mouse development (Liu et al., 1993; Gadea and Lopez-Colome, 2001).

4.3.3. GAT-3

GAT-3 is initially cloned from the rat brain using cDNA library homologous screening technology. Its cDNA has an open reading frame of 1881 nucleotides encoding a protein of 627 amino acids. GAT-3 predicts a single protein of 12 transmembrane domains with multiple putative glycosylation sites on the extracellular loop between transmembrane domain 3 and 4. GAT-3 displays a 52%

amino acid identity with GAT-1. Northern blot and RT-PCR analysis reveal that GAT-3 mRNA is restricted to the brain. Uptake of GABA by GAT-3 is more sensitive to β-alanine than to ACHC, guvacine and nipecotic acid, a property traditionally known as the glial GABA transporter (Borden et al., 1992). Subsequently, GAT-3 is cloned from human and mouse brain (originally termed mouse GAT-4) (Liu et al., 1993; Borden et al., 1994). Interestingly, GAT-3 possesses the highest affinity for GABA among the four plasma membrane GABA transporters isolated from mouse brain (Liu et al., 1993). A lipophilic inhibitor with selectivity for GAT-3, (S)-SNAP-5114 has been developed. Due to its ability to effectively cross the BBB, it may serve as an important tool for evaluating the functional role of GAT-3 in the brain (Borden et al., 1994).

GAT-3 mRNA is widely expressed in the brain, as examined by radiolabelled oligonucleotide probes and *in situ* hybridization histochemistry (Durkin et al., 1995). Immunocytochemical studies reveal that GAT-3 is localized to astrocytic processes in the monkey and rat brain (Minelli et al., 1996; Ribak et al., 1996b; Ng et al., 2000). It is also found in a population of oligodendrocyte-like cells in the rat spinal trigeminal nucleus (Ng and Ong, 2001).

Changes in GAT-3 expression in epilepsy have been shown. GAT-3 mRNA increases bilaterally in the amygdalar nuclei and in the contralateral pyriform cortex and cerebral cortex at 1 hour earlier after amygdala-kindled seizures in the rat (Hirao et al., 1998). The protein levels of GAT-3 in the rat hippocampus undergo upregulation following focal epilepsy induced by amygdaloid ferric iron injection (Ueda and Willmore, 2000). An increase in GAT-3 protein expression has been

demonstrated in the hilus and Ammon's horn in patients with temporal lobe epilepsy (Mathern et al., 1999).

5. Excitotoxic brain injury

5.1. Experimental models of excitotoxcity - Kainate injections

Kainic acid (KA) [2-carboxy-4(1-methyl-ethenyl)-3-pirrolidinacetic acid] is a structural analog of the excitatory amino acid, glutamate that binds to and activates ionotropic, non-NMDA glutamate receptors (Honore et al., 1987; Kaczmarek et al., 1997). It is 30- to 100-fold more potent than glutamate as a neuronal excitant. Systemic and intracerebral administrations of KA into adult rats induce persistent seizures and seizure-mediated brain damage syndrome (Nadler et al., 1978; Coyle, 1983; Sperk, 1994). Within 1 hour after KA injection into the rats, the neuronal circuitry of the hippocampus are activated, and later the animals develop symptoms of robust and recurrent seizures, such as vibrissa tremor, distended eye, upper body tremor, rigidity of the limbs and foaming at the mouth. Pyramidal neurons in the CA1 and CA3 fields of the hippocampus begin to degenerate at 3-4 days post KA injection (Nadler et al., 1986; Ben Ari and Cossart, 2000). KA treated rats have been widely used as a model for studying human temporal lobe epilepsy (Nadler, 1981; Ben Ari, 1985; Sutula, 1990; Sloviter, 1996).

After intraventricular or intracerebral administration, KA produces selective degenerations of neurons, especially in striatal and hippocampal areas of the brain. Axons and nerve terminals are more resistant to the destructive effects of KA than the cell soma (Coyle, 1983; Lerma, 1997). Intraventricular KA injections cause

neuronal death of the affected CA subfields in the hippocampus (Nadler et al., 1978; Malhotra et al., 1990; Ong et al., 1996). In this case, the CA3 subfield ipsilateral to the injection suffers the greatest cellular damage, whilst the neurons in CA1 subfield often survive the KA insult (Nadler et al., 1978; Nadler et al., 1980; Schwob et al., 1980). Also, injections of KA into amygdaloid complex of rats result in pronounced cell death in CA3 subfield (Ben Ari et al., 1980; Pollard et al., 1994a; Pollard et al., 1994b). Aside from neurodegeneration, one of the prominent findings in intraventricular KA injection is the glia reaction in the lesioned area. It is characterized by proliferation and hypertrophy of glial cells in the glial scar (Malhotra et al., 1990; Jorgensen et al., 1993; Ong et al., 1996).

In addition, administration of KA into the ventral globus pallidus (basal forebrain region) of rats produces neurodegeneration of cholinergic neurons, a pattern similar to nerve cells loss in Alzheimer's disease (Johnston et al., 1979). The neuronal excitation caused by KA results in the upregulation of a variety of genes in the hippocampus. These include immediate-early genes, cytokines and membrane transporters (Minami et al., 1991; Simantov et al., 1999; Zagulska-Szymczak et al., 2001).

5.2. Osmotic stress in excitotoxcity

Following KA injections, macroscopic inspection reveals the volume change in the affected brain region. Brains obtained from rats sacrificed shortly after KA systemic administration show an increase in the volume of hemisphere. The temporal lobe shows incisures and appears to be swollen (Sperk, 1994). In rats that

received intraventricular KA injection, the hippocampus, especially ipsilateral to the injection, suffers pronounced shrinkage at late stage. Histopathological findings during the early stage after KA administration include shrinkage and pycnosis of neuronal perikarya and swelling of dendrites and astrocytes (Olney et al., 1979; Schwob et al., 1980; Murabe et al., 1982; Sperk et al., 1983).

Osmotic stress occurs in KA-induced neuronal injury. KA has been shown to produce focal swelling on the dendrites of hippocampal interneuron and primary cortical cultures (Hasbani et al., 1998; Al Noori and Swann, 2000). Upon neuronal excitation, massive influx of ions, particularly Na^+, Cl^- and Ca^{2+}, leads water to flow into neurons and glial cells, and thus cause cellular swelling (Rothman, 1985; Olney et al., 1986; Choi, 1987; Meyer, 1989). A large number of voltage/ligand- gated ion channels, pumps (e.g. Na^+, K^+-ATPase), exchanges (e.g. H-Na exchange) and transporters (e.g. Na, K, 2Cl transporter) are involved in ion movement into or out of cells (Schwartzkroin et al., 1998). In the case of KA induced neuronal injury, the degenerated neurons also release its content into the extracellular space. As a result, dynamic changes in intracellular/extracellular osmolarity in neurons and glial cells occur during neurodegeneration. In fact, changes in osmolarity affect neuronal excitability (Andrew, 1991; Roper et al., 1992; Saly and Andrew, 1993; Huang et al., 1997).

The involvement of osmolyte transporter in KA induced neuronal injury has been reported. Use of Northern Blot and *in situ* hybridization detects the upregulation in the mRNA level of Na^+ / myo-inositol cotransporter in amygdala, hippocampus and neocortex after KA systemic injection (Nonaka et al., 1999). It is

worth to note that osmolytes including betaine, taurine and myo-inositol have been demonstrated to attenuate seizure activity in the rats (Freed, 1985; Ghoz and Freed, 1985; Williams and Jope, 1995; Patishi et al., 1996; El Idrissi et al., 2003).

6. Aims of experimental studies

Osmoregulation in the brain is critical for maintaining a constant milieu in the brain, since the skull is a rigid, non-expandable container, and changes in ion composition would affect excitability (Strange, 1992; Gullans and Verbalis, 1993; Law, 1994a; Lang et al., 1998). The osmolyte transporters might play a key role in osmoregulation in the brain. The expression of taurine transporter (TauT), myo-inositol transporter (SMIT), and betaine / GABA transporter (BGT-1) mRNA levels, for instance, were increased in the brain following acute salt loading (Bitoun and Tappaz, 2000a). Of the three transporters, SMIT and BGT-1 mRNA were increased in all brain regions studied, i.e. the cerebral cortex, striatum and habenula (Bitoun and Tappaz, 2000a).

BGT-1 was first cloned from Madin-Darby canine kidney (MDCK) cells, and shown to transport both betaine and GABA (Yamauchi et al., 1992). Subsequently, it is cloned from the mouse brain (originally named mouse GAT-2) (Lopez-Corcuera et al., 1992), human kidney (Rasola et al., 1995), human brain (Borden et al., 1995b), rat liver (Burnham et al., 1996) and rabbit renal papilla cells (Ferraris et al., 1996). BGT-1 shares sequence similarity with the plasma membrane GABA transporters: GAT-1, GAT-2, GAT-3, and belongs to the family of Na^+- and Cl^--dependent neurotransmitter transporters with 12 putative transmembrane spanning domains (Borden, 1996; Masson et al., 1999; Soudijn and van, I, 2000).

The plasma membrane GABA transporters terminate the synaptic action of GABA. The expressions of GAT-1, GAT-2 and GAT-3 in the brain have been studied by immunocytochemistry. GAT-1 is present in axon terminals of GABAergic neurons and also in astrocytic processes in rat brain (Radian et al., 1990; Minelli et al., 1995; Johnson et al., 1996; Ribak et al., 1996a; Ribak et al., 1996b). GAT-1 is also found in non-pyramidal neurons in human and monkey cerebral cortex (Conti et al., 1998; Ong et al., 1998), and in astrocytic processes in human and monkey cerebral cortex (Conti et al., 1998). GAT-2 is present primarily in the leptomeninges, choroid plexus and ependyma in rat brain (Ikegaki et al., 1994; Durkin et al., 1995; Conti et al., 1999). GAT-3 is only found in glial cells, including astrocytes and a population of oligodendrocyte-like cells in the monkey and rat brains (Minelli et al., 1996; Ribak et al., 1996b; Ng et al., 2000; Ng and Ong, 2001).

In contrast, the distribution and function of BGT-1 in the brain have not been fully elucidated. An examination on the distribution of BGT-1 mRNA in human brain suggests that BGT-1 might not contribute to the removal of the synaptic GABA (Borden et al., 1995b). However, BGT-1 might contribute to osmoregulatory function in the brain, since betaine, which has been widely used as a non-perturbing osmolyte to compensate for hyperosmotic stress (Yancey et al., 1982; Burg, 1995), is a substrate for BGT-1.

The followings are the main aims of this present study.

6.1. Study of distribution and subcellular localization of betaine/GABA transporter BGT-1 in the monkey cerebral neocortex and hippocampus

BGT-1 mRNA has been detected by Northern blot and *in situ* hybridization in mouse, rat and human brain (Lopez-Corcuera et al., 1992; Borden et al., 1995b; Burnham et al., 1996). However, little is known about the distribution of BGT-1 in the brain, especially in primates, and at the ultrastructural level. This portion of the study was carried out, using immunocytochemistry and electron microscopy, to elucidate the distribution of BGT-1 in the monkey cerebral neocortex and hippocampus.

6.2. Study of changes in the expression of GABA transporters in the rat hippocampus after kainate induced neuronal injury

Intraventricular KA injections, a model of temporal lobe epilepsy, causes neuronal death of the affected CA subfields in the hippocampus, and proliferation and hypertrophy of glial cells in the glial scar (Nadler et al., 1978; Malhotra et al., 1990; Ong et al., 1996). To date, little is known about the effects on the expression of GABA transporters after this form of neuronal injury. Since changes in expression of GABA transporters / BGT-1 might result in alterations in levels of GABA / betaine in the extracellular space, with consequent effects on neuronal excitability or osmolarity, this portion of the study was carried out to explore the expression of GABA transporters including BGT-1 in the rat hippocampus, following KA-induced neuronal injury.

6.3. Study of differential effects of betaine and sucrose on BGT-1 expression and betaine transport in human U373MG astrocytoma cells and rat hippocampal astrocytes

In the above studies, BGT-1 immunoreactivity was observed in pyramidal neurons in the monkey and rat cerebral neocortex and the CA fields of hippocampus. BGT-1 expression decreased in neurons but increased in astrocytes after neuronal injury induced by KA. Numerous studies have revealed that osmotic overloading occurs following KA-induced neuronal injury (Rothman, 1985; Olney et al., 1986; Hasbani et al., 1998; Al Noori and Swann, 2000). High levels of betaine (100-300 mM) have been detected in single neurons isolated from the abdominal ganglion from *Aplysia californica* using the technique of NMR spectroscopy (Grant et al., 2000). In view of the known function of betaine as an osmolyte, one possible function of the upregulated BGT-1 might be to protect the astrocytes against increased osmotic stress. On the other hand, it might also be possible that excessive or prolonged BGT-1 expression might be a factor contributing to astrocytic swelling after brain injury. Till date, BGT-1 expression has been studied in astrocytes at the mRNA level (Bitoun and Tappaz, 2000b), but little is known about BGT-1 expression at the protein level, or whether increased BGT-1 is associated with increased betaine transport. It is also not known whether betaine could induce the expression of BGT-1. This portion of the study was therefore carried out, to elucidate the changes in BGT-1 expression at protein level and the accompanied betaine uptake activity *in vitro*, as well as the changes in BGT-1 expression at protein level *in vivo*, in astrocytes after hyperosmotic stress.

CHAPTER 2

MATERIALS AND METHODS

1. Animals

Six adult male or female monkeys (Macaca fascicularis) weighing 1.5-3.5 kg were used in this study, of which, two were used for Western Blot analysis and four were used for immunohistochemical analysis. A total of fifty-two adult male Wistar rats each weighing approximately 200-250 g was used in this study. Monkeys and rats are from Department of Anatomy of NUS, Laboratory Animals Center of NUS, respectively. All the rats received intracerebroventricular drug injection, among which, forty-eight rats were used for immunohistochemistry and the remaining four were used for Western blot analysis.

Prior to surgery or perfusion, all monkeys were deeply anaesthetized with an intraperitoneal injection of Nembutal (30 mg/kg), and all rats were deeply anaesthetized by an intraperitoneal injection of 1.2 ml of 7% chloral hydrate administered in the lower abdomen. Animals were required and cared for in accordance with guidelines published in the NIH Guide for the Care and Use of Laboratory Animals. All procedures involving animals were approved by the Medical Faculty Ethics Committee, National University of Singapore.

2. Drug intracerebroventricular injection

2.1. Kainate injection

Adult male Wistar rats were injected with kainate (Tocris, Bristol, UK). They were anaesthetized with an intraperitoneal injection of 1.2 ml 7% chloral hydrate, and the cranial vault exposed. KA (1 μl of a 1 mg/ml solution in saline) was injected into the right lateral ventricle (coordinates: 1.0 mm caudal to bregma, 1.5 mm lateral

to the mid-line, 4.5 mm from the surface of the cortex) using a Hamilton syringe (Hamilton, Reno, USA). The needle was withdrawn 10 min later, and the scalp sutured. This resulted in seizures after the rats had recovered from the anaesthesia. The experimental controls received an intracerebroventricular injection of 1 μl of normal saline. These rats were sacrificed at 3 days, 1 week, and 3 weeks after injection (four kainate injected and four saline injected rats at each time point) for perfusion.

2.2. Kainate and betaine injection

Rats firstly received kainate injection via right lateral cerebral ventricle, as descried above. At 1 day postinjection, experimental rats were injected intracerebroventricularly in the right ventricle with a solution of 10 μl of 100 mM betaine (Sigma-Aldrich, St Louis, USA, dissolved in normal saline) and control rats were injected intracerebroventricularly with saline. These rats were sacrificed on the third day post-kainate injection for perfusion.

3. Western immunoblot analysis

3.1. Solutions

Homogenization buffer: 0.32 M sucrose, 4 mM Tris-Cl, pH 7.4, 1 mM EDTA and 0.25 mM DTT

Ringer's solution:

NaCl: 85g

KCl: 2.5g

$CaCl_2$: 3g

$NaHCO_3$: 2g

Topped up with distilled water to 10 liters, without pH adjustment

Reagents and solutions for acrylamide gel

Solutions for preparing 10% separating gel for Tris-glycine SDS-Polyacrylamide Gel Electrophoresis (10 ml)

30% acrylamide mix	2.5 ml
1.5 M Tris-HCl (pH 8.8)	2.5 ml
H_2O	4.8 ml
10% SDS	0.2 ml
10% ammonium persulfate	35 µl
TEMED	7.5 µl

Solutions for preparing 5% stacking gel for Tris-glycine SDS-Polyacrylamide Gel Electrophoresis (5ml)

30% acrylamide mix	0.85 ml
1.0 M Tris-HCl (pH 6.8)	1.28 ml
H_2O	2.78 ml
10% SDS	51.23 µl
10% ammonium persulfate	25 µl
TEMED	5 µl

Running buffer: SDS/Glycine electrophoresis buffer

Tris base	3.02 g/L
Glycine	14.4 g/L
SDS	1 g/L

Transfer buffer:

(25 mM) Tris	3.03 g
(192 mM) Glycine	14.4 g
20% Methanol	200 ml

Topped up with distilled water to1 liter, without pH adjustment

TBS solution (pH 7.6)

Tris	2.42 g/L
NaCl	8 g/L

Washing buffer: 0.01% TTBS

TBS	1 L
Tween 20	0.1 ml

Blocking buffer: 5% BSA in washing buffer

BSA	5 g
Washing buffer	100 ml

3.2. Protein extraction

Animals were first deeply anaesthetized and the brains removed. Blocks consisting of the liver and hippocampus were removed and homogenized in 10 volumes of ice-cold homogenization buffer. After centrifugation at 1000g for 15 min, the supernatant was collected. Protein concentrations in the preparation were measured by the Bio-Rad protein assay kit using a spectrophotometer, as described below.

3.3. Measurement of protein concentration

Procedures:

(1) The dye reagent was prepared by diluting 1 part Dye Reagent Concentrate with 4 parts deionized water.

(2) Five dilutions of the BSA standard were prepared.

(3) 200 μl of diluted dye reagent was added to separate microtiter plate wells.

(4) 10 μl of each BSA standard, deionized water and sample solutions were pipetted into each well. Mix the sample and reagent thoroughly.

(5) Incubated at room temperature for 10 minutes, and measured absorbance at 595 nm using a microplate reader.

(6) The standard curve method was used to calculate the concentration of the sample.

3.4. Separation of proteins by running SDS-PAGE gel

Procedures:

(1) The protein concentration in each sample was measured and 2 parts of Laminal buffer (Bio-Rad, Hercules, USA) were added. Samples were heated at 95 °C in water bath for 4 minutes and cooled down to room temperature.

(2) Gel solution was poured into a gel sandwich using a Bio-Rad Minigel apparatus. Deionized water was added on the top of the gel to keep the gel surface flat. The gel was allowed to polymerize for 40 minutes. Subsequently, the stacking gel was poured into the gel sandwich. A comb was carefully inserted into the stacking gel and allowed to polymerize for 20 minutes.

(3) The gel sandwich was put into a Mini-protean electrophoresis chamber (Bio-Rad). A 300 ml of running buffer was added to cover the gel. Sample containing 70 μg protein and protein marker were loaded carefully into each well. The electrode plugs were attached to proper electrodes. Constant voltage was set at 140 V and the gel was run for 75 minutes.

3.5. Transferring protein from SDS-PAGE gel to polyvinylidine difluoride (PVDF) membrane

When the dye front migrated to 1 cm proximal to the bottom of gel, the power was turned off. The gel and two sheets of filter paper, which were of similar size to the gel, were immersed into the transfer buffer for 15-30 minutes. PVDF membrane was pre-wetted in methanol, followed by equilibrating in transfer buffer for at least 10 minutes. The blotting sandwich was assembled according to the instruction of

wet transfer method (Mini TransBlot, Bio-Rad). The proteins were transferred from gel to PVDF membrane at 200 mA constant current for 90 minutes.

3.6. Detection of protein using antibody

After transferring, the membrane was washed with distilled water and then soaked in blocking buffer on a rocking platform for 1 hour. The PVDF membrane was then incubated overnight in an affinity-purified rabbit polyclonal antibody to BGT-1 (Chemicon, Temecula, USA, diluted 4 μg/ml). After washing in washing buffer three times at 10 minutes each, the membrane was incubated with horseradish peroxidase conjugated goat anti-rabbit IgG (Amersham, Little Chalfont, UK) for 1 hour at room temperature. Following three washes at 10 minutes each, the reaction was developed with the supersignal west pico chemiluminescent substrate (Pierce, Rockford, USA). The membrane was incubated for 5 minutes at room temperature without agitation and put into a plastic wrap. In the dark room, a Hyperfilm (Amersham) was placed on top of the membrane and exposed for 30 sec to 1 minute. The film was then developed automatically in a Konica Medical Film Processor.

4. Histology

4.1. Perfusion

Fixatives:

4% paraformaldehyde (PF)

PF 40 g

0.1 M phosphate buffer (pH 7.4) 1000 ml

The pH was adjusted to 7.4 by adding 1N HCl solution.

The PF solution was prepared by heating paraformaldehyde powder in 0.1 M phosphate buffer (pH 7.4). It was subsequently cooled to the room temperature. For immunoperoxidase staining, glutaraldehyde (0.1%) was added into the PF solution before perfusion. However, the glutaraldehyde was omitted for tissues intended for double immunofluorescence staining.

Procedures:

A fully exposed heart was first made by the surgical removal of sternum and ribs. Perfusion was performed under gravity with the reservoirs containing the fixative and Ringer's solution fixed at a height of about 100 cm above the animal. Perfusion was carried out by an insertion of a cannula into the left ventricle, followed by slitting a portion of the right atrium. A Ringer's solution was used to flush the vascular system until the lungs and liver were cleared of blood. The fixative was then administered for at least 1 hour.

4.2. Tissue preparations

Preparation of gelatinized slides:

1.5% gelatin solution:

Gelatin: 1.5 g

Distilled water: 100 ml

Heat until dissolved. Cool and then add:

Chrome alum: 0.15 g

Procedures:

Slides were first dipped in the acid solution (400 ml of 98% sulfuric acid mixed with 1 tea spoon of potassium dichromate) for 2min, and then washed by running tap water for 10min. The slides were rinsed with distilled water and then baked in an oven at 80 °C overnight for drying. The following day, dried slides were dipped in the gelatin solution and then hung to dry with clips. Gelatinized slides were kept in an oven at 37 °C for mounting tissue sections for use in histological or immunohistochemical studies.

Preparation of vibratome sections:

The brains were bisected, and blocks including the left and right temporal cortex and hippocampus were removed and post-fixed in the same fixative overnight. Blocks containing the hippocampus were sectioned coronally at 100 μm thickness using a Vibratome and free-floating sections collected for immunostaining.

Preparation of frozen sections:

The brains were bisected, and blocks including the left and right temporal cortex and hippocampus were removed and post-fixed in the same fixative for additional 2 hours. The tissues were subsequently transferred to a 0.1 M phosphate buffer (pH7.4) containing 15% sucrose and kept overnight at 4 °C. The tissue samples were mounted on a metal chuck using Lipshaw M-1 embedding matrix (Pittsburgh, USA) and rapidly frozen by quenching in liquid nitrogen. Coronal sections of 30 μm thickness were cut using a cryostat (Leica CM 3050). The sections were subsequently collected for free-floating immunofluorescence staining.

4.3. Histochemistry

4.3.1. Nissl staining with cresyl fast violet (CFV)

0.25 % CFV stock solution:

Cresyl Fast Violet (GURR'S, UK) 0.25 g

Deionised water 100 ml

CFV staining solution:

One part of 0.25 % CFV stock solution

Two parts of 0.2 N acetic acid

Procedures:

Free floating sections of the hippocampus were mounted on gelatinized slide. After dry, they were immersed in CFV staining solution at 60 °C oven for 10 minutes, followed by differentiation in 70 % ethanol. The sections were dehydrated in an ascending series of ethanol and cleared with xylene before being coverslipped with Permount as a mountant.

4.3.2. Methyl green staining

0.25% methyl green Staining solution:

Methyl green (GURR'S, UK) 0.25 g

0.1 M acetate buffer (pH 4.8) 100 ml

Procedures:

Free floating sections of the hippocampus were mounted on gelatinized slide and air-dried. After a brief dip in 0.1M acetate buffer (pH 4.8), the sections were immersed in methyl green staining solution for approximately 30 seconds, followed by rinse in deionized water. The sections were then dehydrated in an ascending series of ethanol and cleared with xylene before being coverslipped with Permount as a mountant.

5. Immunohistochemistry

5.1. Immunoperoxidase staining

Antibodies:

Affinity-purified rabbit polyclonal antibodies to GABA transporter GAT-1, GAT-2, GAT-3 and BGT-1 were purchased from Chemicon (Chemicon). The antibody to GAT-1 was raised against amino acid residues 588-599 of rat GAT-1, and has been shown to detect a single band at 60 kDa in rat cortex (Ong et al., 1998). The antibody to GAT-2 was raised against the carboxyl terminus (amino acid residues 593-602) of GAT-2, and had been shown to have no cross-reactivity to the C-termini of other transmitter transporters. The antibody to GAT-3 was raised against the carboxyl terminus (amino acid residues 606-677) of GAT-3 and had been shown not to react with the C-termini of other transmitter transporters (Johnson et al., 1996). The antibody to BGT-1 was raised against the carboxyl terminus (amino acid residues 600-614) of BGT-1 and does not react with the C-termini of other neurotransmitter transporters. It has been characterized in U373 MG human astrocytoma cells (Ruiz-Tachiquin et al., 2002).

Procedures:

(1) Free-floating sections were washed for 3 hrs in phosphate-buffered saline (PBS) at 10 minutes intervals to remove traces of fixative.

0.1 M PBS (pH 7.4)

Di-sodium hydrogen phosphate heptahydrate 26.8 g

Sodium chloride 8.5 g

Distilled water 1000 ml

(2) The sections were incubated for 1 hour in a solution of 5% goat serum (Vector, Burlingame, USA) to block non-specific binding of the antibody.

(3) They were incubated overnight in an affinity- purified rabbit polyclonal antibody to BGT-1 (Chemicon, diluted 4 μg/ml in PBS).

(4) The sections were washed in three changes of PBS at 10 minutes each.

(5) The sections were incubated for 1 hour at room temperature in a 1:200 dilution of biotinylated goat anti-rabbit IgG (Vector). This was followed by three changes of PBS to remove unreacted secondary antibody.

(6) The sections were reacted for 1 hour at room temperature with an avidin-biotinylated horseradish peroxidase complex (Vector).

(7) This was followed by wash in two changes (10 minutes each) of PBS, followed by incubation for 10 minutes in 0.2% nickel chloride solution in 0.1 M Tris buffer (TBS, pH 7.6).

0.1 M TBS: (pH 7.6)

Tris base (Trihydroxymethylaminomethane) 6.0 g

Sodium chloride 8.5 g

Distilled water 1000 ml

(8) The reaction was visualised by treatment for 5 minutes in 0.05% 3, 3, diaminobenzidine tetrahydrochloride (DAB) solution in Tris buffer containing 0.05% hydrogen peroxide. The color reaction was stopped with several washes of Tris buffer, followed by PBS. Some of the sections were mounted on gelatine-coated glass slides, dehydrated, and lightly counterstained with methyl green before

coverslipping, while the remainders were processed for electron microscopy. Control sections were incubated with PBS or pre-immune rabbit serum instead of primary antibody. These showed absence of immunostaining.

5.2. Cell counts

The number of BGT-1 positive glial cells in field CA1/CA3 of the hippocampus and the fimbria were manually counted using a light microscope. The counts were conducted in a "blind" manner at 200X magnification with the help of a grid. An area totaling 200 x 300 μm in each section, and four sections from each rat, were analysed. The mean and standard error was then calculated for each group of rats, at each time interval after kainate injection, and the results subjected to statistical analysis.

5.3. Immunogold staining

Procedures:

(1) Sections intended for immunogold detection were washed in PBS (10 minutes x 6), and then washed in Buffer A for 1 hour (10 minutes x 6).

Buffer A:

Normal goat serum	1 ml
BSA	1 g
Sodium azide	0.1 g
Tween 20	0.1 ml
0.1 M PBS	100 ml pH 8.2

(2) Sections were incubated overnight with antibody to BGT-1 (Chemicon diluted 4 μg/ml in Buffer A) at room temperature with gentle shaking.

(3) After washing for 1 hour (5 minutes x 12) in Buffer A, the sections were reacted for 4 hours at room temperature with goat anti-rabbit IgG conjugated to 1 nm gold particles (British BioCell, Cardiff, UK, diluted 1:200).

(4) The sections were washed in Buffer A for 30 minutes and then in PBS for 30 minutes with gentle agitation to remove excess gold conjugate.

(5) They were fixed in 1% glutaraldehyde for 10 min to strengthen antibody binding to the tissue, and washed thoroughly in distilled water for 30 minutes while agitating to remove excess aldehyde and PBS.

(6) The sections were mounted on clean glass slides and the area surrounding the specimen was dried.

(7) The sections were immersed in fresh silver enhancement solution. The development was monitored using a microscope.

(8) The sections were washed thoroughly in distilled water to stop the reaction.

(9) Some of the sections were mounted on gelatinized slides, dehydrated, and coverslipped, while others were processed for electron microscopy. Control sections were incubated with PBS or preimmune rabbit serum instead of primary antibody. They showed absence of staining.

5.4. Double immunofluorescence labelling

Sections were processed for free-floating immunofluorescence staining. They were incubated in blocking solution composed of 5% goat serum (Vector) and 0.1% Triton X-100 for 1 hour, followed by incubation with rabbit polyclonal antibody to BGT-1 (Chemicon, diluted 4 μg/ml in PBS) and mouse monoclonal antibody to glial fibrillary acidic protein (GFAP) (Chemicon, diluted 1 μg/ml in PBS) overnight. The sections were then washed three times in PBS, and incubated for 1 hour at room temperature in 1:200 dilution of FITC-conjugated goat anti-mouse IgG, and Cy3-conjugated goat anti-rabbit IgG (Chemicon). The sections were mounted and examined using an Olympus FluoView FV500 confocal microscope. Control sections were incubated with PBS instead of primary antibodies. These showed absence of staining.

6. Electron microscopy

Procedures:

(1) Electron microscopy was carried out by subdissecting the immunoperoxidase or immunogold stained sections into smaller rectangular portions that included the cerebral neocortex, or the CA fields / dentate gyrus of the hippocampus. The blocks were osmicated for 1 hour in a solution consisting of:

1% osmium tetroxide (OsO_4)

PBS (pH 7.4)

(2) They were dehydrated in an ascending series of ethanol and acetone as follows:

PBS	5 minutes
25% ethanol	3 minutes
50% ethanol	5 minutes
75% ethanol	5 minutes
95% ethanol	5 minutes
100% ethanol	5 minutes
100% acetone	5 minutes x 2

(3) The tissue blocks were infiltrated as follows:

100% acetone:Araldite (1:1)	10 minutes at room temperature
100% acetone:Araldite (1:4)	20 minutes at room temperature
1st change of fresh Araldite	45 minutes at 40 °C in oven
2nd change of fresh Araldite	30 minutes at 50 °C in oven
3rd change of fresh Araldite	30 minutes at 55 °C in oven

(4) They were flat embedded in fresh Araldite between transparent sheets at 60 °C for 24 hours in an oven.

(5) Ultrathin sections were obtained from the first 5 μm of the sections, mounted on 150-meshed copper grids coated with 0.3% Formvar, and stained with lead citrate, which is prepared as follows:

0.3% Formvar solution:

Formvar	0.3 mg
Chloroform	100 ml

Lead citrate:

Lead nitrate	1.33 g
Sodium citrate	1.76 g
Distilled water	30 ml

The pH value of lead citrate was adjusted to 12 and the volume to 50 ml.

(6) They were viewed using a Philips EM208 or a Jeol 1010EX electron microscope.

7. Cell culture of human U373 MG astrocytoma

Human U373 MG astrocytoma cells were obtained from ECACC (European collection of cell cultures). The cells were cultured in 75 cm^2 culture flasks with medium containing Dulbecco's modified Eagle's medium (DMEM)/nutrient mixture F12 (Invitrogen, Carlsbad, USA) and 10% FCS (Hyclone, Logan, USA). Cells were grown as monolayers at 37 °C in 5% CO_2. When they had reached approximately 90% confluence, the cells were sub-cultured (1:3) after treatment with trypsin / EDTA (Invitrogen). U373 MG cells were plated in 24-well cell culture plates at a density of approximately 0.7 x 10^5 cells/ml, and were used when the cells had reached approximately 80% confluence. The cells were incubated with culture media containing 1 mM, 10 mM or 100 mM betaine or 1 mM, 10 mM or 100 mM sucrose for 12 hours. The osmolarities of sample betaine or sucrose solutions were measured using a vapor pressure osmometer (Wescor, Logan, USA), and were found to be 309 mmol/kg for control medium without addition of betaine or sucrose, 309, 323, and 421 mmol/kg for media containing 1 mM, 10 mM, and 100 mM betaine

respectively; and 309, 324, and 420 mmol/kg for media containing 1 mM, 10 mM, and 100 mM sucrose respectively, i.e. the osmolarities were the same for equal concentrations of betaine or sucrose.

8. Reverse transcription polymerase chain reaction (RT-PCR)

Procedures:

(1) Total RNA was extracted from human U373 MG astrocytoma cells using RNeasy Mini Kit (Qiagen, Valencia, USA) according to the manufacture's instructions. After washed with PBS, cells were directly immersed in 600 μl of Buffer RLT (provided with the kit, containing a highly denaturing guanidinium isothiocyanate which immediately inactivates RNase).

(2) Cells were scraped and passed through a 23-gauge needle for three times.

(3) The clear lysate was transferred to microtube and mixed well with 600 μl of 70% ethanol. The resulted mixture was applied to an RNeasy mini spin column, centrifuged for 15 seconds at 10,000g. During this step, the total RNA binds to the membrane.

(4) The bound RNA was washed with buffer RW1 and RPE sequentially.

(5) High-quality RNA was then eluted in 20 μl of RNase free water. RNA amount was determined spectrophotometrically.

(6) To further eliminate the residue genomic DNA, the extracted RNA was digested with TURBO DNase (Ambion, Austin, USA).

(7) Reverse transcription (RT) was performed using Enhanced Avian RT First Strand Synthesis Kit (Sigma, St. Louis, USA). First strand cDNA was synthesized in a 50 μl reaction mixture containing 2 μg RNA, reverse transcriptase, oligo dT_{23} and RNase inhibitor. This was carried out by incubation at 52 °C for 50 minutes.

(8)The synthesized cDNA was purified by equal mixture of phenol and CIA (chloroform: isoamyl alcohol, 24:1), followed by precipitation with absolute alcohol. After rinsed with 70% alcohol, cDNA was dissolved in 15 μl MilliQ water.

(9) PCR was performed on an Omn-E hybaid thermocycler using Taq DNA polymerase. The BGT-1 specific primers used were as follows: sense 5' -CAT CCT CAC CAT CGC CGT CAT-3', antisense 5'-ACG CAG ACG CTT CCT GAA AGG-3' (Borden et al., 1995a). 2 μl cDNA was amplified in 40 μl final volume containing PCR buffer, $MgCl_2$, 0.25 mM of each dNTP and 2U of Taq DNA polymerase. The following PCR cycling parameters were used: denaturation at 95 °C for 3 minute, 35 cycles with denaturation at 95 °C for 1 minute, annealing at 60 °C for 15 seconds and extension at 72 °C for 1 minute and 20 seconds, followed by one additional extension cycle at 72 °C for 15 minutes.

(10) The resulted PCR products were electrophoresized in 1.5% agarose gel, excised from the gel and eluted into 20 μl buffer using QIAquick Gel Extraction Kit (Qiagen).

(11) The PCR products were then cloned into plasmid vector using TOPO TA Cloning Kit (Invitrogen) according to the manufacture's instructions. The PCR

products were first incubated with TOPO vector at room temperature for 5 minutes. This was followed by chemical transformation into “One Shot” Competent Cells.

(12) The next day, white colonies on agar plates were picked and grown in SOC medium (2% tryptone, 0.5% yeast extract, 10 mM NaCl, 2.5 mM KCl, 10 mM $MgCl_2$, 10 mM $MgSO_4$, 20 mM glucose, 30 μg/ml kanamycin).

(13) After analyzed by PCR and EcoR I digestion, the extracted plasmids inserted with BGT-1 sequence were bidirectionally sequenced using ABI 7300 (Perkin-Elmer, Wellesley, USA) to verify its authenticity.

9. Cell immunofluorescence confocal microscopy

Human U373 MG cells were plated at equal density on polylysine-coated glass coverslips in 24-well plates. After attachment, cells were incubated with culture medium containing betaine or sucrose for 12 hours. Cells were then washed twice in PBS and fixed in 4% paraformaldehyde for 20 minutes at room temperature. Following washes in PBS, cells were incubated in blocking solution composed of 5% normal goat serum (Vector) and 0.1% Trition X-100 in PBS for 1 hour. Coverslips were then incubated overnight at 4 °C in an affinity-purified rabbit polyclonal antibody to BGT-1 (Chemicon, diluted 4 μg/ml in PBS). After three rinses with PBS, coverslips were incubated for 1 hour in a 1:200 Cy3-conjugaed goat anti-rabbit IgG (Chemicon). This was followed by three washes of PBS to remove the unreacted antibody. Coverslips were then reacted for 3 minutes at room temperature with DAPI solution (Molecular Probes, Eugene, USA). Coverslips were

mounted on glass slides and examined using an Olympus FluoView FV500 confocal microscopy. Images were obtained through the center of the cell by examining DAPI nuclear staining. Controls were incubated with PBS or preimmune rabbit serum instead of primary antibodies.

10. Cell-ELISA

Human U373 MG cells were plated at equal density in 24-well plates. After attachment, cells were incubated with culture medium containing betaine or sucrose for 12 hours. Cells were then washed twice in PBS and fixed in 4% paraformaldehyde in 50 mM phosphate buffer, pH 7.4, for 20 min at room temperature. The paraformaldehyde was removed and treated with 95% ethanol for 1 min, followed by air drying. After washed three times with PBS, cells were incubated with 3% H_2O_2 in PBS for 5 min to minimize endogenous peroxidase activity. Cells were incubated with blocking solution composed of 5% normal goat serum (Vector) and 0.1% Trition X-100 in PBS for 1 hour, and then incubated with primary antibodies against BGT-1 (Chemicon) overnight at 4 °C. Cells were washed four times with PBS, incubated with a 1:2000 anti-rabbit peroxidase-conjugated secondary antibody (Amersham Biosciences) for 1 hour at room temperature, and washed five times in PBS. Samples in each well were incubated with 250 μl of Enhanced K-Blue substrate (Neogen, Lexington, USA) for 10 min, after which the colored reaction end product was terminated with the Redstop solution (Neogen). The optical density of samples was determined at 650 nm. Control experiments with PBS were included to determine background value, which was subtracted from the

OD_{650} readings. In order to normalize the reaction to the number of cells in each well, cell quantification assay was performed. After the incubation with Enhanced K-Blue substrate, the cells were washed twice with PBS and twice with deionized water. After drying the wells for 5 min, 200 µl of crystal violet solution [0.04% crystal violet in 4% (v/v) ethanol] was added for 30 min at room temperature. Cells were washed four times with deionized water and 200 µl of 1% SDS solution was added and incubated on a shaker for 1 h at room temperature. The optical density was measured at 595 nm. The OD_{650} value of the ELISA reaction was normalized to the OD_{595} value obtained from the cell quantification assay to give the normalized value of the ELISA reaction. For each experiment four parallel samples were used.

11. [^{14}C] betaine uptake assay

Uptake assay was carried out using methods described previously (Ruiz-Tachiquin et al., 2002) with minor modifications. Human U373 MG cells were plated at equal density in 24-well plates. After attachment, cells were incubated with culture medium containing betaine or sucrose for 12 hours. The culture medium was washed twice with prewarmed HEPES-buffered Krebs (KH) medium (in mM: HEPES 20, NaCl 130, KCl 3.7, $CaCl_2$ 1.8, $MgSO_4$ 1.18, K_2HPO_4 1.8, glucose 11, pH 7.4) and then incubated in 500 µl KH medium containing 0.3 µCi [^{14}C] betaine (American Radiolabelled Chemicals, St., Louis, USA) for 30 minutes at 37 °C. The medium was removed by aspiration, and the monolayers were thoroughly washed with ice-cold KH buffer and solubilized with 0.5 ml 1% SDS. Aliquots of the

suspension were used for liquid scintillation counting by a liquid scintillation counter (Model LS 6800, Beckman-Coulter, Fullerton, USA). The protein content of each well was determined using BCA protein assay (Pierce), and the normalized count calculated by dividing the scintillation count by the protein concentration of each well. For each experiment four parallel samples were used.

12. Statistics

All data were expressed as mean ± SEM, and subjected to statistical analysis using one-way analysis of variance (ANOVA) followed by post hoc Bonferroni's test or Student's t-test when appropriate. P values < 0.05 were considered statistically significant, $P < 0.01$, very significant.

CHAPTER 3

RESULTS

1. Distribution and subcellular localization of betaine/GABA transporter in the monkey cerebral neocortex and hippocampus

1.1. Specificity of antibody

The affinity purified polyclonal antibody to BGT-1 detected a major band at approximately 60 kDa in homogenates of the monkey liver, a result consistent with the findings of Ruiz-Tachiquin et al. in human astrocytoma cells (Ruiz-Tachiquin et al., 2002), but two bands at 60 kDa and 65 kDa in homogenates from the monkey neocortex. The extracellular loops of BGT-1 between transmembrane domains 3 and 4 contain potential sites for N-glycosylation, and the higher molecular weight band is likely a glycosylated form of BGT-1 (Fig. 3).

1.2. Light microscopy

1.2.1. Cerebral neocortex

The cerebral cortex was, in general, lightly labelled for BGT-1. Light staining was observed in layers III (Fig. 4A), V and VI (Fig. 4B) of the cortex, whilst layer IV was almost unstained. Immunoreactivity was observed on cell bodies, particularly in the superficial portion of layer III (Fig. 4A). An apical dendrite could be discerned on most of the labelled cell bodies, and the later were therefore identified as pyramidal neurons (Fig. 4A, B). Large numbers of dendrites were also observed in the neuropil (Fig. 4A, B). Immunoreactivity was not observed in glial cells or mural cells in the walls of blood vessels.

1.2.2. Hippocampus

The hippocampus was more densely labelled for BGT-1 than the cortex. Moderately densely labelled pyramidal cell bodies, and many labelled dendrites were observed. The cell bodies and dendrites of CA1 neurons (Fig. 4C) were more distinctly labelled than those in CA3 (Fig. 4D). The stratum lucidum of CA3, containing the axons of dentate granule neurons, appeared mostly unlabelled (Fig. 4D). The cell bodies of dentate granule neurons were also very lightly labelled or unlabelled.

1.3. Electron microscopy

Immunoperoxidase labelling was observed in the cell bodies and dendrites of pyramidal neurons in the cortex and hippocampus. The labelled neurons contained nuclei with light heterochromatin clumps and cytoplasm with short cisternae of endoplasmic reticulum and features of pyramidal neurons (Feldman, 1984) (Fig. 5A). Neurons with dense heterochromatin clumps in the nucleus, and features of non-pyramidal neurons were unlabelled. Label was also absent from glial cells bodies, including astrocytes and oligodendrocyte-like cells, and astrocytic end feet around blood vessels. Large numbers of immunolabelled dendrites or dendritic spines were observed in the neuropil. The immunolabelled dendrites were of small diameter (less than 1 μm). In contrast, larger diameter dendritic shafts were unlabelled or poorly labelled. The immunolabelled dendritic spines formed asymmetrical synapses with unlabelled axon terminals, containing small round vesicles. Immunoperoxidase reaction product was observed in the cytosol of the dendrites, or the ‘extra-

perisynaptic' region of the cell membranes of the dendrites, i.e. regions away from the synaptic clefts or the perisynaptic area (Fig. 5B).

A similar pattern of staining was observed in the immunogold labelled sections. As in the immunoperoxidase stained sections, label was observed in the cytoplasm of cell bodies of pyramidal neurons (Fig. 6A), and in the cytosol or 'extra-perisynaptic' region of the cell membranes of small diameter dendrites or dendritic spines (Fig. 6B, C).

2. Changes in the expression of GABA transporters in the rat hippocampus after kainate induced neuronal injury

2.1. Western blot analysis

The affinity purified polyclonal antibody to BGT-1 detected a major band at approximately 60 kDa, a result consistent with the findings of Ruiz-Tachiquin et al. (Ruiz-Tachiquin et al., 2002), in the rat liver, but a 60 kDa and a 65 kDa band in both normal, and kainate-injected rat hippocampus. The extracellular loops of BGT-1 between transmembrane domains 3 and 4 contain potential sites for N-glycosylation, and the higher molecular weight band is most likely a glycosylated product of BGT-1 (Fig. 7).

2.2. Light microscopy

2.2.1. CA fields of normal or saline-injected rats

GAT-1 labelling was observed as a fine reticular network, around the unlabelled cell bodies in the CA fields (Fig. 8A). In contrast to GAT-1, very little or

no staining for GAT-2 was observed (Fig. 8B). GAT-3 labelling was observed in occasional glial cell bodies, but in a dense meshwork of fine processes in the neuropil (Fig. 8C). Light BGT-1 labelling was observed in cell bodies of pyramidal neurons and in the neuropil (Fig. 8D).

2.2.2. Three days after kainate injections

Loss of neurons was observed in Nissl stained sections mainly in field CA3 (Fig. 9A), but also in CA1 on the side ipsilateral to the kainate injection. Cell loss was also observed, but was less extensive, in the CA fields of the contralateral hippocampus. No obvious loss of neurons was observed in the dentate gyrus. A decrease in GAT-1 (Fig. 9B) and GAT-3 (Fig. 9C) staining was observed in the CA fields affected by the kainate injection, compared to that of saline-injected rats. No increase or decrease in immunostaining for GAT-2 was observed (data not shown). Loss of BGT-1 immunoreactivity was observed in cell bodies and dendrites of pyramidal neurons, but increased BGT-1 immunoreactivity was observed in a population of glial cells in the degenerating CA fields (Fig. 9D, 12). No change in GAT-1, GAT-3, or BGT-1 expression was observed in the dentate gyrus, compared to that in control rats.

2.2.3. One week after kainate injections

CA3 or CA1 fields affected by kainate showed a loss of neurons, but an increase in glial cell number in Nissl stained sections (Fig. 10A). As in the 3 day post-kainate injected rats, a decrease in GAT-1 (Fig. 10B) and GAT-3 (Fig. 10C) labelling, and

no change in GAT-2 labelling (data not shown) was observed in CA fields of kainate-injected rats. A further increase in BGT-1 immunoreactivity was observed in glial cells in the degenerating CA fields (Fig. 10D). ANOVA statistics showed a significant increase in the number of BGT-1 positive glial cells (Fig. 12). Labelling was observed on the cell bodies (Fig. 10D) and end-feet around blood vessels. Under electron microscopy, labelled cells exhibited morphological features of astrocytes and were doubled labelled for GFAP, an astrocytic marker (see below). No change in GAT-1, GAT-3, or BGT-1 expression was observed in the dentate gyrus, compared to that in control rats.

2.2.4. Three weeks after kainate injections

Very little GAT-1, GAT-2 and GAT-3 staining was observed in the lesioned CA fields at 3 weeks post-kainate injection (Fig. 11A). The density of BGT-1 staining (Fig. 11B) was also reduced, compared to the 1 week post-kainate injected rats, and the number of BGT-1 positive glial cells was significantly less than that at 1 week post-kainate injection (Fig. 11B), as further revealed by ANOVA statistics (Fig. 12). No change in GAT-1, GAT-3, or BGT-1 expression was observed in the dentate gyrus.

2.3. Electron microscopy

Electron microscopy showed that BGT-1 positive glial cells in the lesioned CA fields had large cell bodies with irregular cell outlines. The nucleus contained evenly dispersed fine heterochromatin clumps, and absence of marginated heterochromatin

on the inner aspect of the nuclear envelope. The cytoplasm contained dense bundles of glial filaments. They thus had features of astrocytes (Fig. 11C).

2.4. Double immunofluorescence labelling for BGT-1 and GFAP

The untreated hippocampus, or the unlesioned CA fields of the kainate injected hippocampus (Fig 13A, B), showed BGT-1 labelling in the cell bodies and dendrites of pyramidal neurons in the CA fields. In contrast, areas affected by neuronal loss after kainate injection showed loss of BGT-1 labelling in the stratum pyramidale, consistent with loss of pyramidal neurons, but a large increase in number of BGT-1 labelled glial cells. The latter were double labelled for GFAP, confirming that there were astrocytes (Fig. 13C, D).

3. Differential effects of betaine and sucrose on BGT-1 expression and betaine transport in human U373 MG astrocytoma cells and rat hippocampal astrocytes

3.1. Reverse transcription polymerase chain reaction (RT-PCR)

RT-PCR detected a sharp band of the predicted size in human U373 MG astrocytoma cells using BGT-1 specific primer (Fig. 14), a result consistent with the findings of Ruiz-Tachiquin et al. (Ruiz-Tachiquin et al., 2002). The amplified cDNA segment of BGT-1 was subsequently cloned and bidirectionally sequenced to confirm its sequence. These data, together with the following results of cell ELISA and immunofluorescence confocal microscopy indicate that human U373 MG astrocytoma cells endogenously express the betaine/GABA transporter BGT-1.

3.2. Cell ELISA

U373 MG astrocytoma cells that had been incubated for 12 hours with 1mM, 10 mM and 100 mM betaine showed 20%, 36% and 95% increases in BGT-1 immunointensity, compared to controls incubated with media without additional betaine or sucrose. These increases were statistically significant.

In contrast, cells that had been incubated for 12 hours with 1mM, 10 mM and 100 mM sucrose showed no significant increases in BGT-1, compared to controls (Table 1).

3.3. Immunofluorescence confocal microscopy

U373 MG astrocytoma cells that had been incubated for 12 hours with 1mM, 10 mM and 100 mM betaine showed increases in BGT-1 immunoreactivity, compared to controls incubated with media without additional betaine or sucrose. The increased immunolabelling was present as punctate structures in the cell bodies of the astrocytes, as well as on the cell membrane (Fig. 15A-E).

In contrast to cells that had been incubated with betaine, cells that had been incubated for 12 hours with 1mM, 10 mM and 100 mM sucrose showed no obvious increases in BGT-1 immunoreactivity, compared to controls (Fig. 15F, G, H).

3.4. [^{14}C] betaine uptake assay

Astrocytoma cells that had been incubated for 12 hours with 1mM, 10 mM and 100 mM betaine showed 13%, 37% and 50% increases in [^{14}C] betaine uptake, compared to controls. These increases were statistically significant.

In contrast to cells that had been incubated with 1mM and 10mM betaine, cells that had been incubated for 12 hours with 1 mM and 10 mM sucrose showed no significant increases in [^{14}C] betaine uptake. A rather unexpected and marked (123%) increase in betaine uptake was, however, observed in cells incubated with 100 mM sucrose compared to controls (Table 2).

3.5. Light microscopy revealed by immunoperoxidase labelling for BGT-1

In rats that had been injected with kainate plus saline, loss of BGT-1 immunoreactivity in pyramidal neurons was accompanied by increased BGT-1 immunoreactivity in only a few glial cells in the degenerating CA field (Fig. 16A, B, Table. 3). In contrast, rats that had been injected with kainate plus betaine showed a marked induction of BGT-1 immunoreactivity in glial cells in the degenerating CA3 and the adjacent fimbria (Fig. 16C, 2F, Table. 3). The glial cells had features of astrocytes (see below).

3.6. Double immunofluorescence labelling for BGT-1 and GFAP

As with the immunoperoxidase stained sections, few glial cells were observed in the degenerating CA fields and fimbria in the rats that had received kainate and saline injections (Fig. 17A, B). In contrast, large numbers of glial cells were observed in these regions, in rats that were injected with kainate plus betaine (Fig. 17C, D). The BGT-1 positive cells were double labelled for GFAP, confirming that they were astrocytes.

3.7. Electron microscopy

Electron microscopy revealed that BGT-1 positive glial cells in the degenerating CA fields and the adjacent fimbria areas had large cell bodies with irregular cell outlines. The cytoplasm contained bundles of glial filaments, and the nucleus contained evenly dispersed fine heterochromatin clumps. They thus had morphological features of astrocytes (Fig. 18). The astrocytes in rats that received kainate plus saline showed non-bloated mitochondria with closely packed cristae (Fig. 18A, B). In contrast, large numbers of swollen mitochondria were observed in astrocytes in the degenerating CA3 of rats that had been injected with kainate plus betaine (Fig. 18C, D).

CHAPTER 4

DISCUSSION

1. Distribution and subcellular localization of betaine/GABA transporter BGT-1 in the cerebral neocortex and hippocampus

1.1. Distribution of BGT-1 in cerebral neocortex and hippocampus

BGT-1 was observed in pyramidal neurons in the cerebral neocortex and the CA fields of the hippocampus. Large numbers of small diameter dendrites or dendritic spines were observed in the neuropil. This distribution of BGT-1 is different from that of two other GABA transporters, GAT-1 and GAT-3. GAT-1 is exclusively expressed in axon terminals that formed symmetrical synapses in the human and monkey cerebral cortex and the monkey basal ganglia, although it can also be expressed in astrocytes in the rat cortex (Ong et al., 1998; Minelli et al., 1995). GAT-3 expression is low in the cortex and hippocampus, but been localized to astrocytic processes, in the monkey and rat basal ganglia and brainstem (Ng et al., 2000; Ng and Ong, 2001). GAT-2 is localized mostly in leptomeninges (pia and arachnoid) surrounding the brain (Conti et al., 1999).

The localization of BGT-1 in dendritic spines of pyramidal neurons is consistent with the results of previous cell culture studies. MDCK cells stably transfected with mRNAs to BGT-1 or GAT-1 showed that the BGT-1 was localized to the basolateral membrane, consistent with a dendritic localization, whereas GAT-1 was localized to the apical domain, consistent with an axonal distribution *in vivo* (Pietrini et al., 1994).

1.2. Subcellular localization of BGT-1 revealed by electron microscopy

The immunolabelled small diameter dendrites or dendritic spines made asymmetrical synaptic contacts with unlabelled axon terminals containing small round vesicles, characteristic of glutamatergic terminals. BGT-1 label was observed in an extra-perisynaptic region, away from the post-synaptic density. Immunoreactivity was not observed in portions of dendrites that formed symmetrical synapses, axon terminals, or glial cells.

1.3. Functional implication of BGT-1 in osmoregulation in the central nervous system

The distribution of BGT-1 on dendritic spines, rather than at GABAergic axon terminals, suggests that the transporter is unlikely to play a major role in terminating the action of GABA at a synapse. It may, however, serve to sequester GABA that has diffused away from synaptic regions, thereby assuring the fidelity of transmission, as suggested previously (Borden, 1996). Any GABA taken up is probably broken down. A previous study has shown elevated expression of GABA transaminase, an enzyme important in breakdown of GABA, in hippocampal pyramidal neurons after ischemia-reperfusion injury (Kang et al., 2001).

The osmolyte betaine is more likely to be the physiological substrate of BGT-1 in the brain. BGT-1 transports GABA with a K_m of approximately 20-100 μM, but betaine with a K_m of approximately 200-400 μM (Chen et al., 2004). BGT-1 displays a relatively high degree of sequence identity with the transporter for taurine (Smith et al., 1992), a major osmoregulator in the central nervous system. Betaine is

used as a non-perturbing osmolyte by plants, bacteria, invertebrates and vertebrates to compensate for hypertonic stress (Yancey et al., 1982; Burg 1995). In vertebrates, betaine transport requires Na^+ and Cl^- and is modulated by changes in osmolarity (Nakanishi et al., 1990). Betaine has been detected in the brain, and its levels are increased following salt loading (Heilig et al., 1989), consistent with a role in osmoregulation. High levels of betaine have been detected in single neurons isolated from the abdominal ganglion from *Aplysia californica* using the technique of nuclear magnetic resonance (NMR) spectroscopy (Grant et al., 2000). The presence of BGT-1 in pyramidal neurons therefore suggests that these neurons are likely to utilize betaine to maintain osmolarity. It is postulated that maintenance of osmolarity and prevention of cell shrinkage could be critical to the proper structure and function of proteins on the cell membranes of the neurons.

2. Changes in the expression of GABA transporters in the rat hippocampus after kainate induced neuronal injury

2.1. Decrease in the expression of GAT-1 after kainate induced neuronal injury

In normal rats, GAT-1 labelling was observed as a fine reticular network, around the unlabelled cell bodies of pyramidal neurons in the CA fields. A decrease in GAT-1 immunostaining was observed in the degenerating CA subfields. The decreased GAT-1 staining could be due either to downregulation of the transporter by the GABAergic neurons, or death of these neurons.

2.2. Decrease in the expression of GAT-3 after kainate induced neuronal injury

GAT-3 staining was observed in occasional glial cell bodies, and a meshwork of fine processes in the neuropil in normal rats. A decrease in GAT-3 immunostaining was observed in the degenerating CA subfields. The decreased GAT-3 staining is more likely due to downregulation of the transporter by astrocytes, since BGT-1 expression was concomitantly increased in these cells.

The observed localization of GAT-1, GAT-2 and GAT-3 in the CA fields of the normal rat hippocampus is in agreement with the previous reports on the rat brain (Ribak et al., 1996; Conti et al., 1999). The decrease in GAT-1 and GAT-3 staining in the lesioned CA3 field after kainate lesions might lead to decreased GABA uptake from the extracellular space. The decrease in GAT-1 and GAT-3 staining in the hippocampus after kainate treatment is consistent with previous findings of decreased GAT-1 and GAT-3 expression in the CA3 region of epilepsy patients with mesial temporal sclerosis (Mathern et al., 1999).

2.3. Upregulation of BGT-1 in astrocytes after kainate induced neuronal injury

BGT-1 immunostaining was observed in cell bodies and apical dendrites of pyramidal neurons, a result consistent with that of the study on the monkey brain. In contrast, significantly increased BGT-1 immunoreactivity was observed in glial cells at 1 week after kainate injection. The BGT-1 immunoreactivity in glial cells declined at 3-week post-kainate injection. Labelled glial cells were found to have dense bundles of glial filaments characteristic of astrocytes at electron microscopy, and were double labelled for GFAP, a marker for astrocytes. Non-specific

immunostaining by BGT-1 antibody is unlikely, since a well-characterized antibody, supplied in the affinity-purified form, was used. Our Western immunoblot analyses on the rat liver also confirmed that the antibody detected a band at 60 kDa, consistent with the expected molecular weight of BGT-1. The higher molecular band at 65kDa observed in hippocampal homogenates likely represents a glycosylated form of BGT-1. The transporter is predicted to have two putative glycosylation sites in the extracellular loop between membrane-spanning domains 3 and 4 (Borden et al., 1995).

The increase in BGT-1 expression might lead to an increase in GABA uptake. This effect on GABA uptake is, however, likely to be small, since BGT-1 is a weak GABA transporter (Kwon, 1996). In view of the decreased expression of GAT-1 and GAT-3, it therefore seems unlikely that enhanced GABA uptake in the glial scar could be a factor in contributing to increased excitation of neurons in epilepsy.

2.4. Role of BGT-1 in astrocytes in osmoregulation after kainate induced neuronal injury

The localization of BGT-1 in cell bodies and apical dendrites of pyramidal neurons suggests that neurons have the ability to concentrate betaine, and is consistent with the results of a recent study using single cell nuclear magnetic resonance imaging, which showed high levels (100-300 mM) of betaine in normal neuron (Grant et al. 2000).

Upregulated BGT-1 in astrocytes may play a role in osmoregulation of these cells. BGT-1 transports GABA with a Km of approximately 20-100 μM, but betaine with

a Km of approximately 200-400 μM (Kwon, 1996). Furthermore, BGT-1 exhibits relatively high (61%) sequence similarity to the transporter for taurine (Smith et al., 1992), an important osmoregulator in the central nervous system. The response of BGT-1 to osmotic stress has been well studied, particularly in Madin-Darby canine kidney (MDCK) cells (Uchida et al., 1993a; Uchida et al., 1993b; Takenaka et al., 1995), and cultured astrocytes (Bitoun and Tappaz, 2000b). Astrocytes respond to hyperosmotic stress by an initial shrinkage, followed by recovery of cell volume (Bitoun and Tappaz 2000b). The recovery of cell volume was enhanced by addition of an osmolyte, taurine, into the culture medium (Bitoun and Tappaz 2000b). The osmolytes taurine, sorbitol, myoinositol, and betaine accumulate in cells exposed to hypertonic stress, as a result of transcription of genes containing tonicity-responsive enhancer (TonE), which encode for proteins that catalyse the transport or synthesis of these osmolytes (Handler and Kwon, 2001). The BGT-1 gene contains a TonE (Takenaka et al., 1994) and increased BGT-1 mRNA has been observed in cultured astrocytes following hyperosmotic stress (Bitoun and Tappaz, 2000b).

Previous studies have revealed that osmotic overloading occurs following kainate-induced neuronal injury (Rothman et al., 1985; Olney et al., 1986; Hasbani et al., 1998; Al Noori et al., 2000). It is therefore possible that increased expression of BGT-1 in astrocytes after kainate treatment has a physiological role in enabling these cells to resist shrinkage caused by the hyperosmotic stress. Expression of genes encoding osmolyte transporters in astrocytes has been reported to be prolonged even after cell volume has recovered, probably due to the inertia of the transduction pathway (Bitoun and Tappaz, 2000b). It is therefore conceivable that

prolonged expression of BGT-1 in astrocytes could lead to excessive water influx, and swelling of these cells.

3. Differential effects of betaine and sucrose on BGT-1 expression and betaine transport in human U373 MG astrocytoma cells and rat hippocampal astrocytes

3.1. Effects of betaine or sucrose on BGT-1 expression *in vitro*

Treatment of cultured human U373 MG astrocytoma cells with betaine resulted in an increase in BGT-1 protein as detected by cell-ELISA analysis. A dose-dependent effect on BGT-1 expression was observed. In comparison to betaine, isosmolar concentrations of sucrose had a lesser effect on BGT-1 induction, and did not significantly increase BGT-1 immuno-intensity under these conditions.

The effect of betaine on BGT-1 expression at the protein level was also studied by confocal microscopy. An increase in BGT-1 immunoreactivity was observed in cells treated with increasing concentrations of betaine, consistent with the findings of cell-ELISA. The BGT-1 was mostly present in the cytoplasm, but some immunoreactivity was found on the cell membrane, consistent with its function as an osmolyte transporter.

3.2. Effects of betaine or sucrose on [^{14}C] betaine uptake *in vitro*

Cultured human U373 MG astrocytoma cells that have been incubated with non-radioactive labelled betaine for 12 hours showed increased transport of radioactive betaine with a similar dose-dependent manner. This finding is consistent with that of

the cell-ELISA and immunofluorescence findings, and shows that the betaine induced increases in BGT-1 expression is associated with increased transport of betaine. Consistent with the non-significant change in BGT-1 protein level after sucrose treatment, no significant increase in betaine transport was observed when cells were incubated with 1-10 mM of sucrose. Since the high concentrations of sucrose could mimic any non-specific forms of hyperosmotic stress, these findings could support the notion that betaine is a more effective inducer of BGT-1 expression and activity, than other non-specific forms of osmotic stress.

In contrast to 1 mM and 10 mM sucrose, a marked increase in betaine uptake was observed when cells were incubated for 12 hours with 100 mM sucrose. This is despite the little or no induction in BGT-1 immunoreactivity, and suggests that the uptake is not mediated by BGT-1. It has been reported that in addition to BGT-1, betaine could be taken up by the "amino acid transport system A" under hyperosmotic conditions (Petronini et al., 1994). The activity of amino acid transport system A is induced by high concentrations of sucrose (Petronini et al., 2000). It is therefore possible that both BGT-1 and the amino acid transport system A might be involved in uptake of betaine in astrocytes - BGT-1 being specifically induced by betaine, and amino acid transport system A being non-specifically induced by very high levels of osmotic stress.

3.3. Effects of betaine on BGT-1 expression *in vivo*

Betaine has been suggested as a protective osmolyte (Yancey et al., 1982; Burg, 1995). This effect has been most extensively studied in kidney cells. In response to

hyperosmotic stress, cells increase the BGT-1 expression to increase betaine transport into the cytoplasm to counter the effect of hyperosmotic stress (Kwon and Handler, 1995; Kwon, 1996; Burg et al., 1997). The increase in BGT-1 expression by astrocytes may therefore be a protective mechanism that these cells use to counteract the effect of hyperosmotic stress induced after excitotoxic injury. On the other hand, prolonged and excessive induction of BGT-1 by astrocytes may result in an excessive betaine and water influx into the astrocytes and might be a factor in contributing to astrocytic swelling after excitotoxic injury. The mechanism by which betaine induces BGT-1 expression remains unknown.

The localization of BGT-1 in hippocampal neurons of the normal hippocampus suggests that these neurons contain high levels of betaine. In addition to being an osmolyte, betaine also functions as a donor of 1-carbon (methyl groups) to the methionine cycle, and is important in limiting the toxicity of homocysteine (reviewed in Craig, 2004). It is postulated that the betaine could be released into the extracellular space during neuronal injury. In order to determine whether betaine could induce astrocytic BGT-1 expression *in vivo*, we injected betaine into the cerebral ventricles of rats that have received an intracerebroventricular kainate injection one day earlier. We observed that there was a significant increase in BGT-1 immunoreactivity in astrocytes in rats that receive kainate and betaine injections, compared to those that had received kainate and saline injections. The rats that had been treated with kainate and betaine also showed large number of swollen mitochondria in astrocytes, whereas such swollen mitochondria were not observed in the rats injected with kainate and saline. In this study, a dose of 10 μl of 100mM

betaine was injected into the cerebral ventricles to mimic betaine that could be released from neurons following such injury. Although no information exists as to the level of betaine in mammalian neurons, very high levels of betaine (100-300 mM), has been observed in single neurons from the abdominal ganglion of the sea hare, *Aplysia californica*, using the technique of single neuron nuclear magnetic resonance spectroscopy (Grant et al., 2000). The betaine concentration in these neurons was approximately 9 fold greater than that of another osmolyte, taurine, in these neurons (Grant et al., 2000). The dose that we injected introcerebroventricularly may therefore not be excessive, and may therefore mimic a pathological condition whereby betaine is released from dying neurons.

In view of the above findings, we postulate that the release of betaine from dying neurons may be a factor in contributing to increase BGT-1 expression in astrocytes. This might contribute to astrocytic swelling following head injury or stroke. Further studies are necessary to study the mechanism by which betaine could induce BGT-1 expression and the effects of BGT-1 inhibitors on astrocytic swelling.

CHAPTER 5

CONCLUSIONS

GABA transporters, termed GAT-1, GAT-2, GAT-3, and BGT-1 have been cloned and identified. They show approximately 50% amino acid sequence similarity, and belong to the family of Na^+- and Cl^--dependent neurotransmitter transporters with 12 putative transmembrane spanning domains. In contrast to GAT-1, 2 or 3, the betaine/GABA transporter BGT-1 is capable of utilizing both GABA and betaine as substrates. BGT-1 has been extensively studied in MDCK cells, and it is responsible for the uptake of betaine into kidney cells when adapted to hyperosmotic environments. In addition to being a protective osmolyte, betaine can function as a methyl donor to detoxify the homocysteine.

The expressions of GAT-1, GAT-2 and GAT-3 in the brain have been studied by immunocytochemistry. In contrast, the distribution and subcellular localization of BGT-1 in the brain has yet to be determined. Therefore, this study employed immunocytochemistry and electron microscopy to elucidate the distribution and subcellular localization of BGT-1 in the cerebral neocortex and hippocampus. BGT-1 was observed in pyramidal neurons in the cerebral neocortex and the CA fields of the hippocampus. Large numbers of small diameter dendrites or dendritic spines were observed in the neuropil. These made asymmetrical synaptic contacts with unlabelled axon terminals containing small round vesicles, characteristic of glutamatergic terminals. BGT-1 labelling was observed in an extra-perisynaptic region, away from the post-synaptic density. The distribution of BGT-1 on dendritic spines, rather than at GABAergic axon terminals, suggests that the transporter is unlikely to play a major role in terminating the action of GABA at a synapse. Instead, the osmolyte betaine is more likely to be the physiological substrate of

BGT-1 in the brain, and the presence of the transporter in pyramidal neurons suggests that these neurons utilize betaine to maintain osmolarity.

The functional role of BGT-1 in the brain has not been fully elucidated. BGT-1 might contribute to osmoregulation in the brain, since betaine, a substrate for BGT-1, has been assigned a role in osmoregulation. Osmoregulation is critical for maintaining brain function. Osmotic stress has been shown in neuronal excitotoxcity. Since changes in expression of GABA transporters / BGT-1 might result in alterations in levels of GABA / betaine in the extracellular space, with consequent effects on neuronal excitability or osmolarity, this study investigated the expression of GABA transporters in the rat hippocampus, following kainate-induced neuronal injury. A decrease in GAT-1 and GAT-3 immunostaining, and no change in GAT-2 staining, was observed in the degenerating CA subfields. In contrast, increased BGT-1 immunoreactivity was observed in astrocytes after kainate injection. BGT-1 is a weak transporter of GABA in comparison to other GABA transporters, and the increased expression of BGT-1 in astrocytes might be a protective mechanism against increased osmotic stress known to occur after excitotoxic injury. On the other hand, excessive or prolonged BGT-1 expression might be a factor contributing to astrocytic swelling after brain injury.

BGT-1 expression has been studied in astrocytes at the mRNA level, but little is known about BGT-1 expression at the protein level, or whether increased BGT-1 is associated with increased betaine transport. It is also not known whether betaine could induce the expression of BGT-1. This study further explored the possible changes in betaine transporter expression and function in astrocytes, after treatment

with high concentrations of betaine or sucrose *in vitro*, as well as the effect of betaine on its transporter BGT-1 in reactive astrocytes *in vivo*. Treatment of human U373 MG astrocytoma cells for 12 hours with 1-100 mM of betaine, but not equivalent concentrations of sucrose, resulted in increased BGT-1 immunointensity by ELISA. The increased BGT-1 was present in the cytoplasm and cell membrane. Treatment of cells with 1-100mM betaine also resulted in increased [^{14}C] betaine transport into the cells, consistent with increased BGT-1 transporter function. No increase in betaine uptake was observed when cells were treated with 1 and 10 mM sucrose, but a large increase was observed when cells were treated with 100 mM sucrose. In contrast to rats received intracerebroventricular injection with kainate plus saline, which showed loss of BGT-1 immunoreactivity in neurons and little induction of BGT-1 in astrocytes, a marked increase in BGT-1 immunoreactivity was observed in astrocytes in the degenerating CA fields and fimbria, in rats injected with kainate and betaine. These astrocytes were found to have swollen mitochondria at electron microscopy. In view of the above findings, it is postulated that the release of betaine from dying neurons may be a factor in contributing to increase BGT-1 expression in astrocytes. This might contribute to astrocytic swelling following head injury or stroke.

In summary, the present study has revealed the distribution of betaine/GABA transporter BGT-1 in normal brain and in excitotoxic brain injury, as well as the expression and functional changes of BGT-1 in astrocytes in response to hyperosmolarity *in vitro* and *in vivo*. Overall, the present study has dissected the role of BGT-1 in osmoregulation in the brain. Further studies are necessary to study the

mechanism by which betaine could induce BGT-1 expression and the effects of BGT-1 inhibitors on astrocytic swelling.

CHAPTER 6: REFERENCES

Akbar MT, Rattray M, Williams RJ, Chong NW, Meldrum BS (1998) Reduction of GABA and glutamate transporter messenger RNAs in the severe-seizure genetically epilepsy-prone rat. Neuroscience 85: 1235-1251.

Al Noori S, Swann JW (2000) A role for sodium and chloride in kainic acid-induced beading of inhibitory interneuron dendrites. Neuroscience 101: 337-348.

Alepuz PM, Jovanovic A, Reiser V, Ammerer G (2001) Stress-induced map kinase Hog1 is part of transcription activation complexes. Mol Cell 7: 767-777.

Andrew RD (1991) Seizure and acute osmotic change: clinical and neurophysiological aspects. J Neurol Sci 101: 7-18.

Aoshima H, Tomita K, Sugio S (1988) Expression of amino acid transport systems in Xenopus oocytes injected with mRNA of rat small intestine and kidney. Arch Biochem Biophys 265: 73-81.

Arieff AI (1984) Central nervous system manifestations of disordered sodium metabolism. Clin Endocrinol Metab 13: 269-294.

Attwell D, Barbour B, Szatkowski M (1993) Nonvesicular release of neurotransmitter. Neuron 11: 401-407.

Awapara J, Landua AJ, Fuerst R, Seale B (1950) Free γ-aminobutyric acid in brain. J Biol Chem 187: 35-39.

Bagnasco S, Balaban R, Fales HM, Yang YM, Burg M (1986) Predominant osmotically active organic solutes in rat and rabbit renal medullas. J Biol Chem 261: 5872-5877.

Balaban RS, Burg MB (1987) Osmotically active organic solutes in the renal inner medulla. Kidney Int 31: 562-564.

Barbin G, Pollard H, Gaiarsa JL, Ben Ari Y (1993) Involvement of GABAA receptors in the outgrowth of cultured hippocampal neurons. Neurosci Lett 152: 150-154.

Barron A, Jung JU, Villarejo M (1987) Purification and characterization of a glycine betaine binding protein from Escherichia coli. J Biol Chem 262: 11841-11846.

Batty IH, Michie A, Fennel M, Downes CP (1993) The characteristics, capacity and receptor regulation of inositol uptake in 1321N1 astrocytoma cells. Biochem J 294 (Pt 1): 49-55.

Beetsch JW, Olson JE (1996) Hyperosmotic exposure alters total taurine quantity and cellular transport in rat astrocyte cultures. Biochim Biophys Acta 1290: 141-148.

Behar TN, Li YX, Tran HT, Ma W, Dunlap V, Scott C, Barker JL (1996) GABA stimulates chemotaxis and chemokinesis of embryonic cortical neurons via calcium-dependent mechanisms. J Neurosci 16: 1808-1818.

Behar TN, Schaffner AE, Colton CA, Somogyi R, Olah Z, Lehel C, Barker JL (1994) GABA-induced chemokinesis and NGF-induced chemotaxis of embryonic spinal cord neurons. J Neurosci 14: 29-38.

Ben Ari Y (1985) Limbic seizure and brain damage produced by kainic acid: mechanisms and relevance to human temporal lobe epilepsy. Neuroscience 14: 375-403.

Ben Ari Y, Cossart R (2000) Kainate, a double agent that generates seizures: two decades of progress. Trends Neurosci 23: 580-587.

Ben Ari Y, Tremblay E, Ottersen OP (1980) Injections of kainic acid into the amygdaloid complex of the rat: an electrographic, clinical and histological study in relation to the pathology of epilepsy. Neuroscience 5: 515-528.

Berry GT, Mallee JJ, Kwon HM, Rim JS, Mulla WR, Muenke M, Spinner NB (1995) The human osmoregulatory Na^+/myo-inositol cotransporter gene (SLC5A3): molecular cloning and localization to chromosome 21. Genomics 25: 507-513.

Bitoun M, Tappaz M (2000a) Gene expression of taurine transporter and taurine biosynthetic enzymes in brain of rats with acute or chronic hyperosmotic plasma. A comparative study with gene expression of myo-inositol transporter, betaine transporter and sorbitol biosynthetic enzyme. Brain Res Mol Brain Res 77: 10-18.

Bitoun M, Tappaz M (2000b) Gene expression of the transporters and biosynthetic enzymes of the osmolytes in astrocyte primary cultures exposed to hyperosmotic conditions. Glia 32: 165-176.

Borden LA (1996) GABA transporter heterogeneity: pharmacology and cellular localization. Neurochem Int 29: 335-356.

Borden LA, Dhar TG, Smith KE, Branchek TA, Gluchowski C, Weinshank RL (1994) Cloning of the human homologue of the GABA transporter GAT-3 and identification of a novel inhibitor with selectivity for this site. Receptors Channels 2: 207-213.

Borden LA, Smith KE, Gustafson EL, Branchek TA, Weinshank RL (1995a) Cloning and expression of a betaine/GABA transporter from human brain. J Neurochem 64: 977-984.

Borden LA, Smith KE, Gustafson EL, Branchek TA, Weinshank RL (1995b) Cloning and expression of a betaine/GABA transporter from human brain. J Neurochem 64: 977-984.

Borden LA, Smith KE, Hartig PR, Branchek TA, Weinshank RL (1992) Molecular heterogeneity of the gamma-aminobutyric acid (GABA) transport system. Cloning of two novel high affinity GABA transporters from rat brain. J Biol Chem 267: 21098-21104.

Bowery NG, Enna SJ (2000) gamma-aminobutyric acid (B) receptors: first of the functional metabotropic heterodimers. J Pharmacol Exp Ther 292: 2-7.

Bowery NG, Hill DR, Hudson AL, Doble A, Middlemiss DN, Shaw J, Turnbull M (1980) (-)Baclofen decreases neurotransmitter release in the mammalian CNS by an action at a novel GABA receptor. Nature 283: 92-94.

Brewster JL, de Valoir T, Dwyer ND, Winter E, Gustin MC (1993) An osmosensing signal transduction pathway in yeast. Science 259: 1760-1763.

Burg MB (1995) Molecular basis of osmotic regulation. Am J Physiol 268: F983-F996.

Burg MB, Kwon ED, Kultz D (1997) Regulation of gene expression by hypertonicity. Annu Rev Physiol 59: 437-455.

Burnham CE, Buerk B, Schmidt C, Bucuvalas JC (1996) A liver-specific isoform of the betaine/GABA transporter in the rat: cDNA sequence and organ distribution. Biochim Biophys Acta 1284: 4-8.

Chan PH, Fishman RA (1979) Elevation of rat brain amino acids, ammonia and idiogenic osmoles induced by hyperosmolality. Brain Res 161: 293-301.

Chebabo SR, Hester MA, Aitken PG, Somjen GG (1995) Hypotonic exposure enhances synaptic transmission and triggers spreading depression in rat hippocampal tissue slices. Brain Res 695: 203-216.

Chebib M, Johnston GA (2000) GABA-Activated ligand gated ion channels: medicinal chemistry and molecular biology. J Med Chem 43: 1427-1447.

Chen NH, Reith ME, Quick MW (2004) Synaptic uptake and beyond: the sodium- and chloride-dependent neurotransmitter transporter family SLC6. Pflugers Arch 447: 519-531.

Choi DW (1987) Ionic dependence of glutamate neurotoxicity. J Neurosci 7: 369-379.

Conti F, Melone M, De Biasi S, Minelli A, Brecha NC, Ducati A (1998) Neuronal and glial localization of GAT-1, a high-affinity gamma-aminobutyric acid plasma membrane transporter, in human cerebral cortex: with a note on its distribution in monkey cortex. J Comp Neurol 396: 51-63.

Conti F, Zuccarello LV, Barbaresi P, Minelli A, Brecha NC, Melone M (1999) Neuronal, glial, and epithelial localization of gamma-aminobutyric acid transporter 2, a high-affinity gamma-aminobutyric acid plasma membrane transporter, in the cerebral cortex and neighboring structures. J Comp Neurol 409: 482-494.

Coyle JT (1983) Neurotoxic action of kainic acid. J Neurochem 41: 1-11.

Craig SA (2004) Betaine in human nutrition. Am J Clin Nutr 80: 539-549.

Dahl SC, Handler JS, Kwon HM (2001) Hypertonicity-induced phosphorylation and nuclear localization of the transcription factor TonEBP. Am J Physiol Cell Physiol 280: C248-C253.

Devlin AM, Hajipour L, Gholkar A, Fernandes H, Ramesh V, Morris AA (2004) Cerebral edema associated with betaine treatment in classical homocystinuria. J Pediatr 144: 545-548.

During MJ, Ryder KM, Spencer DD (1995) Hippocampal GABA transporter function in temporal-lobe epilepsy. Nature 376: 174-177.

Durkin MM, Smith KE, Borden LA, Weinshank RL, Branchek TA, Gustafson EL (1995) Localization of messenger RNAs encoding three GABA transporters in rat brain: an in situ hybridization study. Brain Res Mol Brain Res 33: 7-21.

El Idrissi A, Messing J, Scalia J, Trenkner E (2003) Prevention of epileptic seizures by taurine. Adv Exp Med Biol 526: 515-525.

Farrant M (2002) Amino Acids: Inhibitory. In: Neurotransmitters, Drugs and Brain Function (Webster RA, ed), pp 225-250. Chichester: John Wiley & Sons, Ltd.

Ferraris JD, Burg MB, Williams CK, Peters EM, Garcia-Perez A (1996) Betaine transporter cDNA cloning and effect of osmolytes on its mRNA induction. Am J Physiol 270: C650-C654.

Ferraris JD, Persaud P, Williams CK, Chen Y, Burg MB (2002a) cAMP-independent role of PKA in tonicity-induced transactivation of tonicity-responsive enhancer/ osmotic response element-binding protein. Proc Natl Acad Sci U S A 99: 16800-16805.

Ferraris JD, Williams CK, Persaud P, Zhang Z, Chen Y, Burg MB (2002b) Activity of the TonEBP/OREBP transactivation domain varies directly with extracellular NaCl concentration. Proc Natl Acad Sci U S A 99: 739-744.

Finkelstein JD, Martin JJ, Harris BJ, Kyle WE (1982) Regulation of the betaine content of rat liver. Arch Biochem Biophys 218: 169-173.

Fisher SK, Novak JE, Agranoff BW (2002) Inositol and higher inositol phosphates in neural tissues: homeostasis, metabolism and functional significance. J Neurochem 82: 736-754.

Flower RJ, Pollitt RJ, Sanford PA, Smyth DH (1972) Metabolism and transfer of choline in hamster small intestine. J Physiol 226: 473-489.

Fonnum F (1987) Biochemistry, anatomy and pharmacology of GABA neurons. In: Psychopharmacology: the Third Generation of Progress (Meltzer HY, ed), pp 173-182. New York: Raven Press.

Foos TM, Wu JY (2002) The role of taurine in the central nervous system and the modulation of intracellular calcium homeostasis. Neurochem Res 27: 21-26.

Freed WJ (1985) Prevention of strychnine-induced seizures and death by the N-methylated glycine derivatives betaine, dimethylglycine and sarcosine. Pharmacol Biochem Behav 22: 641-643.

Gadea A, Lopez-Colome AM (2001) Glial transporters for glutamate, glycine, and GABA: II. GABA transporters. J Neurosci Res 63: 461-468.

Gaitonde MK (1970) Sulphur amino acids. In: Handbook of Neurochemistry (Lagtha A, ed), pp 225-287. New York: Plenum Press.

Garcia-Perez A, Burg MB (1991) Renal medullary organic osmolytes. Physiol Rev 71: 1081-1115.

Garner MM, Burg MB (1994) Macromolecular crowding and confinement in cells exposed to hypertonicity. Am J Physiol 266: C877-C892.

Ghoz EH, Freed WJ (1985) Effects of betaine on seizures in the rat. Pharmacol Biochem Behav 22: 635-640.

Glenn JL, Vanko M (1959) Choline and aldehyde oxidation by rat liver. Arch Biochem Biophys 82: 145-152.

Grant SC, Aiken NR, Plant HD, Gibbs S, Mareci TH, Webb AG, Blackband SJ (2000) NMR spectroscopy of single neurons. Magn Reson Med 44: 19-22.

Grossman EB, Hebert SC (1989) Renal inner medullary choline dehydrogenase activity: characterization and modulation. Am J Physiol 256: F107-F112.

Guastella J, Nelson N, Nelson H, Czyzyk L, Keynan S, Miedel MC, Davidson N, Lester HA, Kanner BI (1990) Cloning and expression of a rat brain GABA transporter. Science 249: 1303-1306.

Gullans SR, Verbalis JG (1993) Control of brain volume during hyperosmolar and hypoosmolar conditions. Annu Rev Med 44: 289-301.

Hagenbuch B, Lubbert H, Stieger B, Meier PJ (1990) Expression of the hepatocyte Na^+/bile acid cotransporter in Xenopus laevis oocytes. J Biol Chem 265: 5357-5360.

Hager K, Hazama A, Kwon HM, Loo DD, Handler JS, Wright EM (1995) Kinetics and specificity of the renal Na^+/myo-inositol cotransporter expressed in Xenopus oocytes. J Membr Biol 143: 103-113.

Han J, Lee JD, Bibbs L, Ulevitch RJ (1994) A MAP kinase targeted by endotoxin and hyperosmolarity in mammalian cells. Science 265: 808-811.

Han X, Budreau AM, Chesney RW (2000) Cloning and characterization of the promoter region of the rat taurine transporter (TauT) gene. Adv Exp Med Biol 483: 97-108.

Handler JS, Kwon HM (2001) Transcriptional regulation by changes in tonicity. Kidney Int 60: 408-411.

Hasbani MJ, Hyrc KL, Faddis BT, Romano C, Goldberg MP (1998) Distinct roles for sodium, chloride, and calcium in excitotoxic dendritic injury and recovery. Exp Neurol 154: 241-258.

Haubrich DR, Wang PF, Wedeking PW (1975) Distribution and metabolism of intravenously administered choline[methyl- 3-H] and synthesis *in vivo* of acetylcholine in various tissues of guinea pigs. J Pharmacol Exp Ther 193: 246-255.

Hediger MA, Ikeda T, Coady M, Gundersen CB, Wright EM (1987) Expression of size-selected mRNA encoding the intestinal Na/glucose cotransporter in Xenopus laevis oocytes. Proc Natl Acad Sci U S A 84: 2634-2637.

Heilig CW, Stromski ME, Blumenfeld JD, Lee JP, Gullans SR (1989) Characterization of the major brain osmolytes that accumulate in salt-loaded rats. Am J Physiol 257: F1108-F1116.

Hirao T, Morimoto K, Yamamoto Y, Watanabe T, Sato H, Sato K, Sato S, Yamada N, Tanaka K, Suwaki H (1998) Time-dependent and regional expression of GABA transporter mRNAs following amygdala-kindled seizures in rats. Brain Res Mol Brain Res 54: 49-55.

Honda S, Yamamoto M, Saito N (1995) Immunocytochemical localization of three subtypes of GABA transporter in rat retina. Brain Res Mol Brain Res 33: 319-325.

Honore T, Drejer J, Nielsen M, Watkins JC, Olverman HJ (1987) Molecular target size of NMDA antagonist binding sites. Eur J Pharmacol 136: 137-138.

Huang R, Bossut DF, Somjen GG (1997) Enhancement of whole cell synaptic currents by low osmolarity and by low [NaCl] in rat hippocampal slices. J Neurophysiol 77: 2349-2359.

Hussy N, Deleuze C, Desarmenien MG, Moos FC (2000) Osmotic regulation of neuronal activity: a new role for taurine and glial cells in a hypothalamic neuroendocrine structure. Prog Neurobiol 62: 113-134.

Huxtable RJ (1989) Taurine in the central nervous system and the mammalian actions of taurine. Prog Neurobiol 32: 471-533.

Ibsen L, Strange K (1996) In situ localization and osmotic regulation of the Na(+)-myo-inositol cotransporter in rat brain. Am J Physiol 271: F877-F885.

Ikegaki N, Saito N, Hashima M, Tanaka C (1994) Production of specific antibodies against GABA transporter subtypes (GAT1, GAT2, GAT3) and their application to immunocytochemistry. Brain Res Mol Brain Res 26: 47-54.

Inoue K, Shimada S, Minami Y, Morimura H, Miyai A, Yamauchi A, Tohyama M (1996) Cellular localization of Na^+/myo-inositol co-transporter mRNA in the rat brain. Neuroreport 7: 1195-1198.

Isaacks RE, Bender AS, Kim CY, Norenberg MD (1997) Effect of osmolality and myo-inositol deprivation on the transport properties of myo-inositol in primary astrocyte cultures. Neurochem Res 22: 1461-1469.

Isaacks RE, Bender AS, Kim CY, Prieto NM, Norenberg MD (1994) Osmotic regulation of myo-inositol uptake in primary astrocyte cultures. Neurochem Res 19: 331-338.

Isaacson JS, Solis JM, Nicoll RA (1993) Local and diffuse synaptic actions of GABA in the hippocampus. Neuron 10: 165-175.

Isomoto S, Kaibara M, Sakurai-Yamashita Y, Nagayama Y, Uezono Y, Yano K, Taniyama K (1998) Cloning and tissue distribution of novel splice variants of the rat GABAB receptor. Biochem Biophys Res Commun 253: 10-15.

Iversen LL, Neal MJ (1968) The uptake of [^{3}H]GABA by slices of rat cerebral cortex. J Neurochem 15: 1141-1149.

Iversen LL, Neal MJ (1969) Subcellular distribution of endogenous and [^{3}H]-GABA in rat cerebral cortex. Br J Pharmacol 36: 206P.

Jhiang SM, Fithian L, Smanik P, McGill J, Tong Q, Mazzaferri EL (1993) Cloning of the human taurine transporter and characterization of taurine uptake in thyroid cells. FEBS Lett 318: 139-144.

Johnson J, Chen TK, Rickman DW, Evans C, Brecha NC (1996) Multiple gamma-Aminobutyric acid plasma membrane transporters (GAT-1, GAT-2, GAT-3) in the rat retina. J Comp Neurol 375: 212-224.

Johnston MV, McKinney M, Coyle JT (1979) Evidence for a cholinergic projection to neocortex from neurons in basal forebrain. Proc Natl Acad Sci U S A 76: 5392-5396.

Jones DP, Miller LA, Chesney RW (1995) The relative roles of external taurine concentration and medium osmolality in the regulation of taurine transport in LLC-PK1 and MDCK cells. Pediatr Res 37: 227-232.

Jorgensen MB, Finsen BR, Jensen MB, Castellano B, Diemer NH, Zimmer J (1993) Microglial and astroglial reactions to ischemic and kainic acid-induced lesions of the adult rat hippocampus. Exp Neurol 120: 70-88.

Kaczmarek L, Kossut M, Skangiel-Kramska J (1997) Glutamate receptors in cortical plasticity: molecular and cellular biology. Physiol Rev 77: 217-255.

Kaneko T, Takenaka M, Okabe M, Yoshimura Y, Yamauchi A, Horio M, Kwon HM, Handler JS, Imai E (1997) Osmolarity in renal medulla of transgenic mice regulates transcription via 5'-flanking region of canine BGT1 gene. Am J Physiol 272: F610-F616.

Kang TC, Kim HS, Seo MO, Park SK, Kwon HY, Kang JH, Won MH (2001) The changes in the expressions of gamma-aminobutyric acid transporters in the gerbil hippocampal complex following spontaneous seizure. Neurosci Lett 310: 29-32.

Kang YS, Ohtsuki S, Takanaga H, Tomi M, Hosoya K, Terasaki T (2002) Regulation of taurine transport at the blood-brain barrier by tumor necrosis factor-alpha, taurine and hypertonicity. J Neurochem 83: 1188-1195.

Kaupmann K, Schuler V, Mosbacher J, Bischoff S, Bittiger H, Heid J, Froestl W, Leonhard S, Pfaff T, Karschin A, Bettler B (1998) Human gamma-aminobutyric acid type B receptors are differentially expressed and regulate inwardly rectifying K^+ channels. Proc Natl Acad Sci U S A 95: 14991-14996.

Keynan S, Suh YJ, Kanner BI, Rudnick G (1992) Expression of a cloned gamma-aminobutyric acid transporter in mammalian cells. Biochemistry 31: 1974-1979.

Kimelberg HK (1995) Current concepts of brain edema. Review of laboratory investigations. J Neurosurg 83: 1051-1059.

Kimelberg HK, Goderie SK, Higman S, Pang S, Waniewski RA (1990) Swelling-induced release of glutamate, aspartate, and taurine from astrocyte cultures. J Neurosci 10: 1583-1591.

Ko BC, Lam AK, Kapus A, Fan L, Chung SK, Chung SS (2002) Fyn and p38 signaling are both required for maximal hypertonic activation of the osmotic response element-binding protein/tonicity-responsive enhancer-binding protein (OREBP/TonEBP). J Biol Chem 277: 46085-46092.

Ko BC, Turck CW, Lee KW, Yang Y, Chung SS (2000) Purification, identification, and characterization of an osmotic response element binding protein. Biochem Biophys Res Commun 270: 52-61.

Koc H, Mar MH, Ranasinghe A, Swenberg JA, Zeisel SH (2002) Quantitation of choline and its metabolites in tissues and foods by liquid chromatography/electrospray ionization-isotope dilution mass spectrometry. Anal Chem 74: 4734-4740.

Kuner R, Kohr G, Grunewald S, Eisenhardt G, Bach A, Kornau HC (1999) Role of heteromer formation in GABAB receptor function. Science 283: 74-77.

Kwon HM (1996) Transcriptional regulation of the betaine/gamma-aminobutyric acid transporter by hypertonicity. Biochem Soc Trans 24: 853-856.

Kwon HM, Handler JS (1995) Cell volume regulated transporters of compatible osmolytes. Curr Opin Cell Biol 7: 465-471.

Kwon HM, Yamauchi A, Uchida S, Preston AS, Garcia-Perez A, Burg MB, Handler JS (1992) Cloning of the cDNA for a Na^+/myo-inositol cotransporter, a hypertonicity stress protein. J Biol Chem 267: 6297-6301.

Lambert IH (2004) Regulation of the cellular content of the organic osmolyte taurine in mammalian cells. Neurochem Res 29: 27-63.

Lang F, Busch GL, Ritter M, Volkl H, Waldegger S, Gulbins E, Haussinger D (1998) Functional significance of cell volume regulatory mechanisms. Physiol Rev 78: 247-306.

Lauder JM, Liu J, Devaud L, Morrow AL (1998) GABA as a trophic factor for developing monoamine neurons. Perspect Dev Neurobiol 5: 247-259.

Law RO (1994a) Regulation of mammalian brain cell volume. J Exp Zool 268: 90-96.

Law RO (1994b) Taurine efflux and the regulation of cell volume in incubated slices of rat cerebral cortex. Biochim Biophys Acta 1221: 21-28.

Le Rudulier D, Bouillard L (1983) Glycine betaine, an osmotic effector in Klebsiella pneumoniae and other members of the Enterobacteriaceae. Appl Environ Microbiol 46: 152-159.

Lerma J (1997) Kainate reveals its targets. Neuron 19: 1155-1158.

Lien YH (1995) Role of organic osmolytes in myelinolysis. A topographic study in rats after rapid correction of hyponatremia. J Clin Invest 95: 1579-1586.

Lien YH, Shapiro JI, Chan L (1990) Effects of hypernatremia on organic brain osmoles. J Clin Invest 85: 1427-1435.

Lien YH, Shapiro JI, Chan L (1991) Study of brain electrolytes and organic osmolytes during correction of chronic hyponatremia. Implications for the pathogenesis of central pontine myelinolysis. J Clin Invest 88: 303-309.

Liu QR, Lopez-Corcuera B, Mandiyan S, Nelson H, Nelson N (1993) Molecular characterization of four pharmacologically distinct gamma-aminobutyric acid transporters in mouse brain [corrected]. J Biol Chem 268: 2106-2112.

Liu QR, Lopez-Corcuera B, Nelson H, Mandiyan S, Nelson N (1992a) Cloning and expression of a cDNA encoding the transporter of taurine and beta-alanine in mouse brain. Proc Natl Acad Sci U S A 89: 12145-12149.

Liu QR, Mandiyan S, Nelson H, Nelson N (1992b) A family of genes encoding neurotransmitter transporters. Proc Natl Acad Sci U S A 89: 6639-6643.

Lohr J, Acara M (1990) Effect of dimethylaminoethanol, an inhibitor of betaine production, on the disposition of choline in the rat kidney. J Pharmacol Exp Ther 252: 154-158.

Longoni S, Coady MJ, Ikeda T, Philipson KD (1988) Expression of cardiac sarcolemmal Na^{+}-Ca^{2+} exchange activity in Xenopus laevis oocytes. Am J Physiol 255: C870-C873.

Lopez-Corcuera B, Liu QR, Mandiyan S, Nelson H, Nelson N (1992) Expression of a mouse brain cDNA encoding novel gamma-aminobutyric acid transporter. J Biol Chem 267: 17491-17493.

Lopez-Rodriguez C, Aramburu J, Jin L, Rakeman AS, Michino M, Rao A (2001) Bridging the NFAT and NF-kappaB families: NFAT5 dimerization regulates cytokine gene transcription in response to osmotic stress. Immunity 15: 47-58.

Lopez-Rodriguez C, Aramburu J, Rakeman AS, Rao A (1999) NFAT5, a constitutively nuclear NFAT protein that does not cooperate with Fos and Jun. Proc Natl Acad Sci U S A 96: 7214-7219.

Loyher ML, Mutin M, Woo SK, Kwon HM, Tappaz ML (2004) Transcription factor tonicity-responsive enhancer-binding protein (TonEBP) which transactivates osmoprotective genes is expressed and upregulated following acute systemic hypertonicity in neurons in brain. Neuroscience 124: 89-104.

Mager S, Kleinberger-Doron N, Keshet GI, Davidson N, Kanner BI, Lester HA (1996) Ion binding and permeation at the GABA transporter GAT1. J Neurosci 16: 5405-5414.

Mager S, Naeve J, Quick M, Labarca C, Davidson N, Lester HA (1993) Steady states, charge movements, and rates for a cloned GABA transporter expressed in Xenopus oocytes. Neuron 10: 177-188.

Malhotra SK, Shnitka TK, Elbrink J (1990) Reactive astrocytes--a review. Cytobios 61: 133-160.

Marshall FH, White J, Main M, Green A, Wise A (1999) GABA(B) receptors function as heterodimers. Biochem Soc Trans 27: 530-535.

Martin DL (1993) Short-term control of GABA synthesis in brain. Prog Biophys Mol Biol 60: 17-28.

Masson J, Sagne C, Hamon M, El Mestikawy S (1999) Neurotransmitter transporters in the central nervous system. Pharmacol Rev 51: 439-464.

Mathern GW, Mendoza D, Lozada A, Pretorius JK, Dehnes Y, Danbolt NC, Nelson N, Leite JP, Chimelli L, Born DE, Sakamoto AC, Assirati JA, Fried I, Peacock WJ,

Ojemann GA, Adelson PD (1999) Hippocampal GABA and glutamate transporter immunoreactivity in patients with temporal lobe epilepsy. Neurology 52: 453-472.

Matskevitch I, Wagner CA, Stegen C, Broer S, Noll B, Risler T, Kwon HM, Handler JS, Waldegger S, Busch AE, Lang F (1999) Functional characterization of the Betaine/gamma-aminobutyric acid transporter BGT-1 expressed in Xenopus oocytes. J Biol Chem 274: 16709-16716.

McIntire SL, Reimer RJ, Schuske K, Edwards RH, Jorgensen EM (1997) Identification and characterization of the vesicular GABA transporter. Nature 389: 870-876.

McKeever MP, Weir DG, Molloy A, Scott JM (1991) Betaine-homocysteine methyltransferase: organ distribution in man, pig and rat and subcellular distribution in the rat. Clin Sci (Lond) 81: 551-556.

Meyer FB (1989) Calcium, neuronal hyperexcitability and ischemic injury. Brain Res Brain Res Rev 14: 227-243.

Miller B, Schmid H, Chen TJ, Schmolke M, Guder WG (1996) Determination of choline dehydrogenase activity along the rat nephron. Biol Chem Hoppe Seyler 377: 129-137.

Minami M, Kuraishi Y, Satoh M (1991) Effects of kainic acid on messenger RNA levels of IL-1 beta, IL-6, TNF alpha and LIF in the rat brain. Biochem Biophys Res Commun 176: 593-598.

Minelli A, Brecha NC, Karschin C, DeBiasi S, Conti F (1995) GAT-1, a high-affinity GABA plasma membrane transporter, is localized to neurons and astroglia in the cerebral cortex. J Neurosci 15: 7734-7746.

Minelli A, DeBiasi S, Brecha NC, Zuccarello LV, Conti F (1996) GAT-3, a high-affinity GABA plasma membrane transporter, is localized to astrocytic processes, and it is not confined to the vicinity of GABAergic synapses in the cerebral cortex. J Neurosci 16: 6255-6264.

Minton AP (1983) The effect of volume occupancy upon the thermodynamic activity of proteins: some biochemical consequences. Mol Cell Biochem 55: 119-140.

Miyakawa H, Woo SK, Chen CP, Dahl SC, Handler JS, Kwon HM (1998) Cis- and trans-acting factors regulating transcription of the BGT1 gene in response to hypertonicity. Am J Physiol 274: F753-F761.

Miyakawa H, Woo SK, Dahl SC, Handler JS, Kwon HM (1999) Tonicity-responsive enhancer binding protein, a rel-like protein that stimulates transcription in response to hypertonicity. Proc Natl Acad Sci U S A 96: 2538-2542.

Moran J, Maar TE, Pasantes-Morales H (1994) Impaired cell volume regulation in taurine deficient cultured astrocytes. Neurochem Res 19: 415-420.

Murabe Y, Ibata Y, Sano Y (1982) Morphological studies on neuroglia. IV. Proliferative response of non-neuronal elements in the hippocampus of the rat to kainic acid-induced lesions. Cell Tissue Res 222: 223-226.

Nadler JV (1981) Minireview. Kainic acid as a tool for the study of temporal lobe epilepsy. Life Sci 29: 2031-2042.

Nadler JV, Okazaki MM, Gruenthal M, Ault B, Armstrong DR (1986) Kainic acid seizures and neuronal cell death: insights from studies of selective lesions and drugs. Adv Exp Med Biol 203: 673-686.

Nadler JV, Perry BW, Cotman CW (1978) Intraventricular kainic acid preferentially destroys hippocampal pyramidal cells. Nature 271: 676-677.

Nadler JV, Perry BW, Gentry C, Cotman CW (1980) Degeneration of hippocampal CA3 pyramidal cells induced by intraventricular kainic acid. J Comp Neurol 192: 333-359.

Nakanishi T, Balaban RS, Burg MB (1988) Survey of osmolytes in renal cell lines. Am J Physiol 255: C181-C191.

Nakanishi T, Turner RJ, Burg MB (1990) Osmoregulation of betaine transport in mammalian renal medullary cells. Am J Physiol 258: F1061-F1067.

Nelson H, Mandiyan S, Nelson N (1990) Cloning of the human brain GABA transporter. FEBS Lett 269: 181-184.

Ng CH, Ong WY (2001) Increased expression of gamma-aminobutyric acid transporters GAT-1 and GAT-3 in the spinal trigeminal nucleus after facial carrageenan injections. Pain 92: 29-40.

Ng CH, Wang XS, Ong WY (2000) A light and electron microscopic study of the GABA transporter GAT-3 in the monkey basal ganglia and brainstem. J Neurocytol 29: 595-603.

Nonaka M, Kohmura E, Yamashita T, Yamauchi A, Fujinaka T, Yoshimine T, Tohyama M, Hayakawa T (1999) Kainic acid-induced seizure upregulates

Na(+)/myo-inositol cotransporter mRNA in rat brain. Brain Res Mol Brain Res 70: 179-186.

Ohmiya R, Yamada H, Nakashima K, Aiba H, Mizuno T (1995) Osmoregulation of fission yeast: cloning of two distinct genes encoding glycerol-3-phosphate dehydrogenase, one of which is responsible for osmotolerance for growth. Mol Microbiol 18: 963-973.

Oja SS, Saransaari P (1992) Taurine release and swelling of cerebral cortex slices from adult and developing mice in media of different ionic compositions. J Neurosci Res 32: 551-561.

Olney JW, Fuller T, de Gubareff T (1979) Acute dendrotoxic changes in the hippocampus of kainate treated rats. Brain Res 176: 91-100.

Olney JW, Price MT, Samson L, Labruyere J (1986) The role of specific ions in glutamate neurotoxicity. Neurosci Lett 65: 65-71.

Olson JE (1999) Osmolyte contents of cultured astrocytes grown in hypoosmotic medium. Biochim Biophys Acta 1453: 175-179.

Olson JE, Goldfinger MD (1990) Amino acid content of rat cerebral astrocytes adapted to hyperosmotic medium *in vitro*. J Neurosci Res 27: 241-246.

Ong WY, Leong SK, Garey LJ, Reynolds R, Liang AW (1996) An immunocytochemical study of glutamate receptors and glutamine synthetase in the hippocampus of rats injected with kainate. Exp Brain Res 109: 251-267.

Ong WY, Levine JM (1999) A light and electron microscopic study of NG2 chondroitin sulfate proteoglycan-positive oligodendrocyte precursor cells in the normal and kainate-lesioned rat hippocampus. Neuroscience 92: 83-95.

Ong WY, Yeo TT, Balcar VJ, Garey LJ (1998) A light and electron microscopic study of GAT-1-positive cells in the cerebral cortex of man and monkey. J Neurocytol 27: 719-730.

Owens DF, Kriegstein AR (2002) Is there more to GABA than synaptic inhibition? Nat Rev Neurosci 3: 715-727.

Pahlman AK, Granath K, Ansell R, Hohmann S, Adler L (2001) The yeast glycerol 3-phosphatases Gpp1p and Gpp2p are required for glycerol biosynthesis and differentially involved in the cellular responses to osmotic, anaerobic, and oxidative stress. J Biol Chem 276: 3555-3563.

Palkovits M, Elekes I, Lang T, Patthy A (1986) Taurine levels in discrete brain nuclei of rats. J Neurochem 47: 1333-1335.

Paredes A, McManus M, Kwon HM, Strange K (1992) Osmoregulation of Na(+)-inositol cotransporter activity and mRNA levels in brain glial cells. Am J Physiol 263: C1282-C1288.

Pasantes MH, Schousboe A (1988) Volume regulation in astrocytes: a role for taurine as an osmoeffector. J Neurosci Res 20: 503-509.

Pasantes-Morales H, Chacon E, Murray RA, Moran J (1994) Properties of osmolyte fluxes activated during regulatory volume decrease in cultured cerebellar granule neurons. J Neurosci Res 37: 720-727.

Pasantes-Morales H, Franco R, Ordaz B, Ochoa LD (2002) Mechanisms counteracting swelling in brain cells during hyponatremia. Arch Med Res 33: 237-244.

Patishi Y, Belmaker RH, Bersudsky Y, Kofman O (1996) A comparison of the ability of myo-inositol and epi-inositol to attenuate lithium-pilocarpine seizures in rats. Biol Psychiatry 39: 829-832.

Perroud B, Le Rudulier D (1985) Glycine betaine transport in Escherichia coli: osmotic modulation. J Bacteriol 161: 393-401.

Petronini PG, De Angelis E, Borghetti AF, Wheeler KP (1994) Osmotically inducible uptake of betaine via amino acid transport system A in SV-3T3 cells. Biochem J 300 (Pt 1): 45-50.

Petronini PG, Alfieri RR, Losio MN, Caccamo AE, Cavazzoni A, Bonelli MA, Borghetti AF, Wheeler KP (2000) Induction of BGT-1 and amino acid system A transport activities in endothelial cells exposed to hyperosmolarity. Am J Physiol Regul Integr Comp Physiol 279: R1580-R1589.

Phillis JW, Smith-Barbour M, Perkins LM, O'Regan MH (1994) Characterization of glutamate, aspartate, and GABA release from ischemic rat cerebral cortex. Brain Res Bull 34: 457-466.

Pietrini G, Suh YJ, Edelmann L, Rudnick G, Caplan MJ (1994) The axonal gamma-aminobutyric acid transporter GAT-1 is sorted to the apical membranes of polarized epithelial cells. J Biol Chem 269: 4668-4674.

Pin JP, Bockaert J (1989) Two distinct mechanisms, differentially affected by excitatory amino acids, trigger GABA release from fetal mouse striatal neurons in primary culture. J Neurosci 9: 648-656.

Pollard H, Cantagrel S, Charriaut-Marlangue C, Moreau J, Ben Ari Y (1994a) Apoptosis associated DNA fragmentation in epileptic brain damage. Neuroreport 5: 1053-1055.

Pollard H, Charriaut-Marlangue C, Cantagrel S, Represa A, Robain O, Moreau J, Ben Ari Y (1994b) Kainate-induced apoptotic cell death in hippocampal neurons. Neuroscience 63: 7-18.

Porcellati F, Hlaing T, Togawa M, Stevens MJ, Larkin DD, Hosaka Y, Glover TW, Henry DN, Greene DA, Killen PD (1998) Human Na(+)-myo-inositol cotransporter gene: alternate splicing generates diverse transcripts. Am J Physiol 274: C1215-C1225.

Posas F, Chambers JR, Heyman JA, Hoeffler JP, de Nadal E, Arino J (2000) The transcriptional response of yeast to saline stress. J Biol Chem 275: 17249-17255.

Posas F, Wurgler-Murphy SM, Maeda T, Witten EA, Thai TC, Saito H (1996) Yeast HOG1 MAP kinase cascade is regulated by a multistep phosphorelay mechanism in the SLN1-YPD1-SSK1 "two-component" osmosensor. Cell 86: 865-875.

Qian X, Vinnakota S, Edwards C, Sarkar HK (2000) Molecular characterization of taurine transport in bovine aortic endothelial cells. Biochim Biophys Acta 1509: 324-334.

Radian R, Bendahan A, Kanner BI (1986) Purification and identification of the functional sodium- and chloride-coupled gamma-aminobutyric acid transport glycoprotein from rat brain. J Biol Chem 261: 15437-15441.

Radian R, Ottersen OP, Storm-Mathisen J, Castel M, Kanner BI (1990) Immunocytochemical localization of the GABA transporter in rat brain. J Neurosci 10: 1319-1330.

Ramamoorthy S, Leibach FH, Mahesh VB, Han H, Yang-Feng T, Blakely RD, Ganapathy V (1994) Functional characterization and chromosomal localization of a cloned taurine transporter from human placenta. Biochem J 300 (Pt 3): 893-900.

Rasola A, Galietta LJ, Barone V, Romeo G, Bagnasco S (1995) Molecular cloning and functional characterization of a GABA/betaine transporter from human kidney. FEBS Lett 373: 229-233.

Rattray M, Priestley JV (1993) Differential expression of GABA transporter-1 messenger RNA in subpopulations of GABA neurones. Neurosci Lett 156: 163-166.

Rep M, Krantz M, Thevelein JM, Hohmann S (2000) The transcriptional response of Saccharomyces cerevisiae to osmotic shock. Hot1p and Msn2p/Msn4p are required

for the induction of subsets of high osmolarity glycerol pathway-dependent genes. J Biol Chem 275: 8290-8300.

Ribak CE, Tong WM, Brecha NC (1996a) Astrocytic processes compensate for the apparent lack of GABA transporters in the axon terminals of cerebellar Purkinje cells. Anat Embryol (Berl) 194: 379-390.

Ribak CE, Tong WM, Brecha NC (1996b) GABA plasma membrane transporters, GAT-1 and GAT-3, display different distributions in the rat hippocampus. J Comp Neurol 367: 595-606.

Rim JS, Atta MG, Dahl SC, Berry GT, Handler JS, Kwon HM (1998) Transcription of the sodium/myo-inositol cotransporter gene is regulated by multiple tonicity-responsive enhancers spread over 50 kilobase pairs in the 5'-flanking region. J Biol Chem 273: 20615-20621.

Risso S, DeFelice LJ, Blakely RD (1996) Sodium-dependent GABA-induced currents in GAT1-transfected HeLa cells. J Physiol 490 (Pt 3): 691-702.

Roberts E (1976) Introduction. In: GABA in Nervous System Function (Roberts E, Chase TN, Tower DB, eds), pp 1-6. New York: Raven Press.

Roberts E, Frankel S (1950) γ-aminobutyric acid in brain: Its formation from glutamic acid. J Biol Chem 187: 55-63.

Roberts E, Kuriyama K (1968) Biochemical-physiological correlations in studies of the gamma-aminobutyric acid system. Brain Res 8: 1-35.

Robey RB, Kwon HM, Handler JS, Garcia-Perez A, Burg MB (1991) Induction of glycinebetaine uptake into Xenopus oocytes by injection of poly(A)+ RNA from renal cells exposed to high extracellular NaCl. J Biol Chem 266: 10400-10405.

Roper SN, Obenaus A, Dudek FE (1992) Osmolality and nonsynaptic epileptiform bursts in rat CA1 and dentate gyrus. Ann Neurol 31: 81-85.

Rosen AS, Andrew RD (1990) Osmotic effects upon excitability in rat neocortical slices. Neuroscience 38: 579-590.

Rothman SM (1985) The neurotoxicity of excitatory amino acids is produced by passive chloride influx. J Neurosci 5: 1483-1489.

Rothschild HA, Barron ES (1954) The oxidation of betaine aldehyde by betaine aldehyde dehydrogenase. J Biol Chem 209: 511-523.

Ruiz-Tachiquin ME, Sanchez-Lemus E, Soria-Jasso LE, Arias-Montano JA, Ortega A (2002) gamma-aminobutyric acid transporter (BGT-1) expressed in human astrocytoma U373 MG cells: Pharmacological and molecular characterization and phorbol ester-induced inhibition. J Neurosci Res 69: 125-132.

Sagne C, El Mestikawy S, Isambert MF, Hamon M, Henry JP, Giros B, Gasnier B (1997) Cloning of a functional vesicular GABA and glycine transporter by screening of genome databases. FEBS Lett 417: 177-183.

Saly V, Andrew RD (1993) CA3 neuron excitation and epileptiform discharge are sensitive to osmolality. J Neurophysiol 69: 2200-2208.

Sanchez-Olea R, Moran J, Pasantes-Morales H (1992) Changes in taurine transport evoked by hyperosmolarity in cultured astrocytes. J Neurosci Res 32: 86-92.

Saransaari P, Oja SS (2000) Taurine and neural cell damage. Amino Acids 19: 509-526.

Satsu H, Miyamoto Y, Shimizu M (1999) Hypertonicity stimulates taurine uptake and transporter gene expression in Caco-2 cells. Biochim Biophys Acta 1419: 89-96.

Schousboe A, Sanchez OR, Moran J, Pasantes-Morales H (1991) Hyposmolarity-induced taurine release in cerebellar granule cells is associated with diffusion and not with high-affinity transport. J Neurosci Res 30: 661-665.

Schwartzkroin PA, Baraban SC, Hochman DW (1998) Osmolarity, ionic flux, and changes in brain excitability. Epilepsy Res 32: 275-285.

Schwob JE, Fuller T, Price JL, Olney JW (1980) Widespread patterns of neuronal damage following systemic or intracerebral injections of kainic acid: a histological study. Neuroscience 5: 991-1014.

Sigel E, Baur R, Porzig H, Reuter H (1988) mRNA-induced expression of the cardiac Na+-Ca2+ exchanger in Xenopus oocytes. J Biol Chem 263: 14614-14616.

Simantov R, Crispino M, Hoe W, Broutman G, Tocco G, Rothstein JD, Baudry M (1999) Changes in expression of neuronal and glial glutamate transporters in rat hippocampus following kainate-induced seizure activity. Brain Res Mol Brain Res 65: 112-123.

Sivilotti L, Nistri A (1991) GABA receptor mechanisms in the central nervous system. Prog Neurobiol 36: 35-92.

Skiba WE, Wells MS, Mangum JH, Awad WH (1987) Betaine-homocysteine S-methyltransferase. In: Methods in Enzymology (Colowick SP, Kaplan NO, eds), pp 384-388. New York: Academic.

Sloviter RS (1996) Hippocampal pathology and pathophysiology in temporal lobe epilepsy. Neurologia 11 Suppl 4: 29-32.

Smith KE, Borden LA, Wang CH, Hartig PR, Branchek TA, Weinshank RL (1992) Cloning and expression of a high affinity taurine transporter from rat brain. Mol Pharmacol 42: 563-569.

Smolin LA, Benevenga NJ, Berlow S (1981) The use of betaine for the treatment of homocystinuria. J Pediatr 99: 467-472.

Soghomonian JJ, Martin DL (1998) Two isoforms of glutamate decarboxylase: why? Trends Pharmacol Sci 19: 500-505.

Somjen GG (1999) Low external NaCl concentration and low osmolarity enhance voltage-gated Ca currents but depress K currents in freshly isolated rat hippocampal neurons. Brain Res 851: 189-197.

Sone M, Ohno A, Albrecht GJ, Thurau K, Beck FX (1995) Restoration of urine concentrating ability and accumulation of medullary osmolytes after chronic diuresis. Am J Physiol 269: F480-F490.

Soudijn W, van W, I (2000) The GABA transporter and its inhibitors. Curr Med Chem 7: 1063-1079.

Sperk G (1994) Kainic acid seizures in the rat. Prog Neurobiol 42: 1-32.

Sperk G, Lassmann H, Baran H, Kish SJ, Seitelberger F, Hornykiewicz O (1983) Kainic acid induced seizures: neurochemical and histopathological changes. Neuroscience 10: 1301-1315.

Sterns RH, Baer J, Ebersol S, Thomas D, Lohr JW, Kamm DE (1993) Organic osmolytes in acute hyponatremia. Am J Physiol 264: F833-F836.

Stirling DA, Hulton CS, Waddell L, Park SF, Stewart GS, Booth IR, Higgins CF (1989) Molecular characterization of the proU loci of Salmonella typhimurium and Escherichia coli encoding osmoregulated glycine betaine transport systems. Mol Microbiol 3: 1025-1038.

Strange K (1992) Regulation of solute and water balance and cell volume in the central nervous system. J Am Soc Nephrol 3: 12-27.

Strange K, Emma F, Paredes A, Morrison R (1994) Osmoregulatory changes in myo-inositol content and Na+/myo-inositol cotransport in rat cortical astrocytes. Glia 12: 35-43.

Strange K, Morrison R (1992) Volume regulation during recovery from chronic hypertonicity in brain glial cells. Am J Physiol 263: C412-C419.

Strange K, Morrison R, Heilig CW, DiPietro S, Gullans SR (1991) Upregulation of inositol transport mediates inositol accumulation in hyperosmolar brain cells. Am J Physiol 260: C784-C790.

Strange K, Morrison R, Shrode L, Putnam R (1993) Mechanism and regulation of swelling-activated inositol efflux in brain glial cells. Am J Physiol 265: C244-C256.

Stroud JC, Lopez-Rodriguez C, Rao A, Chen L (2002) Structure of a TonEBP-DNA complex reveals DNA encircled by a transcription factor. Nat Struct Biol 9: 90-94.

Sutula TP (1990) Experimental models of temporal lobe epilepsy: new insights from the study of kindling and synaptic reorganization. Epilepsia 31 Suppl 3: S45-S54.

Swartzwelder HS, Bragdon AC, Sutch CP, Ault B, Wilson WA (1986) Baclofen suppresses hippocampal epileptiform activity at low concentrations without suppressing synaptic transmission. J Pharmacol Exp Ther 237: 881-887.

Takanaga H, Ohtsuki S, Hosoya K, Terasaki T (2001) GAT2/BGT-1 as a system responsible for the transport of gamma-aminobutyric acid at the mouse blood-brain barrier. J Cereb Blood Flow Metab 21: 1232-1239.

Takenaka M, Bagnasco SM, Preston AS, Uchida S, Yamauchi A, Kwon HM, Handler JS (1995) The canine betaine gamma-amino-n-butyric acid transporter gene: diverse mRNA isoforms are regulated by hypertonicity and are expressed in a tissue-specific manner. Proc Natl Acad Sci U S A 92: 1072-1076.

Takenaka M, Preston AS, Kwon HM, Handler JS (1994) The tonicity-sensitive element that mediates increased transcription of the betaine transporter gene in response to hypertonic stress. J Biol Chem 269: 29379-29381.

Tappaz ML (2004) Taurine biosynthetic enzymes and taurine transporter: molecular identification and regulations. Neurochem Res 29: 83-96.

Thomsen C, Sorensen PO, Egebjerg J (1997) 1-(3-(9H-carbazol-9-yl)-1-propyl)-4-(2-methoxyphenyl)-4-piperidinol, a novel subtype selective inhibitor of the mouse type II GABA-transporter. Br J Pharmacol 120: 983-985.

Thurston JH, Hauhart RE, Dirgo JA (1980) Taurine: a role in osmotic regulation of mammalian brain and possible clinical significance. Life Sci 26: 1561-1568.

Thurston JH, Hauhart RE, Nelson JS (1987) Adaptive decreases in amino acids (taurine in particular), creatine, and electrolytes prevent cerebral edema in chronically hyponatremic mice: rapid correction (experimental model of central pontine myelinolysis) causes dehydration and shrinkage of brain. Metab Brain Dis 2: 223-241.

Tillakaratne NJ, Medina-Kauwe L, Gibson KM (1995) gamma-Aminobutyric acid (GABA) metabolism in mammalian neural and nonneural tissues. Comp Biochem Physiol A Physiol 112: 247-263.

Tsuge H, Nakano Y, Onishi H, Futamura Y, Ohashi K (1980) A novel purification and some properties of rat liver mitochondrial choline dehydrogenase. Biochim Biophys Acta 614: 274-284.

Uchida S, Kwon HM, Yamauchi A, Preston AS, Marumo F, Handler JS (1992) Molecular cloning of the cDNA for an MDCK cell Na(+)- and Cl(-)-dependent taurine transporter that is regulated by hypertonicity. Proc Natl Acad Sci U S A 89: 8230-8234.

Uchida S, Nakanishi T, Kwon HM, Preston AS, Handler JS (1991) Taurine behaves as an osmolyte in Madin-Darby canine kidney cells. Protection by polarized, regulated transport of taurine. J Clin Invest 88: 656-662.

Uchida S, Yamauchi A, Preston AS, Kwon HM, Handler JS (1993) Medium tonicity regulates expression of the Na(+)- and Cl(-)-dependent betaine transporter in Madin-Darby canine kidney cells by increasing transcription of the transporter gene. J Clin Invest 91: 1604-1607.

Ueda Y, Willmore LJ (2000) Hippocampal gamma-aminobutyric acid transporter alterations following focal epileptogenesis induced in rat amygdala. Brain Res Bull 52: 357-361.

Varon S, Weinstein H, Roberts E (1964) Exogenous and endogenous gamma-aminobutyric acid of mouse brain particulates in a binding system *in vitro*. Biochem Pharmacol 13: 269-279.

Verbalis JG, Gullans SR (1991) Hyponatremia causes large sustained reductions in brain content of multiple organic osmolytes in rats. Brain Res 567: 274-282.

Vitarella D, DiRisio DJ, Kimelberg HK, Aschner M (1994) Potassium and taurine release are highly correlated with regulatory volume decrease in neonatal primary rat astrocyte cultures. J Neurochem 63: 1143-1149.

Walter JH, Wraith JE, White FJ, Bridge C, Till J (1998) Strategies for the treatment of cystathionine beta-synthase deficiency: the experience of the Willink Biochemical Genetics Unit over the past 30 years. Eur J Pediatr 157 Suppl 2: S71-S76.

Watanabe M, Maemura K, Kanbara K, Tamayama T, Hayasaki H (2002) GABA and GABA receptors in the central nervous system and other organs. Int Rev Cytol 213: 1-47.

Weik C, Warskulat U, Bode J, Peters-Regehr T, Haussinger D (1998) Compatible organic osmolytes in rat liver sinusoidal endothelial cells. Hepatology 27: 569-575.

Wiese TJ, Dunlap JA, Conner CE, Grzybowski JA, Lowe WL, Jr., Yorek MA (1996) Osmotic regulation of Na-myo-inositol cotransporter mRNA level and activity in endothelial and neural cells. Am J Physiol 270: C990-C997.

Wilcken DE, Wilcken B (1997) The natural history of vascular disease in homocystinuria and the effects of treatment. J Inherit Metab Dis 20: 295-300.

Wilken DR, McMacken ML, Rodriquez A (1970) Choline and betaine aldehyde oxidation by rat liver mitochondria. Biochim Biophys Acta 216: 305-317.

Williams MB, Jope RS (1995) Modulation by inositol of cholinergic- and serotonergic-induced seizures in lithium-treated rats. Brain Res 685: 169-178.

Wirthensohn G, Guder WG (1982) Studies on renal choline metabolism and phosphatidylcholine synthesis. In: Biochemistry of kidney functions (Morel F, ed), pp 119-128. Amsterdam: Elsevier.

Woo SK, Dahl SC, Handler JS, Kwon HM (2000a) Bidirectional regulation of tonicity-responsive enhancer binding protein in response to changes in tonicity. Am J Physiol Renal Physiol 278: F1006-F1012.

Woo SK, Maouyo D, Handler JS, Kwon HM (2000b) Nuclear redistribution of tonicity-responsive enhancer binding protein requires proteasome activity. Am J Physiol Cell Physiol 278: C323-C330.

Yaghmai R, Kashani AH, Geraghty MT, Okoh J, Pomper M, Tangerman A, Wagner C, Stabler SP, Allen RH, Mudd SH, Braverman N (2002) Progressive cerebral edema associated with high methionine levels and betaine therapy in a patient with cystathionine beta-synthase (CBS) deficiency. Am J Med Genet 108: 57-63.

Yamauchi A, Kwon HM, Uchida S, Preston AS, Handler JS (1991) Myo-inositol and betaine transporters regulated by tonicity are basolateral in MDCK cells. Am J Physiol 261: F197-F202.

Yamauchi A, Uchida S, Kwon HM, Preston AS, Robey RB, Garcia-Perez A, Burg MB, Handler JS (1992) Cloning of a Na(+)- and Cl(-)-dependent betaine transporter that is regulated by hypertonicity. J Biol Chem 267: 649-652.

Yamauchi A, Uchida S, Preston AS, Kwon HM, Handler JS (1993) Hypertonicity stimulates transcription of gene for Na(+)-myo-inositol cotransporter in MDCK cells. Am J Physiol 264: F20-F23.

Yancey PH, Burg MB (1990) Counteracting effects of urea and betaine in mammalian cells in culture. Am J Physiol 258: R198-R204.

Yancey PH, Clark ME, Hand SC, Bowlus RD, Somero GN (1982) Living with water stress: evolution of osmolyte systems. Science 217: 1214-1222.

Zagulska-Szymczak S, Filipkowski RK, Kaczmarek L (2001) Kainate-induced genes in the hippocampus: lessons from expression patterns. Neurochem Int 38: 485-501.

TABLES, TABLE FOOTNOTES, FIGURES AND FIGURE LEGENDS

Table 1. Effect of betaine / sucrose on BGT-1 expression by cell-ELISA. U373 MG cells were incubated for 12 hours with 1mM, 10 mM and 100 mM of betaine or sucrose, and BGT-1 immuno-intensity assayed by cell-ELISA. Betaine, but not sucrose induced increases in BGT-1 immunointensity. Values indicate means and SEM. n = 4 in each group. Statistically significant comparisons by one-way ANOVA and Bonferroni's multiple comparison post-hoc test are as follows: a vs c ($p<0.01$), b vs c ($p<0.05$). Statistically significant comparisons by Student's t-test are as follows: a vs d,e ($P<0.05$), b vs c,d,e ($P< 0.05$), c vs a,d,e, f ($P<0.01$).

Table 1. Effect of betaine / sucrose on BGT-1 expression by cell-ELISA.

Betaine Treatment	BGT-1 staining (ratio to the control)	Sucrose Treatment	BGT-1 staining (ratio to the control)
1mM betaine [a]	1.193 ± 0.021	1mM sucrose [d]	0.881 ± 0.119
10mM betaine [b]	1.356 ± 0.111	10mM sucrose [e]	1.041 ± 0.058
100mM betaine [c]	1.948 ± 0.153	100mM sucrose [f]	1.155 ± 0.110

Table 2. Effect of betaine / sucrose on [^{14}C] betaine transport. U373 MG cells were incubated for 12 hours with 1mM, 10 mM and 100 mM of betaine or sucrose, and betaine uptake assayed by measuring the amount of [^{14}C] betaine taken up into the cells during a 30 min incubation time intervals with [^{14}C] betaine. An increase in betaine uptake was observed when cells were incubated with betaine at 1mM, 10mM and 100mM concentrations, and sucrose at 100mM concentrations. Values indicate means and SEM. n = 4 in each group. Statistically significant comparisons by one-way ANOVA and Bonferroni's multiple comparison post-hoc test are as follows: a vs c ($p<0.05$), d vs f ($p<0.01$), e vs f ($p<0.01$). Statistically significant comparisons by Student's t-test are as follows: a vs c,d,e ($P<0.05$), b vs d,e ($P< 0.05$), c vs d,e ($P<0.05$), f vs a,b,c,d,e ($P<0.01$).

Table 2. Effect of betaine / sucrose on [^{14}C] betaine transport.

Betaine Treatment	[^{14}C] betaine uptake (ratio to the control)	Sucrose Treatment	[^{14}C] betaine uptake (ratio to the control)
1mM betaine [a]	1.126 ± 0.040	1mM sucrose [d]	0.953 ± 0.048
10mM betaine [b]	1.371 ± 0.099	10mM sucrose [e]	0.942 ± 0.047
100mM betaine [c]	1.496 ± 0.135	100mM sucrose [f]	2.227 ± 0.087

Table 3. Effect of betaine on BGT-1 expression *in vivo*. Rats were injected with kainate plus saline or kainate plus betaine, and the number of BGT-1 immunopositive glial cells in the degenerating field CA3 or fimbria counted. Markedly increased numbers of BGT-1 positive glial cells were observed in rats that had received kainate plus betaine, compared to kainate plus saline. Numbers indicate mean and standard error of BGT-1 positive astrocytes per square millimeter. Analyzed by Student's t-test. n = 4 in each group. Significant comparisons are as follows: a vs c ($P<0.01$), b vs d ($P<0.01$).

Table 3. Effect of betaine on BGT-1 expression *in vivo*.

Treatment	Region	No of BGT-1 positive cells
Kainate + Saline [a]	Field CA3	254.2 ± 18.5
Kainate + Saline [b]	Fimbria	312.5 ± 12.5
Kainate + Betaine [c]	Field CA3	1287.5 ± 24.9
Kainate + Betaine [d]	Fimbria	1320.8 ± 47.3

Fig. 1. Schematic diagram depicting the metabolism of betaine. Choline is oxidized by choline dehydrogenase to betaine aldehyde, which is further oxidized to betaine by betaine aldehyde dehydrogenase. Betaine donates a methyl group to homocysteine to form methionine and dimethylglycine, a reaction catalyzed by betaine homocysteine methyltransferase. (The diagram is referred to ‘Garcia-Perez A, Burg MB (1991) Renal medullary organic osmolytes. Physiol Rev 71: 1081-1115.’)

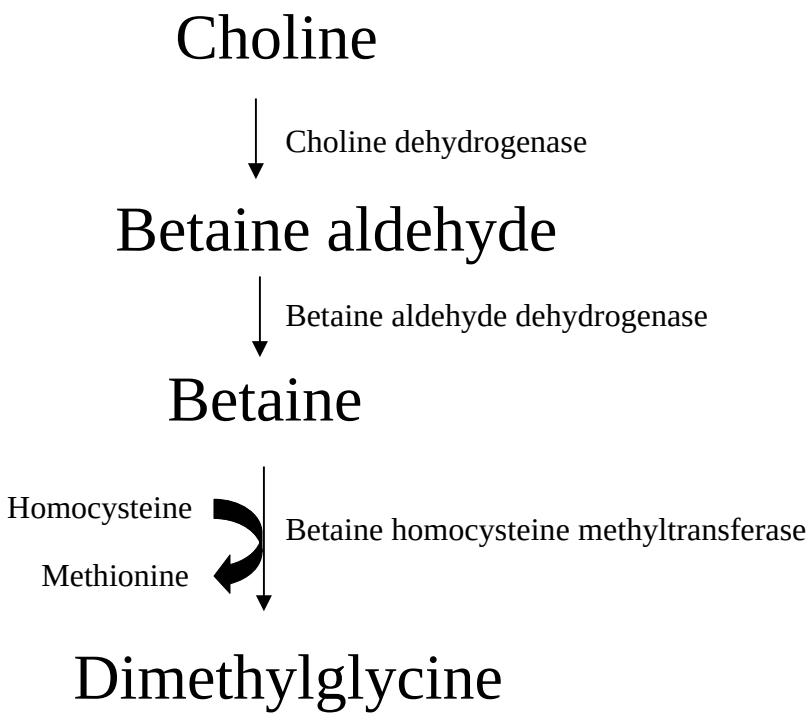
Choline
Choline dehydrogenase
Betaine aldehyde
Betaine aldehyde dehydrogenase
Betaine
Homocysteine
Methionine
Betaine homocysteine methyltransferase
Dimethylglycine

Fig. 2. Illustration of the metabolism of GABA. GABA is synthesized from glutamate by GAD_{67}/GAD_{65} in GABAergic neurons. The synaptically released GABA is up-taken via GABA transporters into axon terminals of GABAergic neurons and surrounding glial cells, where GABA undergoes degradation by mitochondrial enzyme GABA-T. The produced glutamine in glial cells is exported to neurons and converted to glutamate. (The illustration is referred to 'Farrant M (2002) Amino Acids: Inhibitory. In: Neurotransmitters, Drugs and Brain Function (Webster RA, ed), pp 225-250. Chichester: John Wiley & Sons, Ltd.')

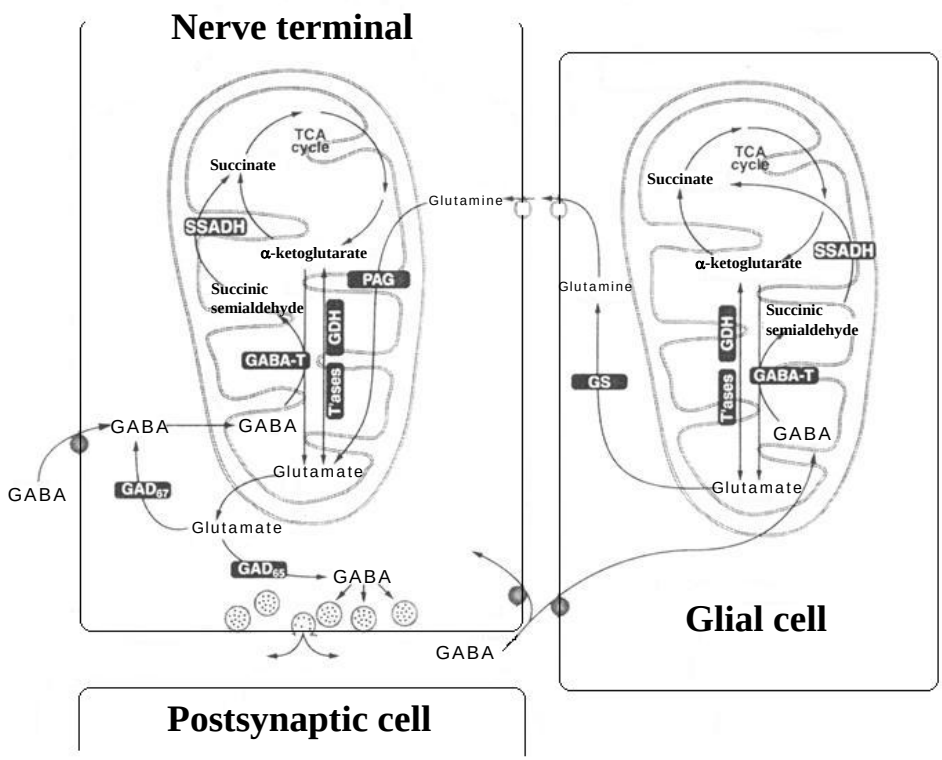
Nerve terminal
TCA cycle
Succinate
SSADH
α-ketoglutarate
PAG
Succinic semialdehyde
GDH
GABA-T
T'ases
GABA
GABA
GABA
GAD67
Glutamate
Glutamate
GAD65
GABA
Glutamine
Glutamine
GS
TCA cycle
Succinate
SSADH
α-ketoglutarate
Succinic semialdehyde
GDH
GABA-T
T'ases
GABA
Glutamate
GABA
Glial cell
Postsynaptic cell

Fig. 3. Western immunoblot analysis of homogenates of the monkey liver and cerebral neocortex. The antibody to BGT-1 detects a major band at approximately 60 kDa in the monkey liver (left panel), but two bands at 60 and 65kDa in homogenates of the monkey cortex (right panel). The higher molecular weight band is likely a glycosylated product of BGT-1.

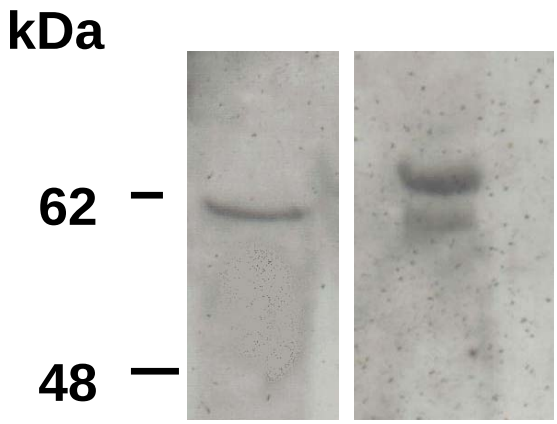
kDa
62
48

Fig. 4. Light micrographs of BGT-1 labelled neurons in the monkey middle temporal cortex (A, B) and hippocampus (C, D). A: immunoperoxidase labelled section through layer III (indicated) of the middle temporal cortex, showing light BGT-1 labelling of pyramidal neurons (arrows). B: immunoperoxidase labelled section through layers V and VI (indicated) of the middle temporal cortex, showing light labelling of pyramidal neurons (arrows). C: immunogold labelled section of field CA1 (indicated) of the hippocampus, showing labelling of pyramidal neuronal cell bodies and dendrites (arrows). D: immunogold labelled section of field CA3 (indicated) of the hippocampus, showing staining of pyramidal neuronal dendrites (arrows). No staining is observed in mossy fibers of dentate granule neurons, in the stratum lucidum (asterisk). Scale: 50 μm.

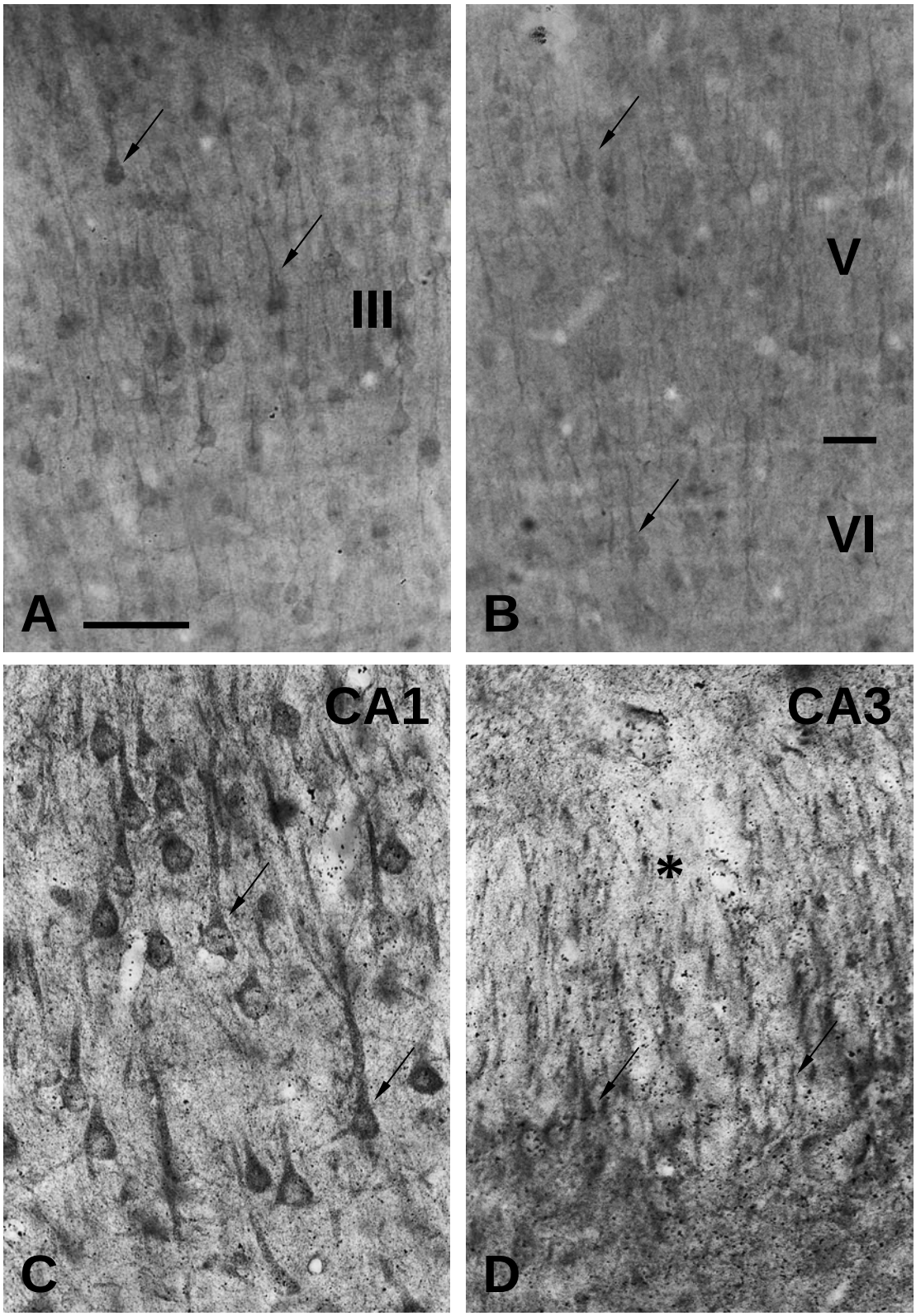
III
A
V
VI
B
CA1
C
CA3
*
D

Fig. 5. Electron micrographs of BGT-1 immunoperoxidase labelled sections through CA fields of the hippocampus (A) and layer V of the middle temporal cortex (B). A: pyramidal neuron (N), showing scattered BGT-1 label in the cytoplasm (arrows). B: synapses (S) between unlabelled axon terminals (AT), and a labelled dendrite (D). BGT-1 label (arrows) is present in the cytosol of the dendrite and in the 'extra-perisynaptic region' i.e. on the cell membrane adjacent to the synapses. Scale: A = 2 μm, B = 0.2 μm.

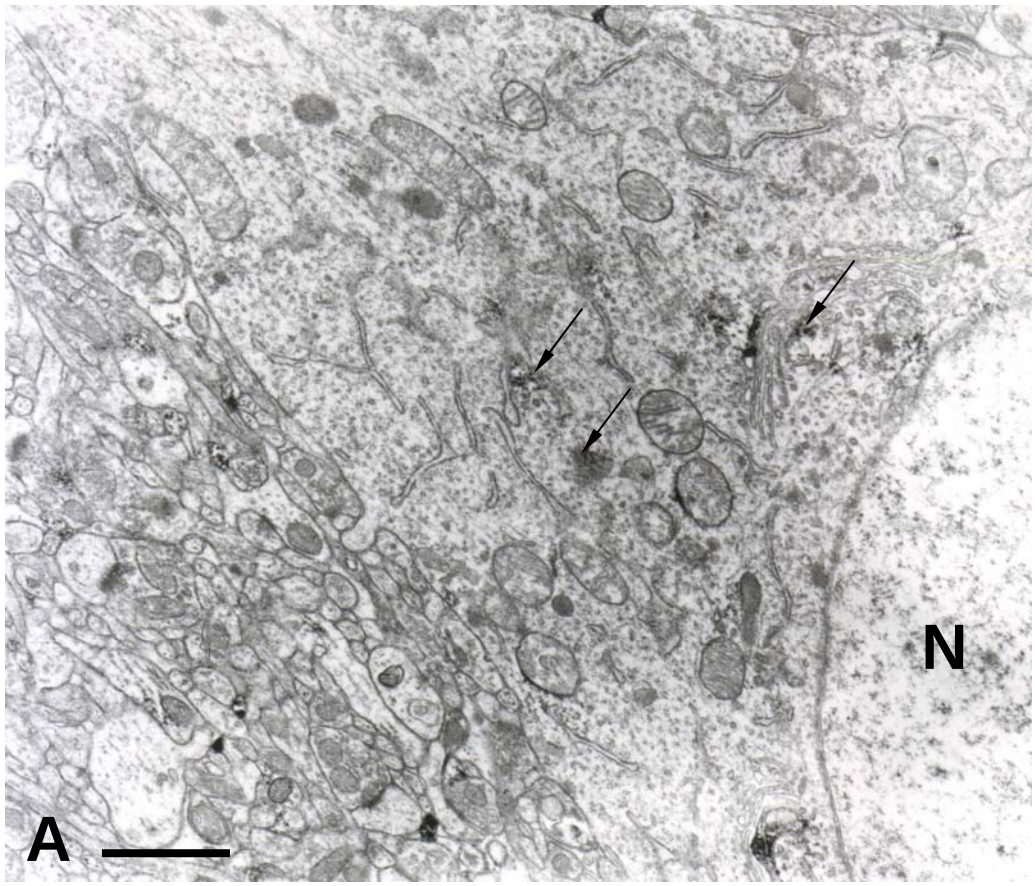
N
A

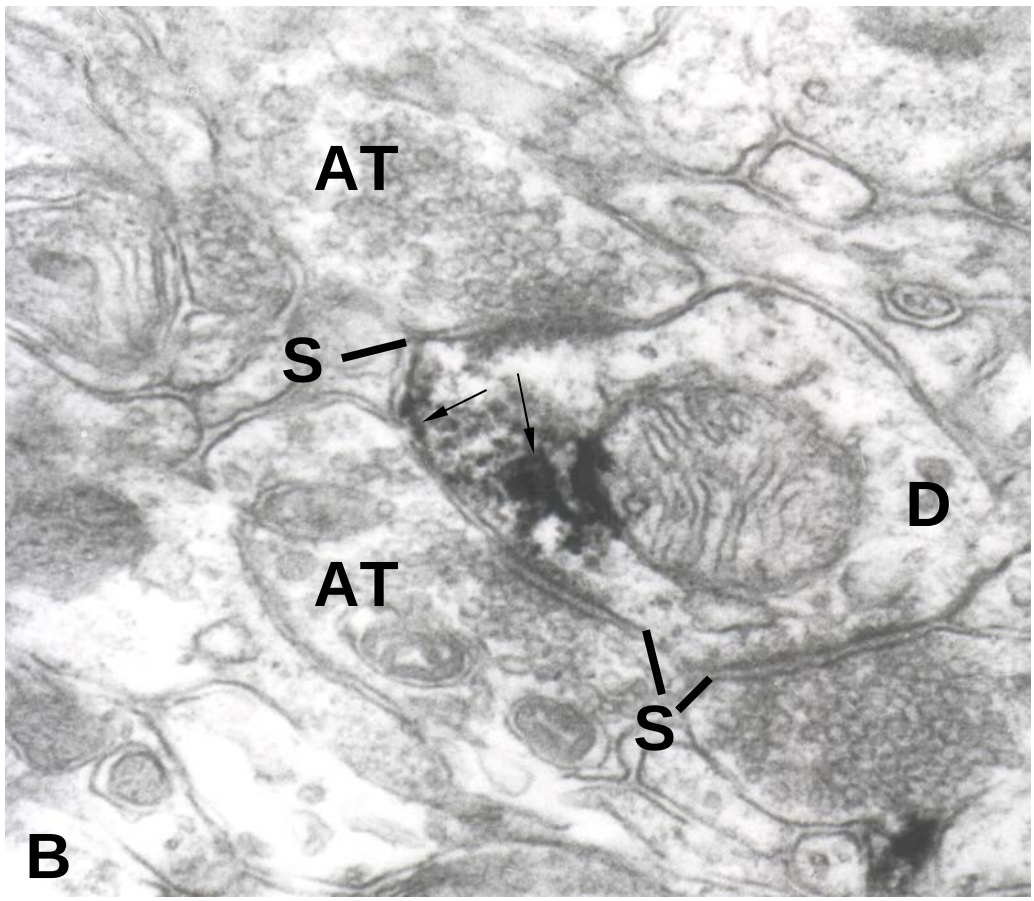
AT
S
D
AT
S
B

Fig. 6. Electron micrographs of BGT-1 immunogold labelled sections through CA fields of the hippocampus. A: pyramidal neuron (N), showing scattered BGT-1 label in the cytoplasm (arrows). B, C: synapses (S) between unlabelled axon terminals (AT), and labelled dendrites (D). BGT-1 label (arrows) is present in the cytosol of the dendrite and in the extra-perisynaptic region. Scale: A = 2 μm, B, C = 0.2 μm.

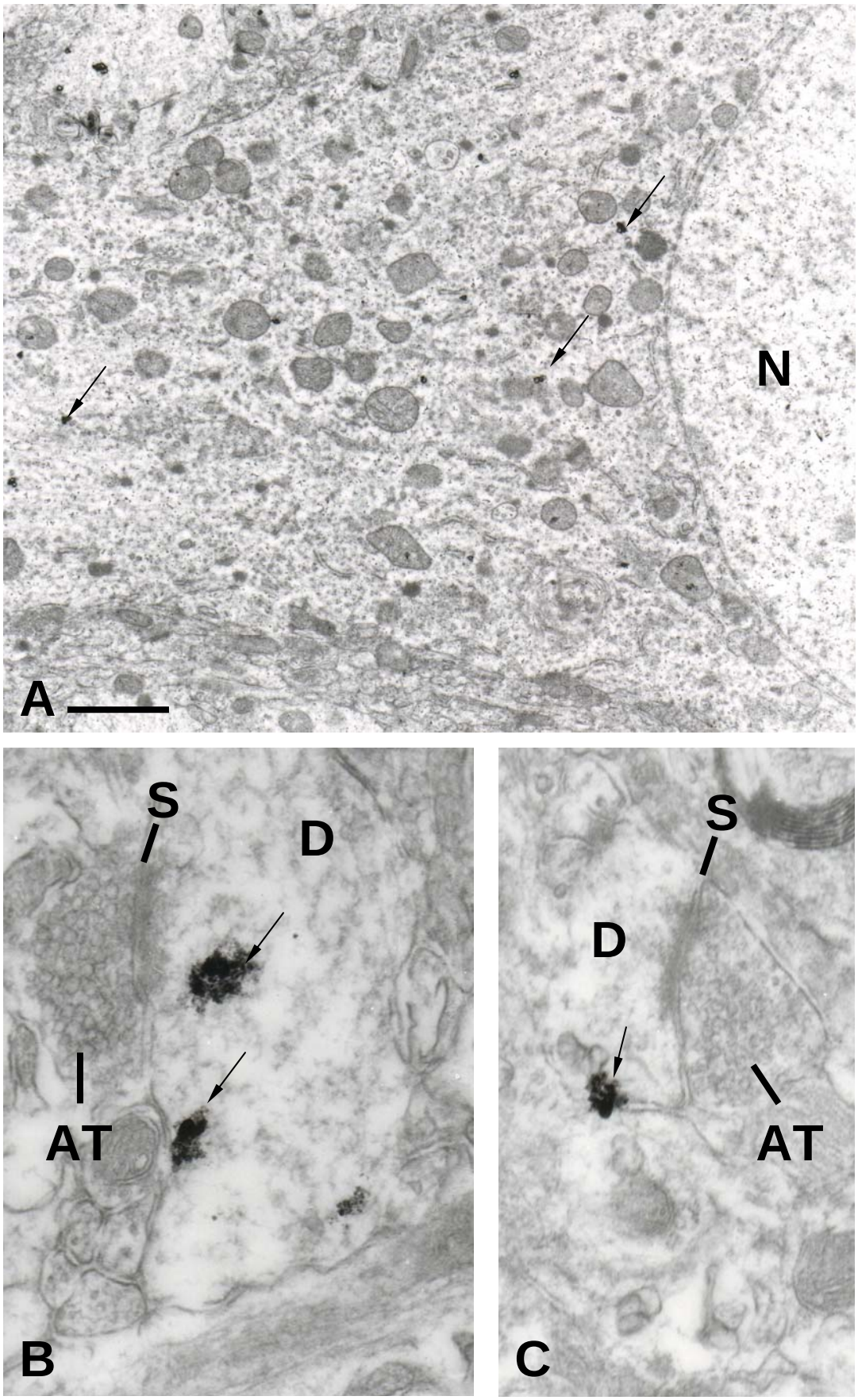
N
A
S
D
AT
B
S
D
AT
C

Fig.7. Western blot analysis of BGT-1. The antibody against BGT-1 recognizes a major band at approximately 60 kDa, a result consistent with the findings of Ruiz-Tachiquin et al. (Ruiz-Tachiquin et al., 2002), in the rat liver (L), but a 60 kDa and a 65 kDa band in both normal (N), and 1 week post kainate-injected (K) rat hippocampus. The 65 kDa band is most likely a glycosylated form of BGT-1.

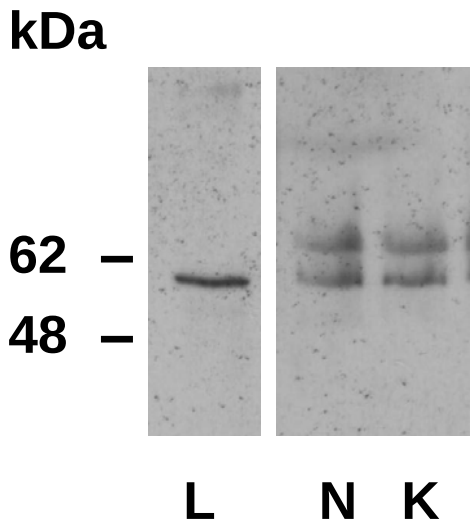
kDa
62
48
L
N
K

Fig. 8. Light micrographs of sections of hippocampal field CA3 from a normal rat. A: GAT-1 label is absent from neuronal cell bodies, but present as a network of fibers in the neuropil (asterisk). B: Very little or no labelling for GAT-2 is observed (asterisk). C: GAT-3 staining is present in occasional glial cell bodies (arrows), but in large numbers of processes in the neuropil (asterisk). D: BGT-1 labelling is present as diffuse staining in the cell bodies of pyramidal neurons in the stratum pyramidale (arrows), and in the neuropil (asterisk). SO, stratum oriens; SP, stratum pyramidale; SR, stratum radiatum. Scale: 50 μm.

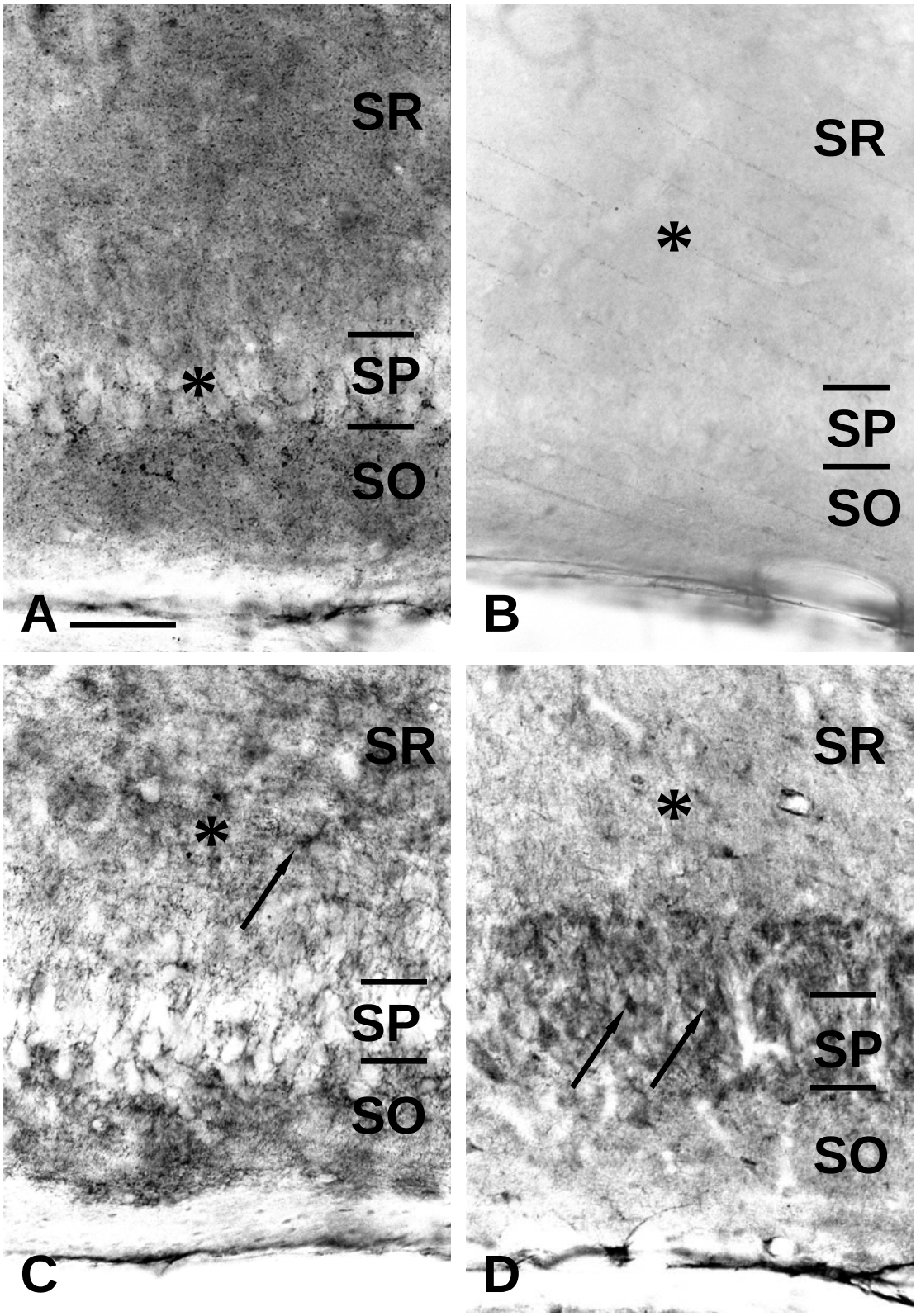
SR
SP
SO
A
SR
SP
SO
B
SR
SP
SO
C
SR
SP
SO
D

Fig. 9. Adjacent sections of field CA3, from a rat that had been injected with kainate 3 days earlier. A: Nissl stained section, showing loss of pyramidal neurons (arrows). B: GAT-1 immunostained section showing a slight decrease in immunostaining in the neuropil (asterisk; compare to Fig. 8A). C: GAT-3 immunostained section showing decreased immunoreactivity in the affected CA field (asterisk; compare to Fig. 8C). D: BGT-1 immunostained section, showing decreased staining in pyramidal neurons, but increased staining in glial cells (arrows), in the lesioned CA fields. Abbreviations as in Fig. 8. Scale: 50 μm.

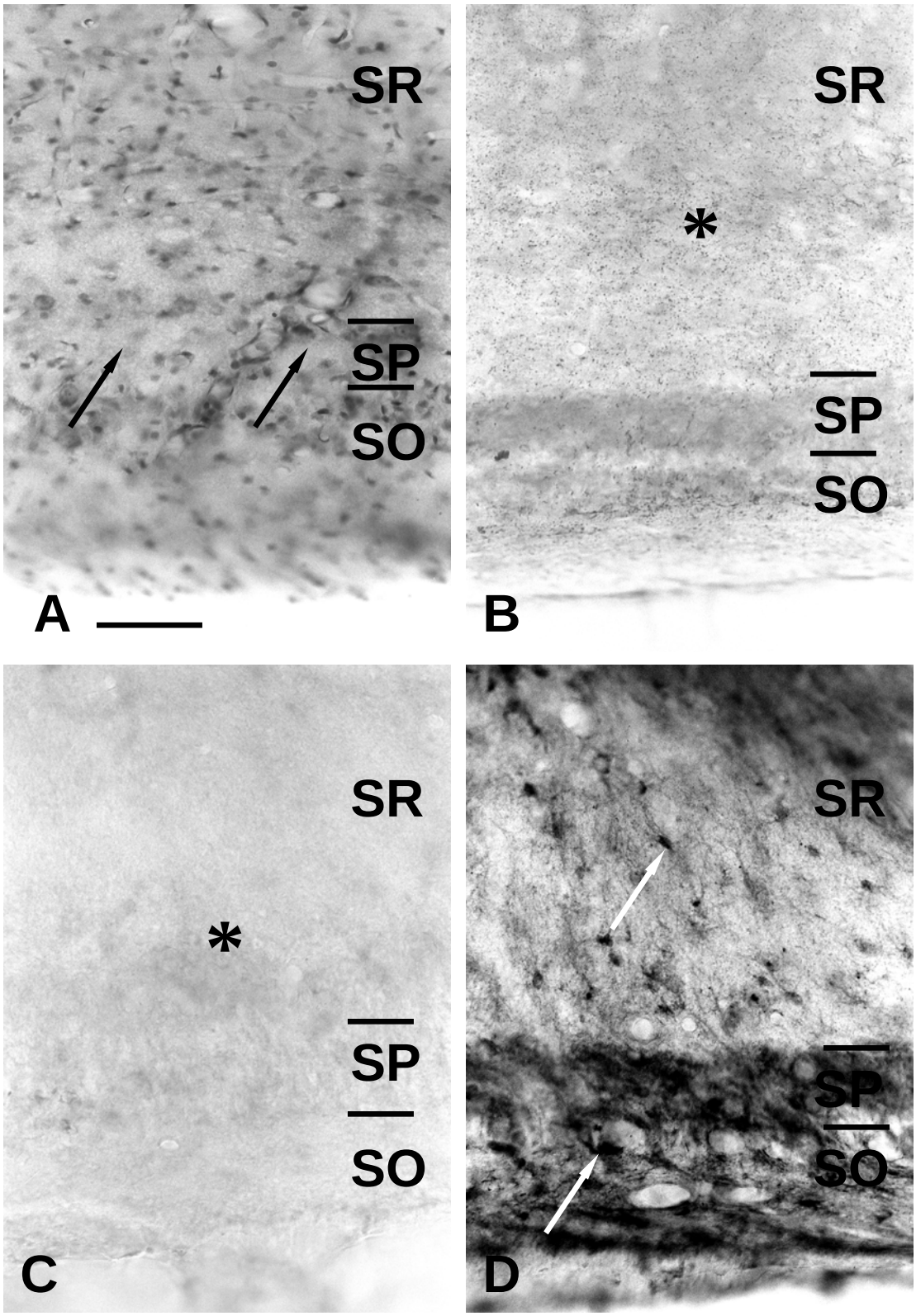
SR
SP
SO
A
SR
*
SP
SO
B
SR
*
SP
SO
C
SR
SP
SO
D

Fig. 10. Adjacent sections of field CA3, from a rat that had been injected with kainate 1 week earlier. A: Nissl stained section, showing loss of pyramidal neurons (arrow), but large numbers of glial cells in the area affected by the kainate injection (asterisk). B: GAT-1 immunostained section showing decreased immunostaining in the neuropil, compared to untreated rats (asterisk; compare to Fig. 8A). C: GAT-3 immunostained section showing decreased immunoreactivity in the affected CA field (asterisk; compare to Fig. 8C). D: BGT-1 immunostained section, showing markedly increased staining in astrocytes, in the lesioned CA fields (arrows). Abbreviations as in Figure 8. Scale: 50 μm.

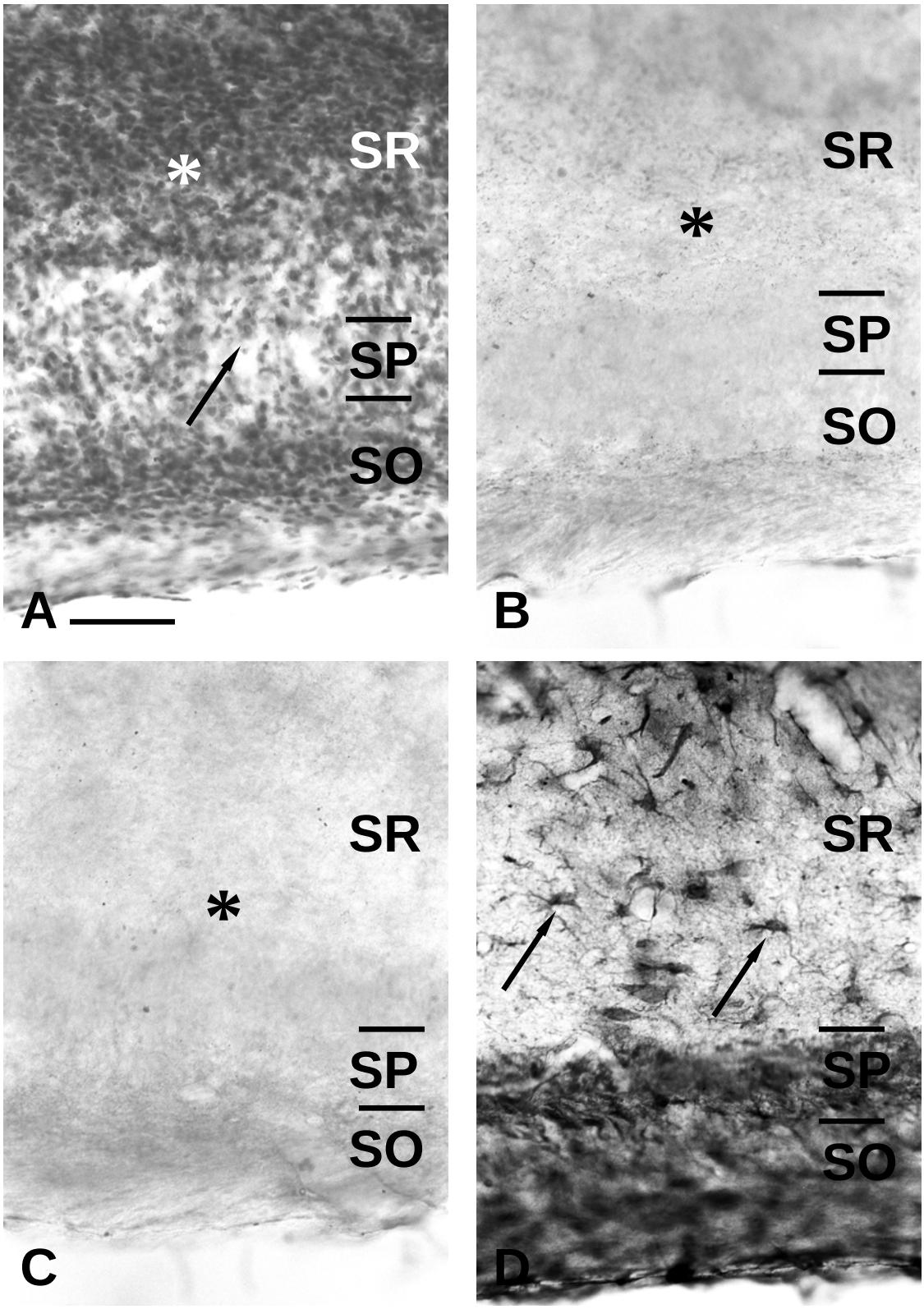
SR
SP
SO
A
B
C
D

Fig. 11. A, B: Adjacent sections of field CA3, from a rat that had been injected with kainate 3 weeks earlier. A: GAT-3 immunostained section showing decreased immunoreactivity in the affected CA field (asterisk; compare to Fig. 8C). B: BGT-1 immunostained section, showing very little staining in glial cell bodies or the neuropil (asterisk), compared to 1-week post-kainate injected hippocampus (compare to Fig. 10D). C: Electron micrograph of BGT-1 immunolabelled astrocytic cell body in field CA3, from a rat which had been injected with kainate 1 week earlier. The immunopositive cells contain dense bundles of glial filaments (F) and are identified as astrocytes. Arrows indicate immunoreactive reaction product. N: nucleus of astrocyte. Abbreviations as in Figure 8. Scale: A, B = 50 μm, C = 0.5 μm.

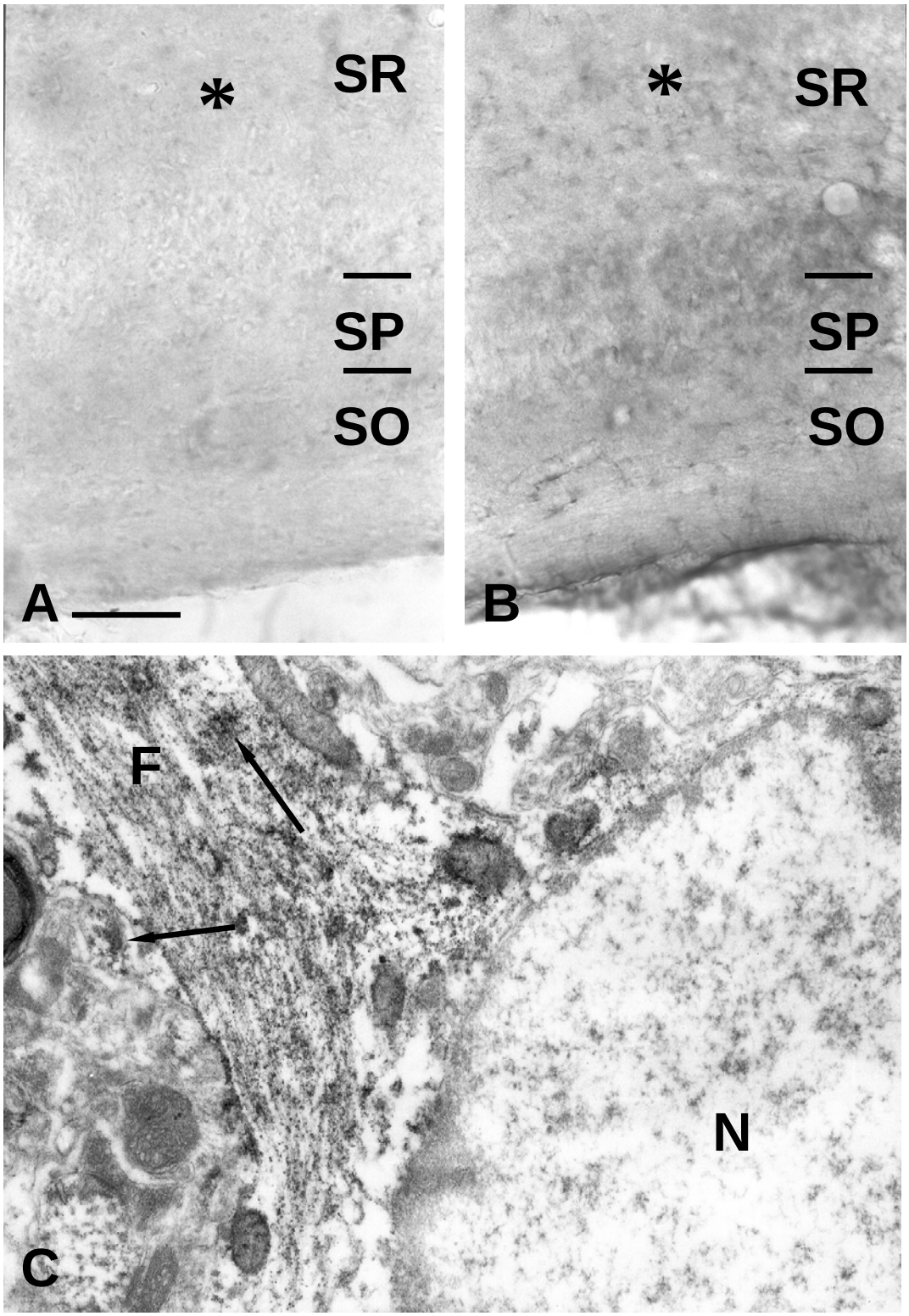
*
SR
SP
SO
A
*
SR
SP
SO
B
F
N
C

Fig. 12. Number of BGT-1 positive astrocytes in lesioned hippocampal CA3 field of saline-injected and kainate-injected rats. A significant increase in the number of BGT-1 positive astrocytes is observed in the 1-week post-kainate injected hippocampus, compared to the 3-day post-kainate injected hippocampus. The number of BGT-1 positive astrocytes declined after 1 week, and significantly fewer BGT-1 positive astrocytes were observed in the 3-week post-kainate injected hippocampus compared to the 1-week post-kainate injected hippocampus. Results were analyzed by 1-way ANOVA with Bonferroni's multiple comparison post-hoc test. Asterisks indicate statistically significant difference, $P < 0.05$. (Saline: pooled data from rats injected with saline 3 days, 1 week and 3 weeks earlier, two rats at each stage. 4 kainate-injected rats are studied at each postinjection interval. 3DK: rats injected with kainate 3 days earlier; 1WK: rats injected with kainate 1 week earlier; 3WK: rats injected with kainate 3 weeks earlier.)

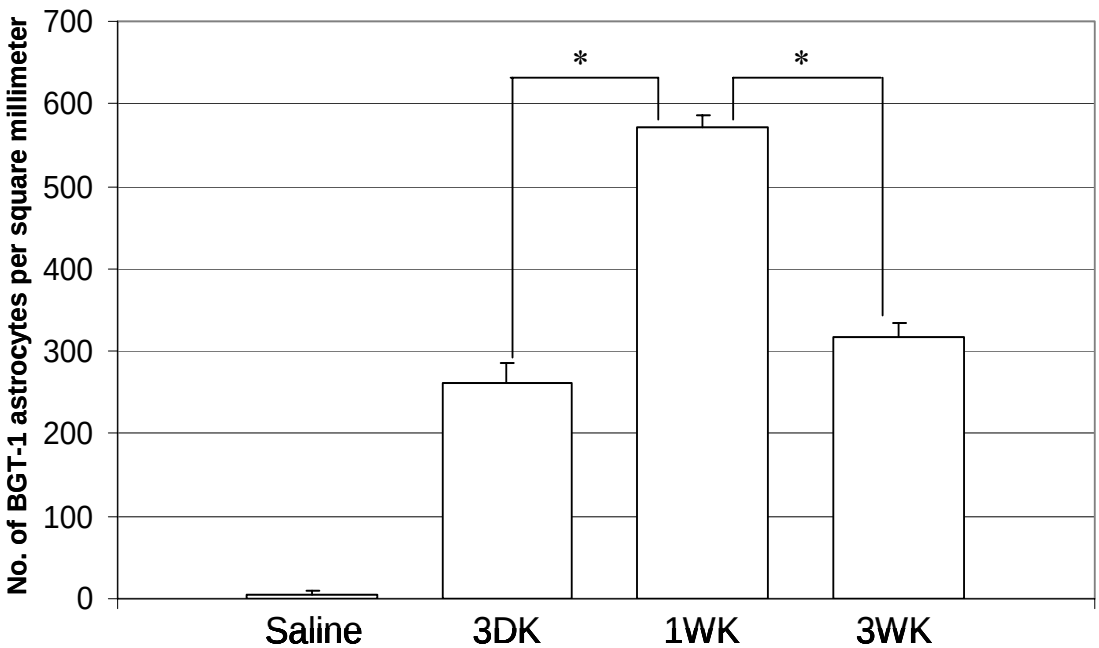
No. of BGT-1 astrocytes per square millimeter
700
600
500
400
300
200
100
0
*
*
Saline
3DK
1WK
3WK

Fig. 13. Double immunofluorescence labelling for BGT-1 and GFAP. A, B, C: The same field from a normal, untreated rat. A: Red channel, showing BGT-1 labelling in the stratum pyramidale (SP, asterisk). B: Green channel showing GFAP immunoreactivity. C: Merged channel showing few BGT-1 positive astrocytes. Arrow indicates a labelled glial cell. D, E, F: The same field from a rat that had been injected with kainate 1 week earlier. D: Red channel showing loss of neuronal labelling in the stratum pyramidale (asterisk; compare to A), but an increase in number of BGT-1 positive glial cells (arrows). E: Green channel showing GFAP positive astrocytes. In contrast to normal astrocytes, which have fine processes branching from the main cellular processes (B), these reactive astrocytes show hypertrophic processes. F: Merged channel showing all the glial cells in D are double labelled for GFAP (arrows), thus confirming that they were astrocytes. Scale: 50 μm.

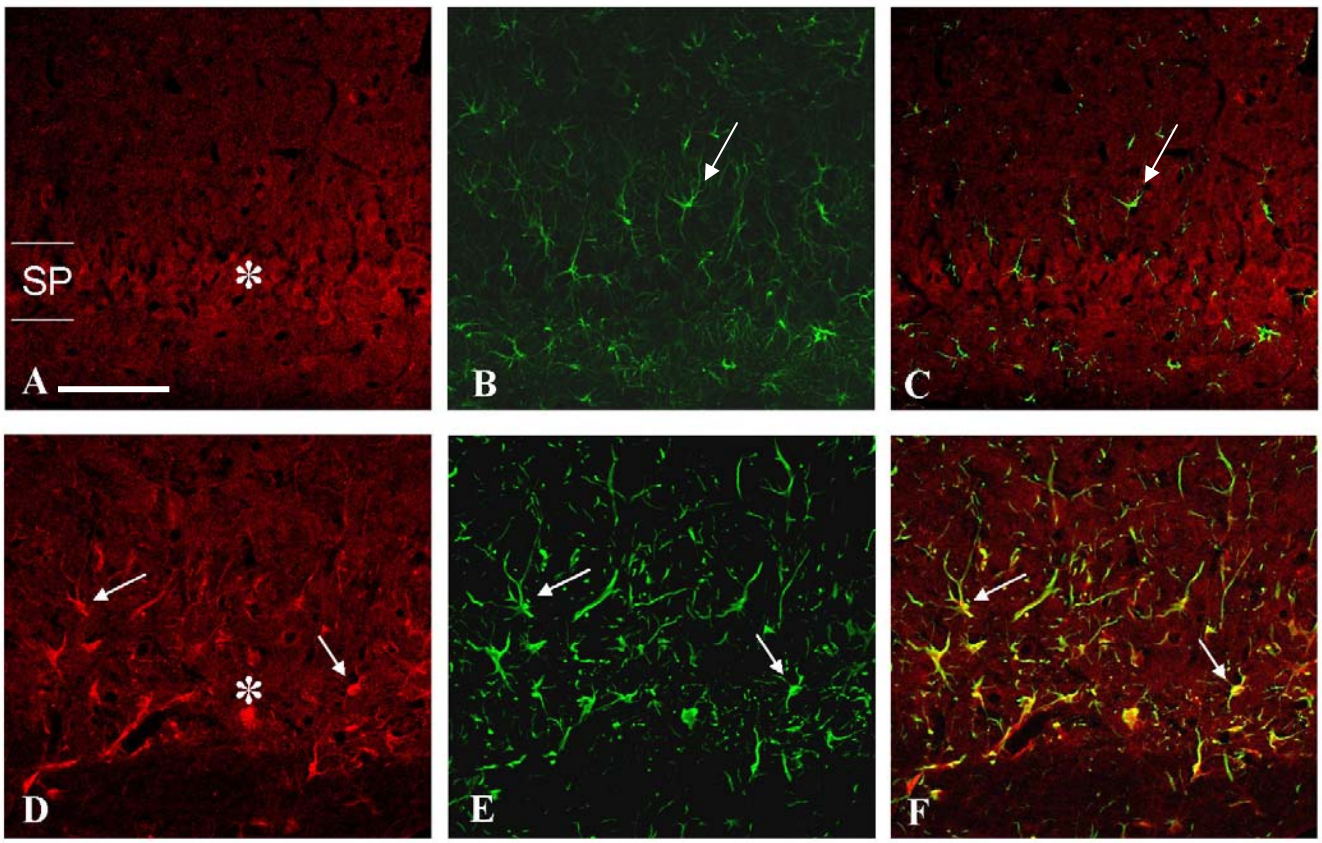
SP
A
B
C
D
E
F

Fig. 14. RT-PCR analysis for the BGT-1 mRNA expression of human U373 MG astrocytoma cells. Lane 1: DNA marker. Lane 2: A sharp band, corresponding to 439 bp, is clearly visible in agarose gel. The band was cut and inserted into plasmid for cloning and sequencing.

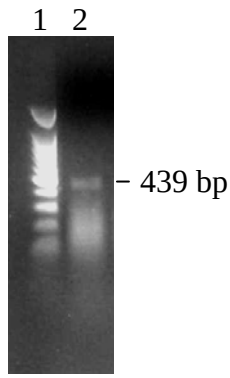
1 2
439 bp

Fig. 15. Effect of betaine or sucrose on BGT-1 immunoreactivity. U373 MG cells were incubated for 12 hours with 1mM, 10 mM and 100 mM of betaine or sucrose, and BGT-1 immunoreactive cells examined using a confocal microscope. A: Negative control in which the primary antibody BGT-1 is omitted. There is absence of red signal, and only the blue nuclear stain (DAPI) is visible. B: Cells incubated with control medium without added betaine or sucrose, showing very low level of BGT-1 immunoreactivity (red fluorescence) in the cytoplasm. C, D, E: Cells incubated with media containing 1mM, 10mM and 100mM betaine respectively, showing a dose-dependent increase in BGT-1 immunoreactivity (red fluorescence, indicated by arrows). Label is mostly present in organelles in the cytoplasm, although some immunoreactivity is visible on the cell membrane (arrow in E). F, G, H: Cells incubated with media containing 1mM, 10mM, 100mM sucrose respectively. There is no obvious increase in immunoreactivity of BGT-1, compared to cells incubated with betaine. Scale: 20 μm.

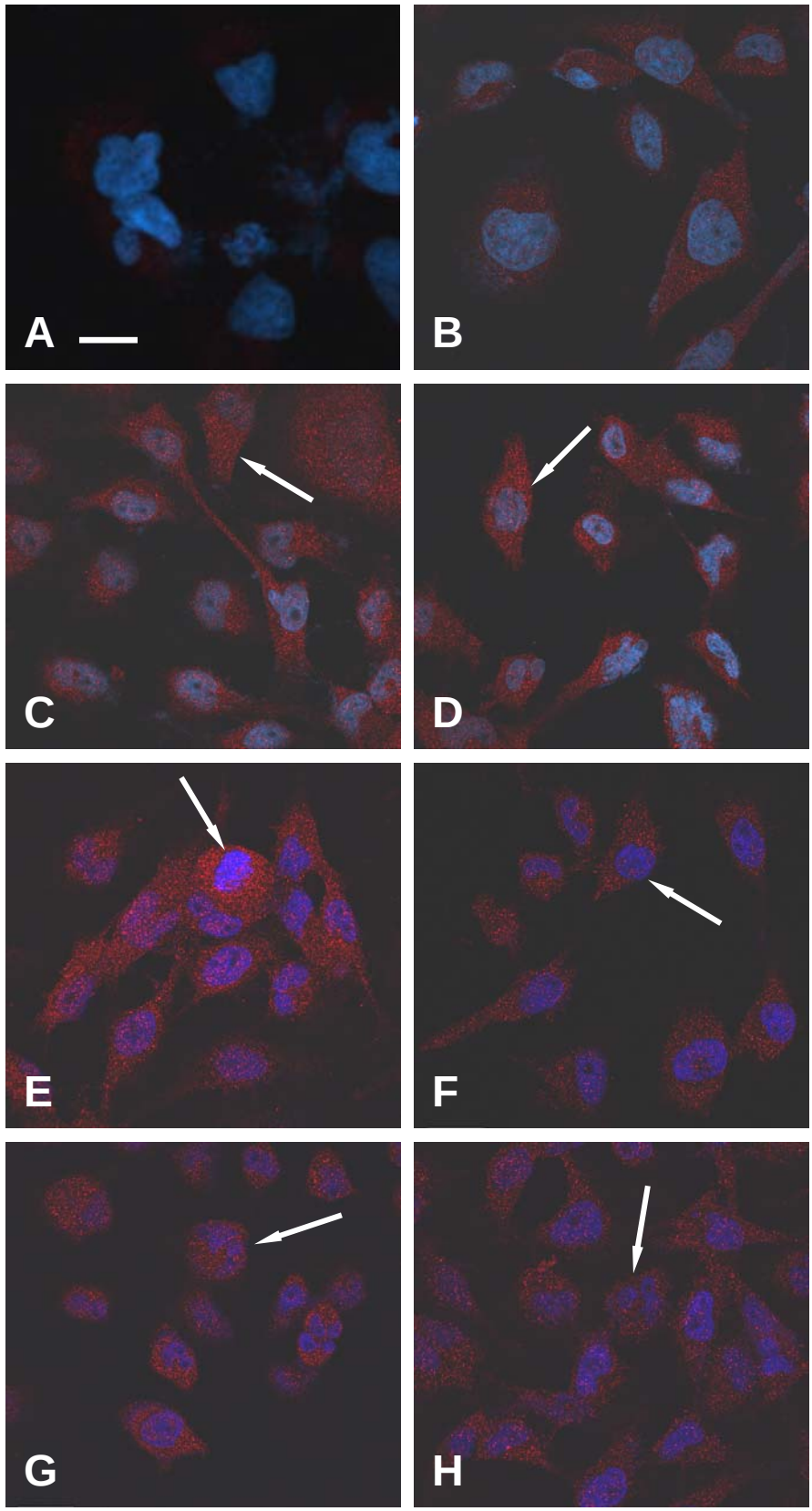
A
B
C
D
E
F
G
H

Fig. 16. Effect of betaine on BGT-1 expression *in vivo*. A: section through the untreated hippocampus showing light BGT-1 immunolabeling in pyramidal neurons (arrows) and in the neuropil (asterisk). B: BGT-1 immunolabeled section of field CA3, from a rat that had been injected with kainate and saline, showing loss of BGT-1 immunoreactivity in pyramidal neurons (asterisk), and little induction of BGT-1 immunoreactivity in glial cells. C: BGT-1 immunolabeled section of the fimbria from a rat that had been injected with kainate and saline, showing only a few BGT-1 immunoreactive glial cells (arrows). D: Nissl stained section from field CA3 from a rat that had been injected with kainate and betaine, showing loss of pyramidal neurons (asterisk). E: BGT-1 immunolabeled section of field CA3 from the same animal as D, showing marked induction of immunoreactivity in glial cells (arrows). F: BGT-1 immunolabeled section of the fimbria from the same animal as D, showing marked induction of immunoreactivity in glial cells (arrows). Abbreviations: CTRL: uninjected control rats. KA: kainate; S: saline; B: betaine. Scale: 100 μm.

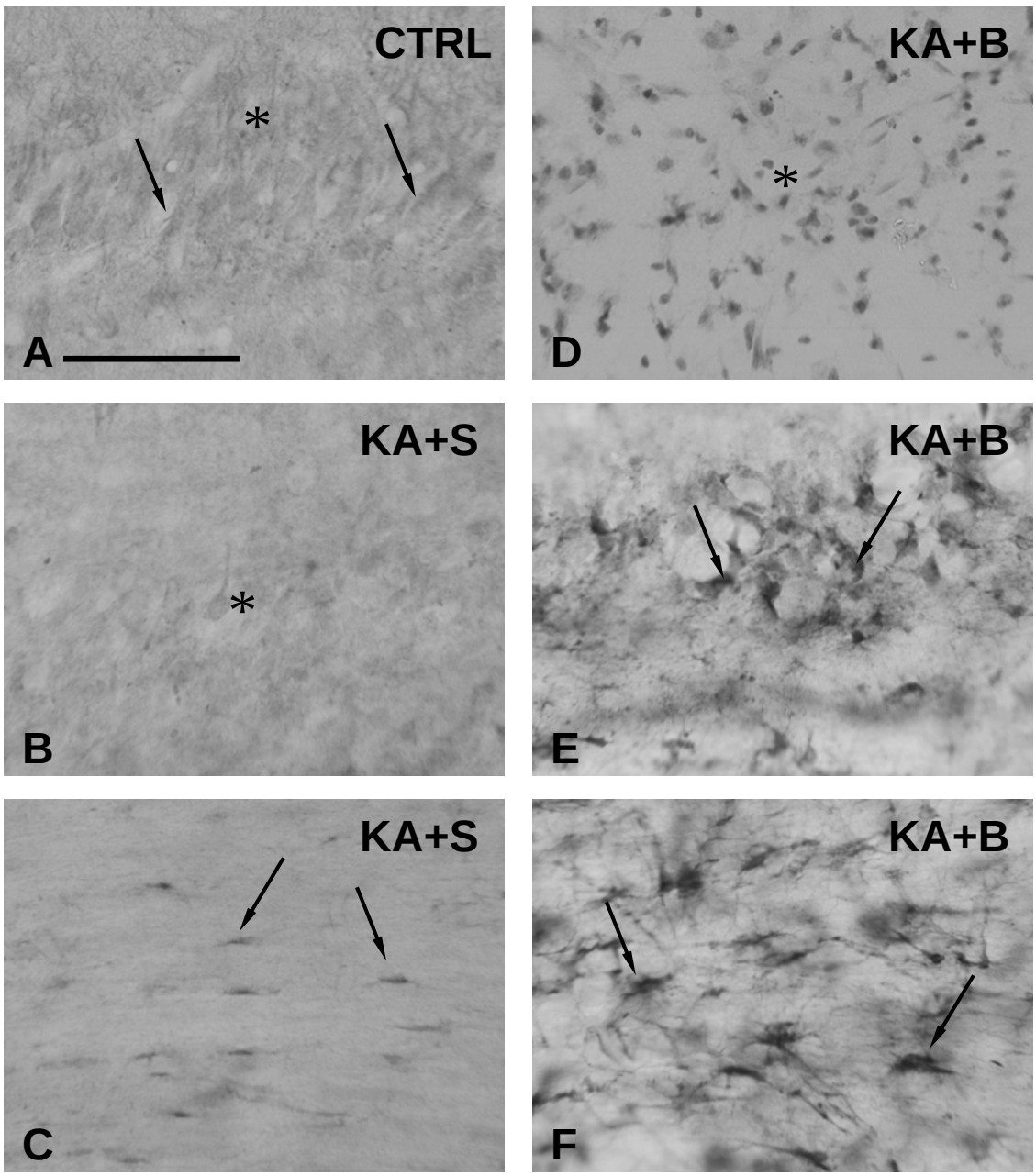
CTRL
A
KA+B
D
KA+S
B
KA+B
E
KA+S
C
KA+B
F

Fig. 17. Double immunofluorescence labeling for BGT-1 and GFAP from sections of the hippocampal CA3 field and its adjacent fimbria on the side ipsilateral to drug injections. A, B, C: Rats injected with kainate plus saline A: Red channel showing BGT-1 labeling in the stratum pyramidale. B: Green channel showing GFAP immunostaining. C: Merged channel showing BGT-1 labelled astrocytes. Arrow indicates a labeled astrocyte. D, E, F: Rats injected with kainate plus betaine D: Red channel showing BGT-1 immunoreactivity. There is a marked increase in number of labeled glial cells (arrows) in the degenerating CA3 fields and the fimbria. E: Green channel showing GFAP immunostaining. F: Merged channel showing that almost all the glial cells in Fig. D are double labeled with GFAP (arrows), indicating that they were astrocytes. Scale: 50 μm.

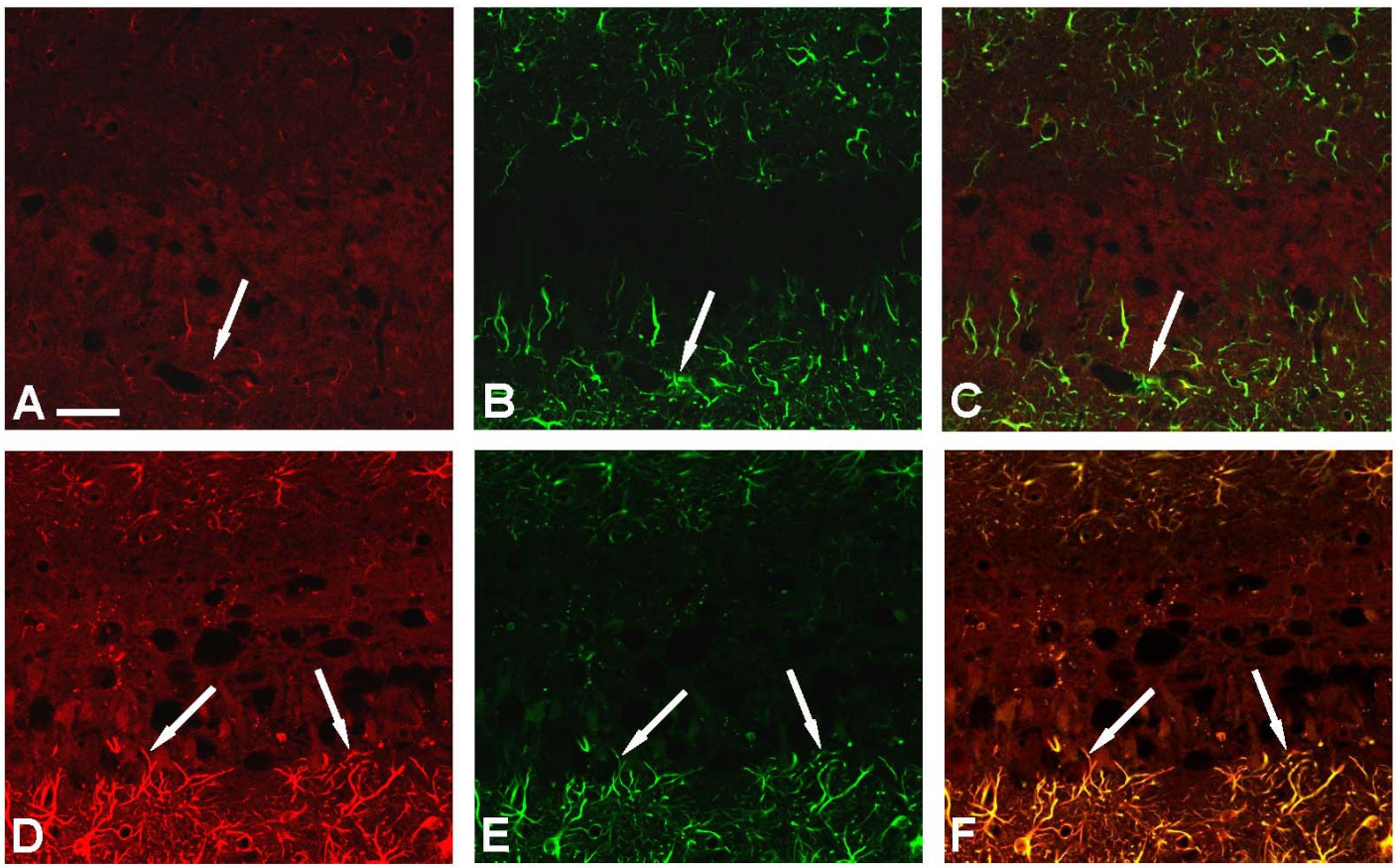
A
B
C
D
E
F

Fig. 18. A, B Electron micrographs of BGT-1 immunolabeled astrocytes in CA3 field in rats that had been injected with kainate and saline. The cytoplasm contains dense bundles of glial filaments (F). The mitochondria (arrows) appear intact and normal. C, D Electron micrographs of BGT-1 immunolabeled astrocytes in rats that received kainate and betaine injections. The cytoplasm contains large numbers of swollen mitochondria (arrows). Arrowheads indicate immunoreactive reaction product. AS: astrocyte. Scale: 1 μm.

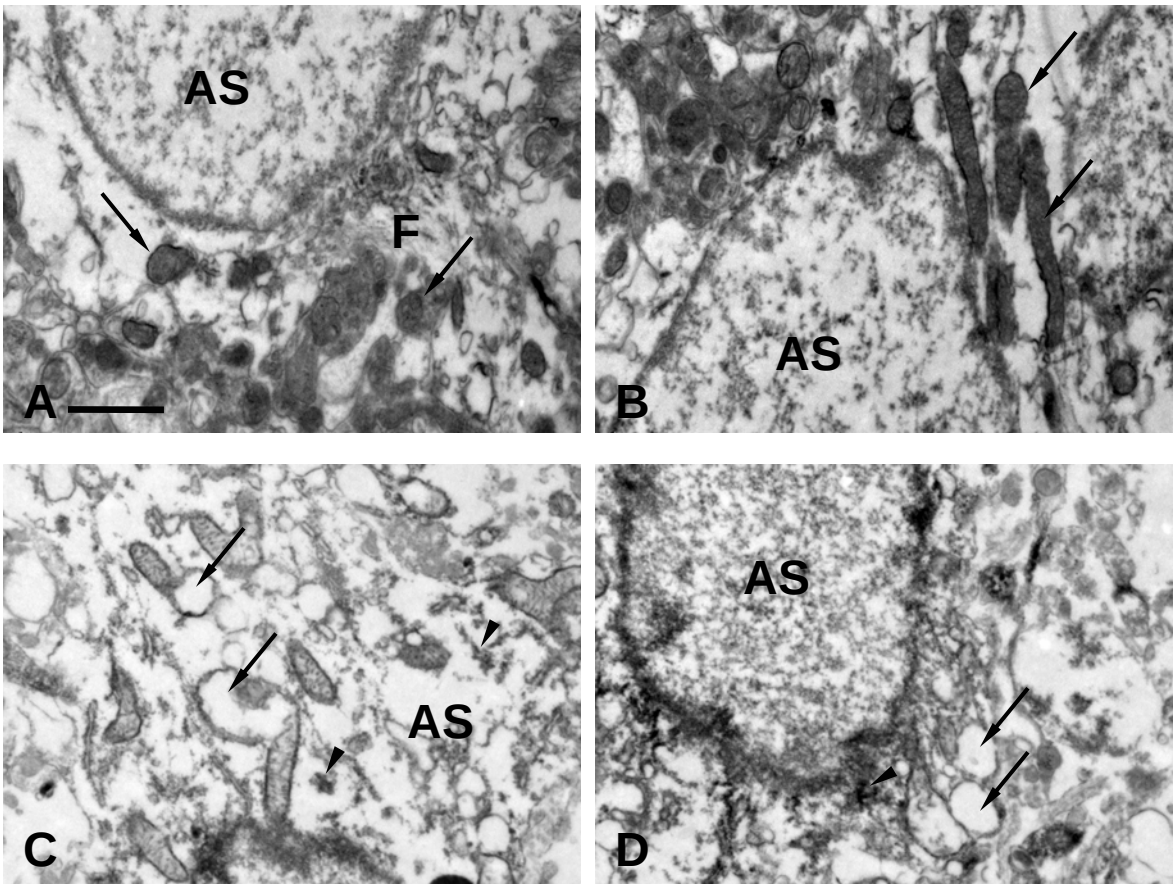
AS
F
A
AS
B
AS
C
AS
D